Epidemiology and biology of powdery mildews and their host plants

Michael Bradshaw

A dissertation
Submitted in partial fulfillment of the
Requirements for the degree of

Doctor of Philosophy

University of Washington
2020

Reading Committee:
Patrick Tobin, Chair
Marianne Elliott
Soo-Hyung Kim
Caroline Strömberg

Program Authorized to Offer Degree:
Environmental and Forest Sciences

University of Washington

Abstract

Epidemiology and biology of powdery mildews and their host plants

Michael Bradshaw

Chair of the Supervisory Committee:

Professor Patrick Tobin

School of Environmental and Forest Science

Powdery mildew is one of the most prevalent plant pathogens in the Pacific Northwest with over 150 different species infecting over 1000 plants. The hot, dry summers and wet, mild winters in this region are optimal for its colonization and spread. Sequencing herbarium specimens for plant pathogens, including powdery mildews, can be challenging but useful in addressing fundamental ecological, epidemiological, and phylogenetic questions in plant-pathogen interactions. In my dissertation, I reviewed the taxonomy and phylogeny of powdery mildews and developed a new sequencing protocol for sequencing herbarium specimens. Using this new sequencing protocol, I conducted a world-wide phylogenetic and taxonomic analysis on powdery mildews on *Viburnum*, in which I described two new species, *E. viburniphila* sp. nov and *E. pseudoviburni* sp. nov, and reduced *E. hedwigii* to synonymy with *E. viburni*; and genetically ascertained the origin and timing of an introduced plant pathogen of which *Acer macrophyllum* (bigleaf maple) is highly susceptible. Additionally, I evaluated 126 plant species within Asteraceae to measure the role of host plant

morphological traits and evolutionary history on their suitability and susceptibility to the powdery mildew, *Golovinomyces latisporus*, and observed that phylogenetic structure, and not plant morphology, is the most consistent predictor of host susceptibility to pathogens. Examining genetic data of ancient herbarium specimens and quantifying host evolutionary history can be useful approaches in deciphering the invasion dynamics and potential impacts of non-native plant pathogens, and addressing ecological, evolutionary and pathological questions related to emerging plant pathogen epidemics.

Table of Contents

List of Tables

List of Figures

Acknowledgments

Chapter 1: Sequencing herbarium specimens of a common detrimental plant disease (powdery mildew).

Abstract

Powdery mildew (Erysiphaceae) is a detrimental plant disease that occurs on a variety of economically important crops. Powdery mildew consists of over 873 species of fungal pathogens that affect over 10,000 plant species. Genetic identification of powdery mildew is accomplished using the internal transcribed spacer (ITS) and large subunit (LSU) regions of the nuclear ribosomal RNA gene cluster. The ITS and LSU regions of powdery mildews can be useful in ecological, epidemiological, phylogenetic and taxonomic investigations. However, sequencing these regions is not without its challenges. For example, powdery mildew sequences are often contaminated with plant and/or fungal DNA. Also, there tends to be a limited amount of DNA present in specimens, and older specimens DNA can fragment over time. The success of sequencing powdery mildew often depends on the primers used for running polymerase chain reaction (PCR). The primers need to be broad enough that they match the majority of powdery mildew DNA yet specific enough that they do not align with other organisms. A review of the taxonomy and phylogeny of the powdery mildews is presented with an emphasis on sequencing the ITS+LSU genomic regions. Additionally, I introduce a new nested primer protocol for sequencing powdery mildew herbarium samples that includes six new powdery mildew specific primers. The new sequencing protocol presented allows specimens up to 130 years old to be sequenced consistently. Sequencing herbarium specimens can be extremely useful for addressing many ecological, epidemiological, phylogenetic and taxonomic problems in multiple plant pathogenic systems including the powdery mildews.

Introduction

Powdery mildew is a widely distributed, detrimental plant disease that occurs on a variety of economically important crops. Symptoms of powdery mildew first appear on its hosts as white powdery spots which can spread over large areas of the plant. This can result in decreased growth, and flower and fruit quantity. Severe infections can lead to the death of the plant and can cost hundreds of millions of dollars to control (Sambucci et al. 2014). Fungi within the family Erysiphaceae (powdery mildews) are obligate, ascomycete pathogens (Braun and Cooke 2012) that have been reported to infect over 10,000 flowering plant species worldwide (Amano 1986). Powdery mildews are one of the most prevalent plant pathogens in the world with an estimated 873 species within 18 genera (Marmolejo et al. 2018) and 5 tribes (Braun and Cook 2012).

The powdery mildews have undergone a long and dynamic co-evolution with their host plants resulting in co-speciation (Takamatsu 2013a). Molecular clocks place the origin of powdery mildews during the Cretaceous period ~100 million years ago (mya), and ~40 million years after the first appearance of angiosperms in the fossil record (Takamatsu 2004). The rapid diversification of angiosperms led to a radiation event of host specific fungi within the Ascomycota (Brundrett 2002). The radiation of powdery mildews that occurred ~76 mya coincides with the large-scale radiation of angiosperms (~108-91 mya) (Takamatsu 2013a). Powdery mildews are believed to have split from a saprotrophic fungus in the family *Myxotrichaceae* that colonizes plant debris (Braun & Cooke 2012). Takamatsu (2004) established that the powdery mildews are a sister group to the *Myxotrichiaceae* and placed the *Myxotrichiaceae* fungus *Byssoascus striatosporus* (G.L. Barron & C. Booth) Arx at the base of the powdery mildew clade in phylogenetic analyses. A recent phylogenetic analysis of the *Leotiomycetes*, using up to 15 concatenated genes across 279 specimens, reassigned the family Erysiphaceae to the order *Helotiales* with *Arachnopezizaceae* as a sister family (forming the "erysiphoid"

clade) (Johnston et al. 2019). Previously, powdery mildews were placed in an order of their own (Erysiphales).

Phylogenetic analyses of the powdery mildews are generally accomplished using data from the internal transcribed spacer regions (ITS) and large subunit (LSU) genomic regions of the nuclear ribosomal RNA gene cluster. The ITS and LSU regions include the divergent ITS1 and ITS2 regions surrounding the 5.8S gene and the large ribosomal subunit genes. The rapid evolutionary rate of the ITS region has resulted in their use in species identification for >30 years (Nilsson et al. 2008). Recently, the Consortium for the Barcode of Life recognized the ITS region as the primary fungal barcode marker (Schoch et al. 2012). The adjacent LSU region follows a similar rate of evolution as the ITS and phylogenetic analyses often provide higher support values when the ITS and LSU regions are used in conjunction (Bradshaw et al. 2020). Sequencing fungi is often accomplished using universal primers situated within the conserved 18S and LSU genes flanking the ITS region. However, these primers anneal to numerous organisms. Using universal primers to sequence obligate parasites, such as powdery mildew, which are intermingled with multiple fungal and plant species, often yields poor results. To account for this, powdery mildew specific primers have been generated (Cunnington et al. 2001; Takamatsu 2001). These primers are commonly used to sequence a wide variety of powdery mildew species (Cunnington et al. 2001; Takamatsu 2001). Although this approach has been useful for sequencing newly collected samples, there has been limited success using these primers for sequencing older herbarium specimens.

The difficulty of sequencing old powdery mildew specimens has been a major deterrent in phylogenetic and taxonomic work on the powdery mildews. In this paper, I review the phylogeny and taxonomy of the powdery mildews with an emphasis on sequencing the ITS and LSU genomic

regions. Additionally, I present a new sequencing protocol that allows herbarium samples >130 years old to be sequenced consistently and reliably.

Phylogeny

The powdery mildews consist of 18 genera that are clearly delineated from ITS + LSU phylogenetic analyses. A phylogenetic tree was constructed from the ITS+LSU sequences of powdery mildew specimens from each Erysiphaceae genus (Figure 1.1). *Byssoascus striatosporus* was selected as an outgroup taxon based on the phylogenetic analyses by Cabrera et al. (2018). We attempted to include only published sequences and the type species for each genus (Table 1.1). Sequences were aligned and edited using MUSCLE in MEGA7:Molecular Evolutionary Genetics Analysis Version 7.0 (Kumar et al. 2016). Major gaps were deleted prior to the phylogenetic analyses. A partition homogeneity test (Farris et al. 1994) was conducted in PAUP 4.0a151 (Swofford 2002) to determine whether the ITS and LSU datasets were congruent with each other. The result of the partition homogeneity test showed no direct conflict between the ITS and LSU rDNA regions (*P*-value=0.65). A GTR+G+I evolutionary model was used for phylogenetic analyses as it the most inclusive model of evolution and includes all other evolutionary models (Abadi et al. 2019). A MCC (maximum clade credibility) phylogenetic tree was constructed for the combined ITS and LSU rDNA, using a yule process speciation model (Gernhard 2008), by Bayesian analyses, in the program BEAST version 1.10.2 (Drummond and Rambaut 2007). The resulting tree was visualized using FigTree ver. 1.3.1 (Rambaut 2009). A maximum likelihood analysis was accomplished using raxmlGUI (Silvestro & Michalak, 2012) under the default settings with a GTR+G+I evolutionary model. Parsimony analysis was done using PAUP 4.0a151 (Swofford 2002). For the parsimony analysis, gaps were treated as missing data and sites were treated as unordered and unweighted. Bootstrap analyses were conducted using 1000 replications with the stepwise addition option set as simple (Felsenstein 1985).

All tree topologies were similar and only the representative maximum clade credibility tree is illustrated in Figure 1.1. Posterior probabilities ≥ 90 are displayed followed by bootstrap values greater than 70% for the maximum likelihood (ML) and maximum parsimony (MP) analyses conducted. Additionally, a tree was constructed using only the LSU sequences. This tree had a similar structure as the ITS+LSU tree but with less support values. Evolutionary events were added to the tree based on information from Braun and Cook (2012) and Takamatsu (2013b). Previous studies evaluating powdery mildew genera tend to construct trees using the combined 18S, 5.8S, and LSU rDNA dataset; however, a tree would not be able to be constructed, using this method that included all of the powdery mildew genera as there are a limited amount of 18S sequences of powdery mildews available on GenBank.

The phylogenetic analyses presented in Figure 1.1 is the first ITS + LSU phylogeny of powdery mildews that includes all of the genera. The analyses revealed that 1) the ITS+LSU sequences are able to accurately delineate the currently described powdery mildew genera as evidenced by the high boot strap values; 2) *Phyllactinia* is not a monophyletic group; 3) the majority of sections within *Erysiphe* and *Podosphaera* are not monophyletic in regards to their ITS+LSU sequences, which is in concordance with Braun and Takamatsu (2000) and Braun and Cook (2012) who introduced and used these sections as non-monophyletic, morphological units; and 4) there is no support using an ITS +LSU tree that *Parauncinula* is part of the Erysiphaceae clade. The clarification of the affiliation of this genus as sister to the Erysiphaceae, outside or inside as a basal position genus, requires further research and the use of additional markers.

The phylogenetic analyses provide the following hypotheses, based on parsimony, for the evolution of morphology of fungi within the Erysiphaceae: 1) The major ancestral traits include conidia in

chains (Euoidium type conidiophores) and chasmothecia with multiple asci; and 2) the major

derived traits include fibrosin bodies, endoparasitisim, monocot hosts, chasmothecia with single asci,

and solitary conidia (Pseudoidium type conidiophores) (Fig. 1.1).

Sequencing

Sequencing herbarium specimens can be extremely useful for addressing many ecological, epidemiological, phylogenetic and taxonomic problems (Lang et al. 2018; Bieker and Martin 2017). However, this has shown to be very difficult with powdery mildews for several reasons. First, powdery mildew sequences are often contaminated with plant and/or fungal DNA (when amplicons are generated from multiple organisms the sequencing results are unreliable, and messy). Also, there tends to be a limited amount of DNA present in specimens. These challenges can be compounded in herbarium specimens in which DNA has been degraded over time, usually into small fragments whose size is less than 500 bp (Pääbo 1989). The success of sequencing old specimens often depends on effectively running DNA extractions and PCR (polymerase chain reaction). We have developed a nested primer protocol (reported below) for consistently sequencing the ITS and LSU regions of DNA of powdery mildew from herbarium specimens that are at least 130 years old.

Past methods have been used to successfully sequence the powdery mildews ITS and LSU genomic regions (Bradshaw et al. 2017; Moparthi et al; 2018; and Bradshaw et al. 2020). The first step of sequencing is to extract the DNA. It should be noted that powdery mildews DNA can successfully be amplified by directly placing the conidia, mycelium, or chasmothecia directly into the PCR master mix (Harrington and Wingfield 1995). Because this method of direct PCR requires newly collected material, DNA extraction, prior to PCR, is recommended for older herbarium specimens. DNA extraction of the powdery mildews is commonly accomplished by using Dneasy plant or soil mini extraction kits (Qiagen, Hilden, Germany), the CTAB method (Rogers and Bendich 1985), or the Chelex method (Walsh et al. 1991; Hirata and Takamatsu 1996). Of the methods listed above, the Chelex method is the most affordable and least time consuming. For example, there are far fewer

steps in the Chelex method, compared to the other commonly used extraction methods, which saves time and decreases the probability for a laboratory mistake.

Following DNA extraction, multiple primers can be used to successfully run PCR on the powdery mildews ITS and LSU genomic regions (Table 1.2). The specificity of the primers was determined using the sequences from the specimens listed in Table 1.1 and Genbank. The primer pairs used often dictate the success of PCR. A list of common primer pair combinations with their optimum annealing temperatures is presented in Table 1.3. The remaining ingredients of the PCR master mix (Taq, Buffer, MgCl, DNTPs) should be calculated in accordance with the directions of the company from which they were purchased. Pre-mixed PCR mixtures are not recommended as they are more expensive and the ingredients cannot be individually adjusted. Adding a mixture of trehalose, bovine serum albumin, and polysorbate-20 (TBT-par) (Samarakoon et al. 2013) or solely bovine serum albumin, to the master mix can improve the sequencing success of old specimens.

When running PCR on herbarium specimens, a nested primer approach yields the greatest success. To ensure that the second primer set is nested within the first primer set, we have created a primer map of the ITS and LSU regions (Fig. 1.2) using the specimens presented in Table 1.1 as well as other commonly used primers for sequencing powdery mildews. Successful sequencing of fresh specimens ITS and LSU regions can be accomplished in one reaction using the primer pairs PM10/PM28R. Because of the limited amount and poor quality of DNA present in old herbarium samples, a multiple reaction, nested approach, is recommended. For the first reaction, AITS/TW14 is recommended, followed by PM10/PM28R for the second reaction. If sequencing a low-quality specimen, amplifications of smaller sections should be attempted for both the first and second PCR reactions (due to the fragmentation of DNA of old specimens). For example, the ITS and LSU

regions should be separated into two separately nested primer approaches. For the ITS region, AITS/PM11 is recommended, followed by PM10/ITS4. For the LSU region, RPM2/NLP2 is recommended, followed by PM28F/PM28R. At least one powdery mildew specific primer should be used in the protocol to ensure that powdery mildew is the only organism being amplified. However, it should be noted that using a powdery mildew specific primer with a universal primer will not guarantee that other fungi won't be amplified. Additionally, the powdery mildew specific primers do not anneal to all powdery mildews (they be easily modified to anneal to each species).

PCR conditions for sequencing the specimens in Table 1.4 are as follows: Activation for 3 minutes (95°) followed by 40 cycles of Denaturation (95°) for 30 seconds, Annealing (see Table 1.3) for 2 minutes, Elongation (72°) for 2 minutes (ramped up slowly at 1° per second). A final elongation (72°) for 10 minutes.

If PCR is successful, DNA can be cleaned up using a variety of kits. An affordable option is the isopropanol precipitation method. The cleaned-up amplicon can be sequenced for a relatively low cost using sanger sequencing from a variety of companies such as Eurofins Genomics (Luxembourg) and Genewiz (New Jersey).

The primers developed for this study were generated using 18S, ITS and LSU sequences from Genbank using the programs Geneious version 11.0.2 (https://www.geneious.com), Tm Calculator v 1.12.0 (New England BioLabs) and OligoAnalyzer (Integrated DNA Technologies). Previous primers developed for the powdery mildews had issues with their annealing temperatures and GC content which prevented sequencing of old specimens. The methods described above were used to generate the sequences provided in Table 1.4 for specimens ranging from 1 to 130 years old.

Discussion

Herbarium specimens can be an opportunistic source of genetic material that can shed light on the recent past, and consequently, sequencing these specimens can be a valuable tool for a broad range of studies. For example, sequences of the ITS+LSU region of plant pathogenic herbarium samples can be used to determine the center of origin and spread of invasive pathogens (Mougou et al. 2008; Brewer and Milgroom 2010), pathogen's virulence structure (Troch et al. 2012), and the evolution of pathogen morphological features (Takamatsu et al. 2016b). Additionally, sequencing herbarium specimens can greatly enhance the phylogeny and taxonomy of various fungal organisms. Herbaria collections contain large numbers of unstudied fungi (Osmundson et al. 2013) including holotype specimens (the specimen used to formally describe a species). Molecular information obtained from these specimens will help clarify numerous taxonomic and phylogenetic issues (Mutanen et al 2015).

Taxonomic and phylogenetic analyses of the powdery mildews are lacking in many areas throughout the world including Africa, Asia and North America (Braun et al. 2002). Sequencing herbarium specimens will allow these phylogenetic gaps in the literature to be filled quickly and efficiently. Most notably, intense, phylogenetic analyses are needed in North America where there is estimated to be over 150 species in the Pacific Northwest alone (Glawe 2004). Braun et al. (2002) described a number of new species based on North American herbarium collections; however, these were based only on morphological observations.

Sequences of herbarium specimens will improve phylogenetic and taxonomic clarity of the powdery mildews. However, higher resolution in genera and species level phylogenetic analyses are limited due to the difficulty in sequencing genomic regions besides the ITS and LSU genomic regions. The ITS and LSU ribosomal RNA gene cluster of the fungal genome contains multiple tandemly

repeated copies. The multiple copies allow the ITS to be sequenced with only a limited amount of genetic material. Because of the obligate nature of powdery mildew, there tends to be a limited amount of DNA available for sequencing. The limited amount of DNA available presents a challenge for sequencing other candidate genes that are not copied throughout the genome. Ellingham et al. (2019) evaluated 7 potential genes (actin, β-tubulin, calmodulin, Chs, EF1-α, Mcm7 and Tsr1) to support species level identification of the powdery mildews. The authors had difficulty obtaining consistent sequences from the majority of the regions. They noted the most success with *MCM7*, which they propose as an appropriate candidate gene, to be used alongside ITS, for differentiation between closely related, phylogenetically young powdery mildew species. In the current study, we had no success sequencing the regions tested in Ellingham et al. (2019) on herbarium specimens. Future research should look to use a similar nested primer approach for other candidate regions (such as those mentioned in Ellingham et al. 2019). Additionally, the ITS and LSU regions are not sufficient to resolve closely allied genera in Ascomycota. For example, there is no support that *Parauncinula*, which was previously placed in Erysiphaceae, based predominately on morphology, should be considered a genus of powdery mildew (Fig. 1.1). Additionally, the genus *Phyllactinia* is not monophyletic; for example, the genus *Leveillula* is nested within the *Phyllactinia* clade (Fig. 1.1). More research is necessary, with additional markers, to clarify higher-level phylogenetic relationships within the powdery mildews. Once protocols for sequencing additional regions is established, genus level clarification can be improved using similar methods to those currently used on other fungi. For example, genera level clarification was obtained in Tubakiaceae using the LSU, ITS, β-tubulin and *EF1-α* regions (Braun et al. 2018).

Although the powdery mildews are one of the world's most common plant pathogens, there are many gaps in their phylogeny and taxonomy. Future research should focus on sequencing herbarium

specimens from understudied regions (Africa, Asia and North America) and improving the

sequencing success of herbarium specimens using other regions besides the ITS and LSU rDNA.

Additionally, the protocol presented in this manuscript should be attempted on other fungal lineages

that are difficult to sequence such as the rusts (Pucciniales).

References

Abadi, S. Azouri, D., Mayrose, I., and Pupko, T. 2019. Model selection may not be a mandatory step for phylogeny reconstruction. Nature Communications, 10: 1-11.

Abasova, L., Aghayeva, D., and Takamatsu, S. 2018. Notes on powdery mildews of the genus *Erysiphe* from Azerbaijan. Current Research in Environmental and Applied Mycology, 8: 30-53.

Adhikari, M., Meeboon, J., Takamatsu, S., and Braun, U. 2018. *Leveillula buddlejae* sp. nov., a new species with an asexual morph resembling phylogenetically basal *Phyllactinia* species. Mycoscience. 59: 71-74.

Aylward, Janneke, Steenkamp, Emma T, Dreyer, Léanne L, Roets, Francois, Wingfield, Brenda D, and Wingfield, Michael J. 2017. A plant pathology perspective of fungal genome sequencing. IMA Fungus. 8: 1-15.

Bassoriello, M., and Jordan, K. 2012. First Report of *Magnaporthe poae*, Cause of Summer Patch Disease on Annual Bluegrass, in Canada. Plant Disease. 96: 1698.

Bieker, V., and Martin, M. 2018. Implications and future prospects for evolutionary analyses of DNA in historical herbarium collections. Botany Letters. 165: 409-418.

Bradshaw, M. 2018. First Report of Powdery Mildew Caused by *Erysiphe aquilegiae* var. *aquilegiae* on *Aquilegia vulgaris* in the United States. Plant Health Progress. 19:69-70

Bradshaw, M., Braun, U., Gotz, M., and Takamatsu S. 2017. Phylogeny and Taxonomy of the *Chrysanthemum* x *morifolium* Powdery Mildew. Mycologia.10: 508-519.

Bradshaw, M., Braun, U., Wang, S., Shuyan, L., Feng, J., Shin, H.D, Choi, Y.J., Takamatsu, S, Bulgakov, T., and Tobin, P.C. 2020. Phylogeny and taxonomy of powdery mildew on *Viburnum* species. Mycologia. Online. https://doi.org/10.1080/00275514.2020.1739508

Braun, U., and Cook, Roger T. A. 2012. *Taxonomic manual of the Erysiphales (powdery mildews)* (CBS biodiversity series ; no. 1). Utrecht, The Netherlands: CBS-KNAW Fungal Biodiversity Centre.

Braun, U., Nakashima, C., Crous, P.W., Groenewald, J.Z., Moreno-Rico, O., Rooney-Latham, S., Blomquist, C.L., Haas, J., and Marmolejo, J. 2018. Phylogeny and taxonomy of the genus Tubakia s. lat. Fungal Systematics and Evolution. 1: 41-99.

Braun, U., Bradshaw, M., Zhao, T., Cho, S., and Shin, H. 2018. Taxonomy of the *Golovinomyces cynoglossi* Complex (Erysiphales,Ascomycota) Disentangled by Phylogenetic Analyses and Reassessments of Morphological Traits. Mycobiology. 46: 192-204.

Brundrett, M. 2002. Coevolution of roots and mycorrhizas of land plants. New Phytologist. 154: 275-304.

Cabrera, M., Álvarez, R., and Takamatsu, S. 2018. Morphology and molecular phylogeny of
Brasiliomyces malachrae, a unique powdery mildew distributed in Central and South
America. Mycoscience. 59: 461-466.

Cho, S. E., Shin, H. D., Takamatsu, S. H., and Lee, S. 2018. *Cystotheca kusanoi* comb. nov.: A
redescription with new morphological observations. Mycotaxon. 133: 401-414.

Cooke, D., Drenth, A., Duncan, J., Wagels, G., and Brasier, C. 2000. A Molecular Phylogeny of
Phytophthora and Related Oomycetes. Fungal Genetics and Biology. 30: 17-32.

Cunnington, J., Takamatsu, H., Lawrie, S., and Pascoe, A. 2003. Molecular identification of
anamorphic powdery mildews (Erysiphales). Australasian Plant Pathology. 32: 421-428.

Divarangkoon, R., Meeboon, J., Monkhung, S., To-Anun, C., & Takamatsu, R. 2011. Two new
species of *Erysiphe* (Erysiphales, Ascomycota) from Thailand. Mycosphere. 2: 231-238.

Drummond, A., & Rambaut, A. 2007. BEAST: Bayesian evolutionary analysis by sampling trees.
BMC Evolutionary Biology. 7: 214.

Gernhard, T. 2008. The conditioned reconstructed process. Journal of Theoretical Biology. 253:
769-778.

Glawe, D. A. 2004. Taxonomic diversity of Erysiphales (powdery mildew fungi) in the Pacific
Northwest, Phytopathology. 94 (S152).

Farris, J., Källersjö, M., Kluge, A., and Bult, C. 1994. Testing Significance of Incongruence. Cladistics. 10: 315-319.

Felsenstein, J. 1985. Confidence Limits on Phylogenies : An Approach Using the Bootstrap. Evolution. 39: 783–791.

Hambleton, S., Egger, K., and Currah, R. 1998. The genus *Oidiodendron*: Species delimitation and phylogenetic relationships based on nuclear ribosomal DNA analysis. Mycologia. 90: 854-868.

Harrington, T., and Wingfield, B. 1995. A PCR-based identification method for species of *Armillaria*. Mycologia. 87: 280-288.

Heluta, V., Takamatsu, S., Harada, M., and Voytyuk, V. 2010. Molecular phylogeny and taxonomy of Eurasian *Neoerysiphe* species infecting Asteraceae and *Geranium*. Persoonia. 24: 81-92.

Hirata, T., and Takamatsu, S. 1996. Nucleotide sequence diversity of rDNA internal transcribed spacers extracted from conidia and cleistothecia of several powdery mildew fungi. Mycoscience, 37: 283-288.

Hirose, S., Tanda, S., Kiss, L., Grigaliunaite, B., Havrylenko, M., and Takamatsu, S. 2005. Molecular phylogeny and evolution of the maple powdery mildew (Sawadaea, Erysiphaceae) inferred from nuclear rDNA sequences. Mycological Research, 109: 912-922.

Inuma, T., Khodaparast, S., and Takamatsu, S. 2007. Multilocus phylogenetic analyses within *Blumeria graminis*, a powdery mildew fungus of cereals. Molecular Phylogenetics and Evolution. 44: 741-751.

Johnston, P., Quijada, L., Christopher A. Smith, C., Baral, H.-O., Hosoya, T., Baschien, C., Pärtel, K., Zhuang, W.-Y., Haelewaters, D., Park, D., Carl S., López-Giráldez, F., Zheng Wang, Z., and Townsend, J. 2019. A multigene phylogeny toward a new phylogenetic classification of Leotiomycetes. IMI Fungus. 10: 1-22.

Khodaparast, S., Takamatsu, S., and Hedjaroude, G. 2001. Phylogenetic structure of the genus *Leveillula* (Erysiphales: Erysiphaceae) inferred from the nucleotide sequences of the rDNA ITS region with special reference to the *L. taurica* species complex. Mycological Research. 105: 909-918.

Khodaparast, S., Takamatsu, A., Harada, S., Abbasi, M., and Samadi, M. 2012. Additional rDNA ITS sequences and its phylogenetic consequences for the genus *Leveillula* with emphasis on conidium morphology. Mycological Progress. 11: 741-752.

Kumar, S., Stecher, G., and Tamura, K. 2016. MEGA7: Molecular Evolutionary Genetics Analysis Version 7.0 for Bigger Datasets. Molecular Biology and Evolution. 33: 1870-1874.

Lang, P., Willems, F., Scheepens, J., Burbano, H., and Bossdorf, O. 2018. Using herbaria to study global environmental change. New Phytologist. 221: 110-122.

Liberato, J., Barreto, R., Niinomi, S., and Takamatsu, S. 2006. *Queirozia turbinata* (Phyllactinieae, Erysiphaceae): A powdery mildew with a dematiaceous anamorph. Mycological Research. 110: 567-574.

Marmolejo, J., Siahaan, S., Takamatsu, S., and Braun, U. 2018. Three new records of powdery mildews found in Mexico with one genus and one new species proposed. Mycoscience. 59: 1-7.

Meeboon, J., Takamatsu, S., and Hidayat, I. 2012. *Erysiphe javanica* sp. nov., a new tropical powdery mildew from Indonesia. Mycotaxon. 12: 189-194.

Meeboon, J., and Takamatsu, S. 2013a. Molecular phylogeny reveals the presence of cryptic speciation within *Erysiphe japonica* (≡Typhulochaeta japonica), a powdery mildew on *Quercus* spp. Mycoscience. 54: 69-74.

Meeboon, J., Takamatsu, S., and Hidayat, I. 2013b. *Pseudoidium javanicum*, a new species of powdery mildew on *Acalypha* spp. from Indonesia. Mycoscience. 54: 183-187.

Meeboon, J., Siahaan, S., Fujioka, K., and Takamatsu, S. 2017. Molecular phylogeny and taxonomy of *Parauncinula* (Erysiphales) and two new species *P. polyspora* and *P. uncinata*. Mycoscience. 58: 361-368.

Meeboon, J., and Takamatsu, S. 2017a. *Microidium phyllanthi-reticulati* sp. nov. on *Phyllanthus reticulatus*. Mycotaxon, 132: 289-297.

Meeboon, J., and Takamatsu, S. 2017b. First found of *Erysiphe elevata* on *Eucalyptus camaldulensis* and *Phyllactinia lagerstroemiae* sp. nov. on *Lagerstroemia* from Thailand. Mycoscience. 58: 253-260.

Matsuda, S., and Takamatsu. 2003. Evolution of host–parasite relationships of *Golovinomyces* (Ascomycete: Erysiphaceae) inferred from nuclear rDNA sequences. Molecular Phylogenetics and Evolution. 27: 314-327.

Moparthi, S., Bradshaw, M., and Grove, G. 2017a. First Report of Powdery Mildew Caused by *Golovinomyces spadiceus* on *Helianthus annuus* in the USA. Plant Disease. First Look Online. https://apsjournals.apsnet.org/doi/abs/10.1094/PDIS-09-17-1434-PDN

Moparthi, S., Frost, M., Hamm, K., Bradshaw, P., and Buck, J. 2018a. First report of powdery mildew caused by *Golovinomyces spadiceus* on okra in the United States. Plant Disease. 102: 1664.

Moparthi, S., Bradshaw, M., and Grove, G. 2018b. First Report of Powdery Mildew on *Verbascum Thapsus* caused by *Golovinomyces verbasci* in the USA. Plant Disease. First Look Online. https://apsjournals.apsnet.org/doi/abs/10.1094/PDIS-09-17-1453-PDN

Moparthi, S., Grove, G., Pandey, B., Bradshaw, M., Latham, S., Braun, U., Meeboon, J., and Romberg, M. 2019. Phylogeny and taxonomy of *Podosphaera cerasi*, sp. nov., and *Podosphaera prunicola* sensu lato. Mycologia. 111: 647-659.

Mori, Y., Sato, Y., and Takamatsu, S. 2000. Evolutionary analysis of the powdery mildew fungi using nucleotide sequences of the nuclear ribosomal DNA. Mycologia, 92: 74-93.

Mougou, A., Dutech, C., and Desprez-Loustau, M. 2008. New insights into the identity and origin of the causal agent of oak powdery mildew in Europe. Forest Pathology. 38: 275-287.

Pääbo, S. 1989. Ancient DNA: Extraction, Characterization, Molecular Cloning, and Enzymatic Amplification. Proceedings of the National Academy of Sciences of the United States of America. 86: 1939-1943.

Mutanen, M., Kekkonen, M., Prosser, S., Hebert, P., and Kaila, L. 2015. One species in eight: DNA barcodes from type specimens resolve a taxonomic quagmire. Molecular Ecology Resources. 15: 967-984.

Nilsson, R. H., Ryberg, M., Abarenkov, K., Sjökvist, E., and Kristiansson, E. 2009. The ITS region as a target for characterization of fungal communities using emerging sequencing technologies. FEMS Microbiol. Lett. 296: 97–101. doi: 10.1111/j.1574-6968.2009.01618.x

Osmundson, T.W., Robert, V.A., Schoch, C.L., Baker, L.J., Smith, A., Robich, G., Mizzan, L., and Garbelotto, M.M. 2013. Filling Gaps in Biodiversity Knowledge for Macrofungi: Contributions and Assessment of an Herbarium Collection DNA Barcode Sequencing Project. PLoS ONE. 8: e62419. https://doi.org/10.1371/journal.pone.0062419

Qiu, P., Liu, S., Bradshaw, M., Latham-Rooney, S., Takamatsu, S., Bulgakov, T., Tang, S., Feng, J., Temitope, T., Li, Y., Wang, L., and Braun, U. 2020. Multi-locus phylogeny and taxonomy of an unresolved, heteroenous species complex within the genus *Golovinomyces* (Ascomycota, Erysiphales),

including *G. ambrosiae, G. circumfusus* and *G. spadiceus*. BMC Microbiology 20:51. doi:10.1186/s12866-020-01731-9

Rogers, S., and Bendich, O. 1985. Extraction of DNA from milligram amounts of fresh, herbarium and mummified plant tissues. Plant Molecular Biology, 5: 69-76.

Rambaut A. 2009. Fig Tree ver. 1.3.1. Available at: http://tree.bio.ed.ac.uk/software/figtree.

Samarakoon, T., Wang, S., and Alford, M. 2013. Enhancing PCR amplification of DNA from recalcitrant plant specimens using a trehalose-based additive. Applications in Plant Sciences: 1

Sambucci, O. S., Alston, J. M. and Fuller, K. B. 2014. The Costs of Powdery Mildew Management in Grapes and the Value of Resistant Varieties: Evidence from California, California – Center for Wine Economics. Robert Mondavi Institute: Center for Wine Economics. Available at: http://vinecon.ucdavis.edu/2014/09/11/the-costs-of-powdery-mildew-management-in-grapes-and-the-value-of-resistant-varieties-evidence-from-california/.

Schoch, C. L., Seifert, K. A., Huhndorf, S., Robert, V., Spouge, J. L., Levesque, C. A., et al. 2012. Nuclear ribosomal internal transcribed spacer (ITS) region as a universal DNA barcode marker for Fungi. Proc. Natl. Acad. Sci. U.S.A. 109: 6241–6246. doi: 10.1073/pnas.1117018109

Scholin, C., Herzog, M., Sogin, M., and Anderson, D. 1994. Identification of group and strain specific genetic markers for globally distributed Alexandrium (Dinophyceae). II. Sequence analysis of a Fragment of the LSU rRNA gene 1. Journal of Phycology, 30: 999-1011.

Seko, Y., Bolay, A., Kiss, L., Heluta, V., Grigaliunaite, B., and Takamatsu, S. 2008. Molecular evidence in support of recent migration of a powdery mildew fungus on *Syringa* spp. into Europe from East Asia. Plant Pathology. 57: 243-250.

Silvestro, D., and Michalak, I. 2012. RaxmlGUI: A graphical front-end for RAxML. Organisms Diversity & Evolution. 12: 335-337.

Sugiyama, M., and Mikawa, T. 2001. Phylogenetic analysis of the non-pathogenic genus *Spiromastix* (Onygenaceae) and related onygenalean taxa based on large subunit ribosomal DNA sequences. Mycoscience. 42: 413-421.

Swofford D. 2002. PAUP*: phylogenetic analysis using parsimony (*and other methods). Sunderland, Massachusetts, Sinauer.

Takamatsu, S., and Kano, Y. 2001. PCR primers useful for nucleotide sequencing of rDNA of the powdery mildew fungi. Mycoscience. 4: 135-139.

Takamatsu, S. 2004. Phylogeny and evolution of the powdery mildew fungi (Erysiphales, Ascomycota) inferred from nuclear ribosomal DNA sequences. Mycoscience. 45: 147-157.

Takamatsu, S., Havrylenko, M., Wolcan, S., Matsuda, S., and Niinomi, S. 2008a. Molecular phylogeny and evolution of the genus Neoerysiphe (Erysiphaceae, Ascomycota). Mycological Research. 112: 639-649.

Takamatsu, S., Inagaki, M., Niinomi, S., Khodaparast, S., Shin, H., Grigaliunaite, B., and Havrylenko, M. 2008b. Comprehensive molecular phylogenetic analysis and evolution of the genus *Phyllactinia* (Ascomycota: Erysiphales) and its allied genera. Mycological Research, 112: 299-315.

Takamatsu, S., Niinomi, M., Harada, S., and Havrylenko, M. 2010. Molecular phylogenetic analyses reveal a close evolutionary relationship between *Podosphaera* (Erysiphales: Erysiphaceae) and its rosaceous hosts. Persoonia. 24: 38-48.

Takamatsu, S. 2013a. Origin and evolution of the powdery mildews (Ascomycota, Erysiphales). Mycoscience. 54: 75-86.

Takamatsu, S. 2013b. Molecular phylogeny reveals phenotypic evolution of powdery mildews (Erysiphales, Ascomycota). Journal of General Plant Pathology 79: 218–226, http://dx.doi.org/10.1007/s10327-013-0447-5.

Takamatsu, S., Ito, H., Shiroya, Y., Kiss, L., and Heluta, V. 2015. First comprehensive phylogenetic analysis of the genus *Erysiphe* (Erysiphales, Erysiphaceae) I. The Microsphaera lineage. Mycologia. 107: 475-489.

Takamatsu, S., Siahaan, S., Moreno-Rico, O., Cabrera de Álvarez, M., and Braun, U. 2016a. Early evolution of endoparasitic group in powdery mildews: Molecular phylogeny suggests missing link between *Phyllactinia* and *Leveillula*. Mycologia. 108: 837-850.

Takamatsu, S., Shiroya, Y., and Seko, Y. 2016b. Geographical and spatial distributions of two *Erysiphe* species occurring on lilacs (Syringa spp.). Mycoscience. 57: 349-355.

Taylor D.L., and Bruns T.D. 1999. Community structure of ectomycorrhizal fungi in a Pinus muricata forest: minimal overlap between the mature forest and resistant propagule communities. Mol Ecol 8: 1837–1850

To-anun, C., Kom-un, S., Sunawan, A., Fangfuk, W., Sato, Y., and Takamatsu, S. 2005. A new subgenus, Microidium , of *Oidium* (Erysiphaceae) on *Phyllanthus* spp. Mycoscience. 46: 1-8.

Troch, V., Audenaert, K., Bekaert, B., Höfte, M., and Haesaert, G. 2012. Phylogeography and virulence structure of the powdery mildew population on its 'new' host triticale. BMC Evolutionary Biology. 12:76.

Walsh, P., Metzger, D., and Higuchi, R. 1991. Chelex 100 as a medium for simple extraction of DNA for PCR-based typing from forensic material. BioTechniques. 10: 506-13.

White T.J., Bruns, T., Lee, S., Taylor, J. 1990. Amplification and direct sequencing of fungal ribosomal RNA genes for phylogenetics. In: Innis, MA, Gelfand DH, Sninsky JJ, White TJ, Eds., PCR Protocols: A Guide to Methods and Applications. Academic Press San Diego. 315–332.

Chapter 2: Phylogeny and taxonomy of powdery mildew on *Viburnum* species

Abstract

The phylogeny and taxonomy of powdery mildew on *Viburnum* species is evaluated and discussed. Morphological and phylogenetic analyses revealed two new species and demonstrated that *Erysiphe hedwigii* and *E. viburni* should be reduced to synonymy and are referred to herein as *E. viburni*. The two new species, *E. viburniphila* and *E. pseudoviburni*, previously hidden under *E. viburni* (incl. *E. hedwigii*), are described on the basis of European, North American, and East Asian powdery mildew collections on *Viburnum edule*, *V. tinus, V. odoratissimum* var. *awabuki* and *V. sieboldii*. The sexual morph of *E. viburniphila* is similar to *E. viburni*, however, morphological differences exist in their asexual morphs. Analyses of sequences from the ITS and LSU genomic region of *Erysiphe* species obtained on *Viburnum* species (and other closely allied *Eryisphe* species) throughout the world reveled that *E. viburniphila* and *E. pseudoviburni* are in two different monophyletic groups that are separate from all other *Erysiphe* species. *Erysiphe hedwigii* and *E. viburni* on *Viburnum* species have often been recognized as separate species based on morphological differences in the size of their chasmothecia and number of chasmothecial appendages. Taxonomic conclusions based on these morphological distinctions within these species are unreliable (these characters are rather variable, and often have overlapping ranges). The present phylogenetic analyses suggest that *E. hedwigii* has to be reduced to synonymy with *E. viburni*. To fix the application of the species names *E. hedwigii* and *E. viburni*, epitypes have been designated for these taxa with ex-epitype sequences. Additionally, the Asian

species *E. miranda* is phylogenetically confirmed as species of its own, described in detail and

discussed.

Introduction

Powdery mildew is a widely distributed, detrimental disease of grasses, vegetables, fruits and ornamental plants. Powdery mildews are ascomycetes that are obligate parasites (Braun and Cooke 2012), and have been reported to infect up to 10,000 plant species worldwide (Amano 1986). Powdery mildew decreases the aesthetics and ornamental value of infected plants by decreasing their growth, their flower and fruit quantity, and their leaf aesthetics, which in turn, can greatly decrease their salability (Westcott and Horst 1990). Numerous species within *Viburnum* (Adoxaceae, previously Caprifoliaceae s. lat.) are cultivated throughout the world for the ornamental value of their flowers and foliage. The genus comprises between 150 and 200 species (depending on the particular species concepts), of mostly evergreen and deciduous shrubs. The native range of *Viburnum* spp. includes the temperate northern hemisphere, with a few species in the subtropical montane regions of Africa, Asia and South America (Winkworth and Donoghue 2005, Wu et al. 2011).

Viburnum species are common hosts for powdery mildews within *Erysiphe*. Braun and Cook (2012) recognized five *Erysiphe* spp. infecting plants within *Viburnum*, including *E. viburnicola* U. Braun & S. Takam. (*Erysiphe* sect. Uncinula), *E. hedwigii* (Lév.) U. Braun & S. Takam., *E. miranda* (V.P. Heluta) U. Braun & S. Takam., *E. shinanoensis* (Tanda) U. Braun & S. Takam., and *E. viburni* Duby (Erysiphe sect. Microsphaera). Meeboon and Takamatsu (2015) described an additional *Erysiphe* species on *Viburnum* called E. *viburni-plicati* Meeboon & S. Takam. *Erysiphe viburni-plicati* is an unusual species characterized by having chasmothecia with dichotomously branched appendages and a single ascus. The purpose of the present study was to evaluate the taxonomy and phylogeny of the powdery mildews on *Viburnum* species with a focus on the *E. viburni* complex.

The *E. viburni* complex has a taxonomic history dating back to Salmon (1900). Salmon (1900) assigned *E. viburni* to *Microsphaera alni* (DC.) G. Winter (sensu latissimo), which, at the time, comprised a large portion of species within *Erysiphe* sect. Microsphaera in its current sense. Later, Blumer (1933) recognized two species, *Microsphaera hedwigii* Lév. and M. viburni (Duby) S. Blumer (nom. illeg., non M. viburni Howe). Braun (1995) followed the taxonomy of Blumer (1933), but corrected the nomenclature and reintroduced the name *M. sparsa*, which is the oldest available name for this fungus in *Microsphaera*. Based on the new phylogenetic genus concept of the Erysiphaceae, introduced in Braun and Takamatsu (2000), Braun and Cook (2012) assigned *M. sparsa* to *Erysiphe* and replaced the species name with E. *viburni* (the oldest valid name for this species in *Erysiphe*). Currently, there are several unresolved issues around the taxonomy of the *E. viburni* complex requiring a phylogenetic approach: 1) Are *E. hedwigii* and *E. viburni* two different species? 2) Are there genetic and taxonomic differences among collections of these species from Asia, Europe and North America, or is it a single species? To answer these questions, powdery mildews with a Pseudoidium-type asexual structure were collected throughout the world on multiple *Viburnum* species. Phylogenetic analyses of European and North American collections of the specimens were conducted to reassess this species complex and to address their phylogeny and taxonomy. Furthermore, morphological re-examinations of *E. hedwigii* and *E. viburni* were conducted. Analyses were supplemented by epitypifications with ex-epitype sequences for the genetic characterization of these species.

Materials and Methods

Sample collection.

Powdery mildews were collected at the University of Washington, which includes the Center for Urban Horticulture and the Washington State Arboretum, on *V. edule*, *V. opulus* and *V. tinus* in June and October of 2018 and June of 2019. The anamorph and teleomorph (if developed) were morphologically and genetically examined. Powdery mildew was also collected in the fall of 2018 in China on *V. sargentii* (= *V. opulus* subsp. *calvescens*) and in July of 2019 in Korea on *V. sargentii*. Herbarium specimens of powdery mildew were obtained for this study on *V. carlesii*, *V. lantana*, and *V. opulus* from Germany, on *V. tinus* from Russia and Switzerland and on *V. sargentii* from China and Korea, *V. odoratissimum* var. *awabuki* from Korea, and *V. sieboldii* from Japan. A list of all of the specimens used in this study is presented in Table 2.1.

Morphological examinations.

Morphological examinations of the asexual morph of recently collected samples were accomplished by placing clear adhesive tape on powdery mildew colonies and setting the tape onto a slide containing a drop of distilled water. If the specimens had dried, examinations were done following the lactic acid protocol (Shin 1988). Examinations of the sexual morph were accomplished by using a clean needle to mount chasmothecia onto a microscope slide containing a 3% NaOH solution. Pictures were taken of the slides using a compound microscope with an Olympus SC50 camera attached. At least 20 measurements of conidia and other structures were acquired, from which the mean, and upper and lower bounds of the range, were estimated. For the Scanning Electron

Microscope (SEM), chasmothecia were vaporized with gold and examined by a 'TM3030 Plus Tabletop Microscope' (Hitachi).

DNA analyses.

DNA analyses were conducted in China, Korea and the USA. Whole-cell DNA of the specimens from China and Korea were extracted from mycelium and chasmothecia or mycelium and conidia using the Chelax-100 method (Walsh et al. 1991 and Hirata and Takamatsu 1996). The partial sequence of the large subunit (LSU) rDNA including the D1 and D2 regions were amplified by polymerase chain reaction (PCR) with the primer sets LSU1 (5'-ACCCGCTGAACTTAAGCATA-3') and LSU2 (5'-CCTTGGTCCGTGTTTCAAGA-3') (Scholin et al. 1994) or TW14 (5'–GCTATCCTGAGGGAAACTTC–3') (Mori et al., 2000) and PM3 (5'–GKGCTYTMCGCGTAGT–3') (Takamatsu and Kano 2001). The complete internal transcribed spacer (ITS) rDNA regions including 5.8S were amplified with the primers ITS5 (5'-GGAAGTAAAAGTCGTAACAAGG-3') and ITS4 (5'-TCCTCCGCTTATTGATATGC-3') (White et al. 1990). The amplified DNA products were purified using Mag-MK PCR Products Purification Kit or an AccuPrep PCR Purification Kit (Bioneer, Daejeon, Korea), following the manufacturers' protocols. Nucleotide sequences of the samples were sequenced with the same primers by direct sequencing in a 3730xl DNA Analyzer (Applied Biosystems) by Sangon Biotech (Shanghai, China) and Macrogen (Seoul, Korea). The sequence reactions were conducted using the BigDye™ Terminator v3.1 Cycle Sequencing Kit (Applied Biosystems) per the manufacturer's protocol.

DNA analyses on the remaining specimens was accomplished at the University of Washington, USA. PCR was conducted by placing mycelium and chasmothecia or mycelium and conidia from the

cultures directly into the PCR mix (Harrington and Wingfield 1995). If direct PCR was unsuccessful, whole-cell DNA was extracted from mycelium and chasmothecia or mycelium and conidia with the Dneasy plant mini kit (Qiagen, Hilden, Germany), following the manufacturers protocol. The nucleotide sequences of the LSU rDNA and the ITS region were amplified by PCR with the primer pairs TW14 (Mori et al., 2000) and PM3 (Takamatsu and Kano 2001) for the LSU rDNA and PM1 (5´-TCGGACTGGCCYAGGGAGA-3') and PM2 (5´-TCACTCGCCGTTACTGAGGT-3') (Cunnington et al. 2003) for the ITS region. If PCR failed, a second amplification was accomplished using 2 µL from the first reaction and the primer pairs LSU1 and LSU2 for the LSU rDNA and ITS5 (White et al. 1990) and PM6 (5'–GYCRCYCTGTCGCGAG–3') (Takamatsu and Kano 2001) and ITS4 and PM7 (5'–RYYGACCCTCCCACCCGTGY–3') (Seko et al. 2008) for the ITS region. If PCR failed a second time, PCR was attempted with the primer pairs PM6 and T4 (5'– TCAACAACGGATCTCTTGGC–3') (Hirata and Takamatsu 1996) and PM7 and T3 (5'– ACGCTCGAACAGGCATGCCC–3') (Hirata and Takamatsu 1996). DNA was purified by isopropanol precipitation. Purified amplicons were sent to Eurofins (Luxembourg) to be directly sequenced in both the forward and reverse direction using the primer pairs above.

Phylogenetic analyses.

Sequences were manually trimmed using Geneious version 11.0.2 (https://www.geneious.com) and deposited into Genbank. Sequences were combined with other sequences from Genbank (Table 2.1) and aligned and manually edited using MUSCLE in MEGA7: Molecular Evolutionary Genetics Analysis Version 7.0 (Tamura et al., 2013). Alignments were deposited in TreeBASE (http://www.treebase.org/) under the accession number 25537. A partition homogeneity test (Farris et al. 1995) was conducted in PAUP 4.0a151 (Swofford, 2002) to determine whether the ITS and

LSU datasets were congruent with each other. After the datasets were determined to be congruent,

models of evolution for the combined dataset was found to be GTR+G+I by jModelTest 2

(Darriba et al. 2012). A MCC (maximum clade credibility) phylogenetic tree was constructed for the

combined ITS and LSU rDNA, using a yule process speciation model (Gernhard 2008), by Bayesian

analyses, in the program BEAST version 1.10.2 (Drummond and Rambaut 2007). The resulting tree

was visualized using FigTree ver. 1.3.1 (Rambaut 2009). A maximum likelihood analysis was

accomplished using raxmlGUI (Silvestro & Michalak, 2012) under the default settings with a

GTR+G+I evolutionary model. Parsimony analysis was done using PAUP 4.0a151 (Swofford 2002).

For the parsimony analysis, gaps were treated as missing data and sites were treated as unordered

and unweighted. Bootstrap analyses were conducted using 1000 replications with the stepwise

addition option set as simple (Felsenstein, 1985). Bootstrap supports below 70% were dropped for

both analyses.

Results

Morphological and molecular analyses conducted on these specimens revealed that *E. hedwigii* and *E. viburni* are in fact one fungal species. In addition, phylogenetic analyses of North American powdery mildew collections of *Erysiphe* on *V. edule* and *V. tinus* and East Asian powdery mildew collections on *V. odoratissimum* var. *awabuki* and *V. sieboldii* revealed two undescribed species within the *E. viburni* complex described herein as *Erysiphe viburniphila* sp. nov. and *Erysiphe pseudoviburni* sp. nov.

Phylogenetic analyses.

Amplicons for all of the specimens obtained were deposited in Genbank (Table 2.1). Sequences from the ITS and LSU rDNA regions were combined for phylogenetic analyses. The phylogenetic analyses contained 53 sequences from powdery mildew specimens throughout the world including the outgroup taxon *E. glycines* which was selected based on Takamatsu et al. (1999) and Mori et al. (2000).

The result of the partition homogeneity test showed no direct conflict between the ITS and LSU rDNA regions (*P*-value=0.88). A maximum clade credibility tree was constructed using Bayesian analyses from the combined ITS and LSU sequences. Posterior probabilities $\geq$ 90 are displayed followed by bootstrap values greater than 70% for the maximum likelihood (ML) and maximum parsimony (MP) analyses conducted (Fig. 2.1). All tree topologies were similar and only the representative maximum clade credibility tree is illustrated in Figure 1.1. The phylogenetic analyses revealed that 1) *Erysiphe miranda* specimens from Korea and China are nested within the same clade with high support values, 2) *Erysiphe hedwigi* and *E. viburni* specimens are nested within the same

40

clade with high support values and 3) two undescribed species formed monophyletic groups

separate to all other powdery mildew species with high support values (Fig. 2.1).

Taxonomy

Erysiphe viburniphila M. Bradshaw., sp. nov.   Figs. 2.2–2.3

MycoBank: MB 832452

Illustrations: Figs 2.4–2.5.

Typification: On *Viburnum tinus*, *Adoxaceae* [= *Viburnaceae*, *Caprifoliaceae* s. lat.]; United States, Washington State, University of Washington main campus (Coordinates: 47.65103234 °N, 122.31286579 °W), Seattle, WA, June 26th, 2019, M. Bradshaw (**holotype** WTU-F-71046). Genbank number of the ITS-LSU sequence of the holotype: MN431631.

Etymology: Named after the type genus (*Viburnum*) + -phila (from Ancient Greek *φίλος* (phílos, loving).

Mycelium amphigenous, forming small to large white to grayish white patches, often confluent and persistent on the upper leaf surface, but usually sparse and evanescent below; hyphae septate, hyaline, 3–6 μm wide; hyphal appressoria 2–5 μm diam., solitary, slightly lobed but can occasionally be nipple-shaped; conidiophores arising from upper surface of the mother cell, with a basal septum at the base of the mother cell, erect, (86–)125(–161.5 μm long, foot-cells straight, cylindrical, (38–)78.5(–124.5) μm × (5–)7(–8.5) μm, followed by 1 to 3 shorter cells, (11–)24(–43.5) μm × (6.5–)8(–10) μm, forming conidia singly; conidia ellipsoid-doliiform, (24.5–)33(–44) μm × (11–)14(–18) μm with a length to width ratio of (1.8–)2.4(–3.3); germ tubes tend to form terminally and are (0.3–)1.6(–3.3) times as long as the conidial width with a simple or lobed terminal appressorium. Chasmothecia (description based on HAL 355 F, European material from Switzerland)

amphigenous, scattered to subgregarious, subglobose to depressed globose, 80–100 μm diam.; peridium cells rounded in outline to angular-irregular, 8–25 μm diam., walls thick; with 3 to 6 more or less equatorial appendages, radiating, straight to mostly somewhat curved, (0.5–)0.75–1.2 times as long as the chasmothecial diam., mostly about as long as the diam. [(50–)60–100 μm in length], 7–9 μm wide below, gradually narrowing towards the tip, 5–6(–7) μm wide just below the branched apical portion, aseptate or with a single septum at the very base, hyaline throughout or brown at the base, usually below the basal septum, wall almost smooth to irregularly verruculose-rugose and thickened, 3–4 μm wide below and 1–3 μm wide above, apex regularly dichotomously branched, 3–4(–5) times, branched portion 20–50 μm diam., branches of all orders short or primary branches somewhat elongated, 10–15 μm, tips of the ultimate branchlets distinctly recurved when mature; asci 2–4, subglobose to broad ellipsoid-ovoid, sessile or subsessile, 40–60 × 30–50 μm, wall to 2.5 μm wide, terminal oculus inconspicuous, (10–)15(–20) μm diam., 5–7-spored; ascospores broad ellipsoid-ovoid, 18–24 × 10–15 μm, colorless.

Host range and distribution: Over 15 specimens of *Viburnum* species were examined for powdery mildew throughout the world. *E. viburniphila* was collected on *V. tinus* from Washington State and Switzerland and *V. edule* from Washington State. Considering that *E. viburniphila* was located in both Switzerland and Washington State, it is likely that the range of this powdery mildew species includes the entire United States and Europe. Future research can evaluate the host range and worldwide distribution of *E. viburniphila.*

Additional specimens examined: USA, Washington State, King County, University of Washington (Coordinates: 47.64913570 °N, 122.31105890 °W) on *V. tinus*, June 14th, 2018, M. Bradshaw (WTU-F-71044), Genbank number of the ITS-LSU sequence: MN431629; Washington State, King County,

University of Washington (Coordinates: 47.65201435 °N, 122.30807593 °W), on *V. tinus*, June 26th, 2019, M. Bradshaw (WTU-F-71045), Genbank number of the ITS-LSU sequence: MN431630; Washington State, King County, University of Washington (Coordinates: 47.65610462 °N, 122.30749084 °W) on *V. edule*, Oct. 20th 2018, M. Bradshaw (WTU-F-71047), Genbank number of the ITS-LSU sequence: MN431632. Switzerland, Vaud, Morges, Rte. de Lausanne 8, on *V. tinus*, Mar. 17th, 1999, A. Bolay (HAL 355 F). Switzerland, Genève, Jardin botanique, Oct. 16th, 1995, A. Bolay (G00566225); ibid., Nov. 15th, 1995, A. Bolay (G00566226); ibid., Nov. 15th 1996, A. Bolay (G00566224); ibid., Aug. 4th, 1997, A. Bolay (G00566227); ibid., Oct. 21st, 1998, A. Bolay (G00566228); ibid., Oct. 28th, 2002, A. Bolay (G00566229); Vaud, Morges, Rte. de Lausanne 8, on *V. tinus*, Mar. 17th, 1999, A. Bolay (HAL 355 F).

Notes: Erysiphe viburniphila is morphologically and phylogenetically distinct from all other *Erysiphe* species. *Erysiphe viburniphila* forms a separate clade that is clearly distinct from other *Viburnum* powdery mildew species (Fig. 2.1). Chasmothecia were noticed in October of 2018 on *V. tinus* and *V. edule* in Washington State. The majority of the chasmothecia on these specimens were very immature. A couple were mature enough to identify as *Phyllactinia* sp. There was an insufficient amount of material to sequence the *Phyllactinia* species. A *Phyllactinia* species as well as a *E. viburniphila* specimen was observed on the host *V. tinus* from Switzerland (HAL 355 F), including abundant chasmothecia (the chasmothecia formed on *V. tinus* largely agree with the sexual morph of *E. viburni* collections previously assigned to *E. hedwigii*). The LSU region of the *Phyllactinia* sp. on *V. tinus* from Switzerland (HAL000355) was sequenced (Genbank number: MN431633) and aligned 99% with multiple *Phyllactinia* species including *Phyllactinia guttata* (Genbank number: AB080461), *Phyllactinia moricola* (Genbank number: LC371326) and *Phyllactinia philadelphi* (Genbank number: AB080431).

Erysiphe pseudoviburni Y.J. Choi, H.D. Shin, & S. Takamatsu sp. nov.   Figs 2.6-2.7.

= *M. hedwigii* auct. p.p.

= *M. viburni* auct. p.p.

MycoBank: MB 832453

Typification: On *Viburnum odoratissimum* var. *awabuki* (≡ *Viburnum awabuki*), *Adoxaceae* [= *Viburnaceae*, *Caprifoliaceae* s. lat.]; Korea, Jeju, Halla Arboretum (Coordinates: 33°28′07.1″ N; 126°29′28.9″ E), 13 June 2013, H.D. Shin (**holotype** KUS-F27310). Genbank number of the ITS-LSU sequence of the holotype: MN431595.

Etymology: Composed of the prefix pseudo- (false) and viburni, the epithet of *Erysiphe viburni,* referring to the close genetic affinity between the two species.

Mycelium, amphigenous, evanescent or almost persistent on the upper surface of the leaves, effuse or in patches; hyphal cells about 30–75 × 4–7 μm; hyphal appressoria lobed to multilobed, in opposite pairs or solitary, 4–8(–10) μm diam.; conidiophores arising ± centrally from upper surface of the mother cell, erect, 70–110(–130) μm long, foot-cells straight, subcylindrical, 22–40 × 7–9(–10) μm, followed by 1–3 shorter cells, forming conidia singly; conidia ellipsoid-ovoid, cylindrical, 30–45 × 15–20 μm, germ tubes on an end, short to moderately long, conidial appressoria usually multilobed. Chasmothecia (description based on MUMH 4071, East Asian material from Japan) amphigenous, scattered, subglobose, 94–120(–131) μm diam.; peridium cells irregularly polygonal, ca 15–25 μm diam., walls thick; with (5–)7–12 more or less equatorial appendages, radiating, straight to mostly somewhat curved, 78–101 μm long (≤1.0 times as long as the chasmothecial diam.), 7.5–9 μm wide below, gradually narrowing towards the tip, 6–7 μm wide just below the branched apical

portion, aseptate or with a single septum at the very base, hyaline throughout or brown at the base, usually below the basal septum, wall thin to somewhat thickened throughout, smooth to rough, apex regularly dichotomously branched 4–5 times, branched portion 48–74 × 35–53 μm in size, branches of all orders short, primary branch 5–13 μm long, tips of the ultimate branchlets recurved when mature; asci (2–)3–4, subglobose to broad ellipsoid-ovoid, sessile or subsessile, 44–57(–67) × 38–51 μm, wall 2–3 μm wide, terminal oculus inconspicuous, ca 13–16 μm diam., 4–6(–7)-spored; ascospores broad ellipsoid-ovoid, 23–33 × 12–17 μm, colorless.

Host range and distribution: on *Viburnum* (*odoratissimum, sieboldii*); Asia (Japan, Korea).

Additional specimens examined: Korea, Jeju, Halla Arboretum, on *Viburnum odoratissimum* var. *awabuki*, Jun. 13th, 2013, H.D. Shin (KUS-F27319); ditto, Oct. 1st, 2013, H.D. Shin (KUS-F27665); ditto, Apr. 3rd, 2018, H.D. Shin (KUS-F30420); Japan, Mie Prefecture, Mt. Fujiwara, on *Viburnum sieboldii*, Sep. 23th, 1994, S. Takamatsu (TNS-F-87187, formerly MUMH 1), Genbank number of the ITS-LSU sequence: LC009904; Japan, Niigata Prefecture, Mt. Yahiko, on *Viburnum sieboldii* var. *obovatifolium*,Oct. 18th, 1996, S. Takamatsu (MUMH 263); Japan, Mie Prefecture, Mt. Kirara-mine, on *Viburnum sieboldii*, Nov. 5th, 2005, S. Takamatsu (MUMH 4071).

Notes: Erysiphe pseudoviburni is morphologically and phylogenetically distinct from all other *Erysiphe* species. *Erysiphe pseudoviburni* forms a monophyletic clade that is a sister group to *E. viburni* (Fig. 2.1). Morphologically, differences between *E. viburni* and *E. pseudoviburni,* have been noted in the size of their foot-cells (*E. viburni* foot-cells can be up to 80 μm whereas *E. pseudoviburni* foot-cells range from 22–40 μm), and in the length of their appendages [*E. viburni* appendages are (0.5–)1–1.5(–2) times as long as the chasmothecial diam. whereas *E. pseudoviburni* appendage length is ≤1 times as

long as the chasmothecial diam.]. *E. pseudoviburni* is a sister species of *E. viburni*, most likely originating from Asia.

Erysiphe viburni Duby, Bot. gall. **2**: 872, 1830 Figs 2.8–2.10

≡ *Microsphaera viburni* (Duby) G. Winter, in Kunze, Fungi Sel. Exs. 576, 1880, nom. illeg., non *M. viburni* Howe, 1874.

≡ *M. viburni* (Duby) S. Blumer, Beitr. Krypt.-Fl. Schweiz **7**(1): 310, 1933, nom. illeg., non *M. viburni* Howe, 1874.

= *Erysiphe penicillata* f. *viburni-opuli* Fr., Syst. mycol. **3**: 244, 1829.

= *Erysiphe penicillata* g. *viburni-lantanae* Fr., Syst. mycol. **3**: 244, 1829.

≡ *M. viburni-opuli* (Fr.) Cif. & Sousa da Câmara, Quad. Lab. Crittog. Ist. Bot. Univ. Pavia **21**: 21, 1962.

= (?) *Erysiphe viburni* Schwein., Trans. Amer. Philos. Soc. **4**: 269, 1834, nom. illeg., non *E. viburni* Duby 1830, type host – *Viburnum* sp. (type not preserved).

≡ *Microsphaera viburni* Howe, Bull. Torrey Bot. Club **5**: 43, 1874, nom. nov. (as "(Schwein.) Howe", based on *E. viburni* Schwein.).

=*Microsphaera hedwigii* Lév., Ann. Sci. Nat., Bot., Sér. 3, **15**: 155 & 381, 1851 [lectotype (designated by Braun 1987): on *Viburnum lantana*, France, Mendon, ex herb. Léveillé, in herb. Berkeley (K(M) 116634); **epitype** (designated here, MycoBank, MBT388578): Germany, Saxony, Dippoldiswalde, Karsdorf, forest school, on *V. lantana*, Sep. 21st, 2006, F. Klencke (GLM-103736); Genbank number of the ITS-LSU sequence of the epitype: MN431618].

≡ *Erysiphe hedwigii* (Lév.) U. Braun & S. Takam., Schlechtendalia **4**: 9, 2000.

= (?) *Microsphaera sparsa* Howe, in Cooke & Peck, J. Bot., N.S., **1**: 171, 1872 [holotype: USA, New York, New Baltimore, 1870, on *Viburnum lentago*, E.C. Howe (NYS)].

= *Caloclada penicillata* f. *lantanae* Pass., in Rabenh., Fungi Eur. Exs. 2031, 1876.

= *Microsphaera penicillata* f. *viburni-lantanae* Sacc., Mycoth. Ven. 61, 1876.

= *Caloclada penicillata* f. *viburni-opuli* Rostr., in Thüm., Mycoth. Univ. 958, 1881.

= *M. viburni* f. *viburni-lentaginis* Thüm., Mycoth. Univ. 2055, 1881.

= *Microsphaera penicillata* f. *viburni* Jacz. (Jaczewski 1927: 351).

= *M. alni* auct. p.p.

= *Microsphaera penicillata* auct. p.p.

= *M. hedwigii* auct. p.p.

Illustrations: Léveillé (1851: Pl. 8, Fig. 19), Magnus (1898: Pl. II, Figs 5–6, 11), Jaczewski (1927: 351–252, Figs 98–99), Blumer (1933: 310, Fig. 118, 312, Figs 119–120; 1967: 203, Fig. 93, 206, Fig. 96), Tanda et al. (1973: 137, Pl. IX; 1977: 29, Pl. VI), Tanda & Nomura (1978: 31, Pl. VII), Zhao (1979: 91, Fig. 50), Braun (1981: 509, Figs 6–8; 1982: 152, Fig. 10; 1984: 226, Pl. 1, Fig. 6; 1987: 417, Pl. 184, Figs A–C; 1995: 285, Pl. 70, Fig. A–B), Chen et al. (1987: 194, Fig. 99), Salata (1985: 172, Fig. 69, Pl. XXXIII), Heluta (1989: 92, Fig. 18), Eliade (1990: 445, Pl. 12, Fig. 54–55), Fakirova (1991: 79, Pl. 26, Fig. 1), Nomura (1992: 260–261, Figs 170–171; 1997: 140, Figs 171–172), Chen & Yao (1993: 109, Pl. 13, Fig. 36 a–b), Simonyan (1994: 156, Fig. 31), Paulech (1995: 204–205, Fig. 94–95), Grigaliūnaitė (1997: 128, Fig. 77), Braun and Cook (2012: 519, Fig. 652 A–B).

Exs.: Allescher & Schnabl, Fungi Bav. 529. Baglietto, Cesati & Notaris, Erb. Critt. Ital., Ser. II, 1166. Barthol., Fungi Columb. 3337. Brenckle, Fungi Dakot. 280. Desm., Pl. Crypt. Fr. 922 A,B. Ellis, N. Amer. Fungi 432. Fuckel, Fungi Rhen. Exs. 659, 691. Kari, Fungi Exs. Fenn. 56. Kellerm., Ohio Fungi 48. Kochm., Mycoth. Polon. 135. Krypt. Exs. 128c,d. Kunze, Fungi Sel. Exs. 176, 237, 576. Linh., Fungi Hung. Exs. 257. Poelt, Pl. Graec. Fungi 445, 717. Rabenh., Fungi Eur. Exs. 2031. Racib., Mycoth. Polon. 161 II. Rehm, Ascomyc. 299. Sacc., Mycoth. Ven. 618, 619. Syd., Mycoth. Germ. 163, 1897, 2326. Thüm., Fungi Austr. Exs. 139. Thüm., Mycoth. Univ. 155, 958, 2055.

Triebel, Microf. Exs. 33. Wartm. & Schenk, Schweiz. Krypt. 424. Weese, Eumyc. Sel. Exs. 161.
Westend., Herb. Crypt. Belg. 112. Wilson & Seaver, Ascomyc. Lower Fungi 85. Winter, Fungi Helv.
Exs. 576.

Typification: On *Viburnum opulus*, *Adoxaceae* [= *Viburnaceae*, *Caprifoliaceae* s. lat.]; France, herb Duby,
No. 153 (**holotype** STR). **Epitype** (designated here, MycoBank, MBT388579): Germany,
Brandenburg, Landkreis Ostprignitz-Ruppin, Rheinsberg, on *Viburnum opulus*, Sep. 29th, 2006, H.
Boyle & S. Hoeflich (GLM-F74776). Genbank number of the ITS-LSU sequence of the epitype:
MN431619.

Mycelium, amphigenous, evanescent or almost persistent on the upper surface of the leaves, effuse
or in patches; hyphal cells about 40–75 × (3.5–)4–6(–10) μm; hyphal appressoria lobed to
multilobed, in opposite pairs or solitary, 3–12 μm diam.; conidiophores arising ± centrally from
upper surface of the mother cell, erect, 55–120(–130) μm long, foot-cells straight, subcylindrical to
slightly curved-sinuous at the base, 20–85 × 5–10(–12) μm long, followed by 1–3 shorter cells,
forming conidia singly; conidia ellipsoid-ovoid, cylindrical, 25–40(–47.5) × 11–23 μm, germ tubes on
an end, short to moderately long, conidial appressoria usually multilobed. Chasmothecia scattered to
almost gregarious, depressed globose, (60–)75–130 μm diam.; peridium cells not very conspicuous,
polygonal, about 8–30 μm diam.; appendages 3–22, equatorial, stiff, mostly curved, (0.5–)1–1.5(–2)
times as long as the chasmothecial diam., about 5–10 μm wide, aseptate or with 1–2 septa at the
base, hyaline but pigmented at the base, walls smooth to rough, moderately thick throughout or thin
above and thick towards the base, apices (3–)4–5(–6) times regularly and densely dichotomously
branched, compact or often somewhat looser with primary branches characteristically elongated,
horizontally spread, tips distinctly recurved; asci about 2–8, broad ellipsoid-obovoid, saccate, 40–75

× 30–60 μm, sessile or short-stalked, 4–8-spored; ascospores ellipsoid-ovoid to subglobose, (15–)18–26(–30) × 10–18 μm, colorless.

Host range and distribution: (1) Phylogenetically known hosts – on *Viburnum* (*carlesii*, *edule*, *lantana*, *opulus*, *tinus*); (2) Phylogenetically unknown hosts – on *Viburnum* (*acerifolium*, *affine*, *alnifolium*, *burejaeticum*, *cassinoides*, *cotinifolium*, *dentatum*, *dilatatum*, *ellipticum*, *erosum*, *foetidum*, *fordiae*, *lentago*, *nudum*, *phlebotrichum*, *plicatum* and varieties, *prunifolium*, *pubescens*, *scabrellum*, *sempervirens*, *setigerum*, *trilobum*, *wrightii*, sp.), *Adoxaceae* [= *Viburnaceae*, *Caprifoliaceae* s. lat.]; Asia (Central Asia, China, India, Japan, Korea, Russia, Siberia, Far East, Turkey), Caucasus (Armenia), Europe (Austria, Belgium, Bulgaria, Czech Republic, Denmark, Finland, France, Germany, Hungary, Italy, the Netherlands, Norway, Poland, Romania, Russia, Serbia, Slovakia, Spain, Sweden, Switzerland, Turkey, UK, Ukraine, North America (Canada, USA), and introduced into New Zealand. Russia, Krasnodar region, Sochi, the park of Sanatorium n.a. M.V. Frunze, on *V. tinus*, Oct. 15th, 2018, T.S. Bulgakov (HAL 3304F).

Additional specimens examined: Germany, Saxony, Görlitz, historical center, on *Viburnum carlesii*, Oct. 15th, 2007, S. Hoeflich (GLM-F81204); Rheinland-Pfalz, Kell am See, on *V. lantana*, Aug. 13th, 2000, U. Braun (HAL 687 F); Saxony, Boxberg, O.L., Uhyst, St. Peter and Paul, church park, on *V. opulus*, Sep. 24th, 2009, H. Boyle & S. Hoeflich (GLM-F99785). Russia, Krasnodar Region, Sochi, on *V. tinus*, Oct. 15th, 2018, T.S. Bulgakov (HAL 3304F).

Notes: When two species are reduced to synonymy it is important to designate epitypes for both of the old species to ensure that they are synonyms. The decision to reduce *E. hedwigii* to synonymy is based on the present phylogenetic results and thus epitypification from a sequenced specimen was necessary.

Erysiphe miranda (Heluta) U. Braun & S. Takam., Schlechtendalia **4**: 11, 2000.

≡ *Microsphaera miranda* Heluta, Ukrayins'k. Bot. Zhurn. **47**(5): 80, 1990.

Illustrations: Heluta (1990: 80, Figs 2–3), Shin (2000: 145, Fig. 51, as "*Microsphaera sparsa*"), Liu (2010: 100, Fig. 45, as "*Erysiphe hedwigii*"), Braun and Cook (2012: 483, Fig. 591).

Typification: On *Viburnum sargentii* (=*Viburnum opulus* var. *calvescens*), *Adoxaceae* [= *Viburnaceae*, *Caprifoliaceae* s. lat.]; Russia, Far East, Primorsky Kray, Khasan'sky Rayon, nature reserve "Kedrovaya Pad", Oct. 1st, 1989, V.P. Heluta (**holotype** KW). Isotype: VLA.

Mycelium amphigenous, effuse, cobwebby, evanescent to subpersistent; hyphae branching at right or narrow angle, septate, straight to sinuous, occasionally geniculate, hyphal cells 40–75 × 4–6 μm; hyphal appressoria well-developed, moderately lobed, solitary or in opposite pairs; conidiophores solitary per hyphal cell, arising from the upper surface of the mother cell, more or less in the middle of the supporting cell, erect, 55–85 × 7–9 μm, foot cells straight, cylindrical to somewhat flexuous-sinuous, about 20–40 μm long, followed by 2–3 cells shorter than the foot cell, about as long or even longer; conidia solitary, ellipsoid-ovoid, subcylindrical, 28–40 × 12–17 μm, length/width ratio 1.7–2.6, germ tubes perihilar, short, ending in lobed to multilobed appressoria. Chasmothecia scattered to almost gregarious, depressed globose, base finally almost umbilicate, 70–95(–110) μm diam.; peridium cells irregularly polygonal, 5–25 μm diam.; appendages 3–10(–16), around the equatorial zone and below, almost straight to curved, short, 0.7–1.5 times as long as the chasmothecial diam., 7–10 μm wide below and 5–7 μm wide above, aseptate or with a single septum at the base, hyaline throughout or brownish at the very base, wall thin to somewhat thickened throughout, smooth to rough, apices (3–)4–5 times regularly and relatively tightly dichotomously

branched or primary branches somewhat elongated, tips short, at first straight, later straight to curved; asci 2–5, subglobose to broad obovoid, 45–65 × 35–50(–60) μm, sessile to short-stalked, (3–)5–7(–8)-spored; ascospores broad ellipsoid-ovoid, 17–27(–30) × 10.5–16.5 μm, colorless.

Notes: Bunkina (1979, 1991) described *Microsphaera sparsa* on *Viburnum sargentii* from the Far East of Russia with much larger chasmothecia [(78–)100–126(–130) μm diam.] with more numerous asci (4–12), compared with typical *E. miranda.* The identity of theses collections is unclear and needs to be re-examined.

Discussion

The results of this study and the phylogenetic analyses cast doubt upon the monophyly of *Erysiphe viburni* (s. lat.). Blumer (1933, 1967) recognized two species, *Microsphaera viburni* (type host *Viburnum opulus*) and *M. hedwigii* (type host *Viburnum lantana*), which were said to be differentiated in the size of their chasmothecia and the number of chasmothecial appendages. Braun (1987, 1995) maintained the Blumer (1933, 1967) species concept of two *Erysiphe* species on *Viburnum* hosts. However, *M. viburni* (nom, illeg.) was replaced by *M. sparsa*, the correct name within *Microsphaera* for this species. Braun and Cook (2012) continued to follow the Blumer species concept (1933, 1967), but replaced *M. sparsa* with *Erysiphe viburni* (the correct name for *M. sparsa* in the genus *Erysiphe*). The differences between *E. hedwigii* and *E. viburni* are slight, i.e., overlapping chasmothecial sizes and numbers of chasmothecial appendages. Therefore, it is not surprising that there is controversy surrounding the species concept proposed by Blumer (1933, 1967). While some authors followed Blumer (1933, 1967) and Braun (1987, 1995, and maintained two species [Sandu-Ville (1967), Eliade (1990), Simonyan (1994), and Bolay (2005)], others regarded the European powdery mildew on *Viburnum* as a single species, referred to as *M. hedwigii*, with *M. viburni* as synonym (Fakirova 1991, Grigaliūnaitė 1997) or *M. sparsa*, with *M. hedwigii* as synonym (Sałata 1985, Bunkina 1991). The phylogenetic results from this study suggest that *E. hedwigii* has to be reduced to synonymy with *E. viburni*. The *E. viburni* clade (Fig. 2.1) encompasses sequences retrieved from European and North American powdery mildew collections on several hosts. It should be noted that the phylogeny of *E. viburni* in Asia is not clear. A sequence obtained from a collection on *V. sieboldii* in Japan forms a separate clade with sequences of powdery mildew on *Viburnum odoratissimum* var. *awabuki* from Korea and is described here as *Erysiphe pseudoviburni*. Powdery mildew on additional Asian *Viburnum* spp., previously referred to as *E. hedwigii* or *E. viburni* might belong to the latter species, but are still in

need to be morphologically and genetically analyzed. The slight morphological differences in the sexual morphs of the two "taxa" (*E. hedwigii* and *E. viburni*) are undoubtedly minor phenotypic variations influenced by the different substrates (hosts). This phenomenon was observed in *E. hedwigii* where smaller chasmothecia with fewer appendages were reported on *Viburnum lantana*, its type host, as well as on several other *Viburnum* spp., including *V. tinus* (Bolay 2005). Consequently, I propose to reduce *E. hedwigii* to synonymy with *E. viburni* and designate epitypes with ex-epitype sequences to stabilize these names genetically.

The phylogenetic analysis of North American specimens revealed an undescribed species on *Viburnum tinus*, and (rarely) on *V. edule*. This species, described as *E. viburniphila*, is genetically and morphologically (in particular with specific characters of the asexual morph) distinct from *E. viburni*. To ascertain the origin of this species, a specimen on *V. tinus* from Europe was included in the phylogenetic analysis, which revealed that the European collection is conspecific with the North American one (*Viburnum tinus* is a Mediterranean species, but is also widely used as an ornamental shrub). Furthermore, the sexual morph (chasmothecia) on *V. tinus* is common in Europe, which is in contrast to North American collections. The inability of this species to produce its sexual morph in North America suggests that *E. viburniphila* is an introduced pathogen in North America and has a Mediterranean origin. Chasmothecia of *E. viburniphila* (European collections) are rather small with few, short appendages and agree well with the sexual morph of *E. viburni* collections previously referred to as *E. hedwigii*. Thus, it is not surprising that *Erysiphe* on *V. tinus* in Europe has previously been identified as *E. hedwigii* (see Braun and Cook 2012). The current study emphasizes that a reliable identification of this pathogen can only be accomplished with careful morphological examinations of the asexual morph and, if possible, genetic comparisons. Because *E. viburni* and *E. viburniphila* have overlapping host ranges (Fig 2.1), identifying the fungus based solely on host species

is insufficient. For example, *V. tinus* outside its native range can be infected by *E. viburni* (see the collections from Russia and the United Kingdom on this host), and *E. viburniphila* can infect *V. edule* (a *Viburnum* species native to Canada and the northern parts of the USA).

Sequences obtained in this study from Chinese and Korean powdery mildew collections on *V. sargentii* (=*Viburnum opulus* var. *calvescens*) were included in the phylogenetic examinations. The sequences retrieved from these specimens formed a well-supported clade representing *Erysiphe miranda*, which is distantly related to *E. viburni. Erysiphe miranda* appears to be common and widespread in Asia [*V. sargentii*, often treated as variety or subspecies of *V. opulus*, is closely allied to the latter European species, but phylogenetically clearly separate from *V. opulus* and, therefore, maintained on the species level by Donoghue et al. (2004), Winkworth and Donoghue (2005), and Clement et al. (2014), which is the preferred status of the taxon concerned]. *Erysiphe miranda* is probably common and widespread in the natural range of *V. sargentii*. In addition, phylogenetic analyses of Korean collections on *V. odoratissimum* var. *awabuki* revealed a cryptic undescribed species that lies in a monophyetic group with a specimen from Japan on *V. sieboldii*.

Microsphaera viburni Howe (as "(Schwein.) Howe") and *M. sparsa* Howe are tentatively treated as synonyms of *Erysiphe viburni* Duby, but the true identity of these species described on the basis of North American powdery mildew specimens on *Viburnum* species (including *V. lentago*) remains unclear. Future research can evaluate epitypifications, and analyze ex-epitype sequences of powdery mildew on the type host of *M. sparsa*, *Viburnum lentago* [which currently belongs to a separate clade and section of *Viburnum* (sect. *Lentago* DC., Clement et al. 2014)]. Furthermore, additional research evaluating collections of *E. viburni* s. lat. on a wide array of host species might clarify if there are additional cryptic powdery mildew species hidden under *E. viburni* s. lat.

References

Amano K. 1986. Host range and geographical distribution of the powdery mildew fungi (2nd ed.).
Tokyo, Japan: Scientific Societies Press. 741 p.

Blumer S. 1933. Die Erysiphaceen Mitteleuropas unter besonderer Berücksichtigung der Schweiz.
Beiträge zur Kryptogamenflora der Schweiz 7:1–483.

Blumer S. 1967. Echte Mehltaupilze (Erysiphaceae). G. Fischer Verlag, Jena. 436 p.

Bolay A. 2005. Les Oïdiums de Suisse (Erysiphacées). Cryptogamica Helvetica 20:1–173.

Bradshaw, M., Braun, U., Wang, S., Shuyan, L., Feng, J., Shin, H.D, Choi, Y.J., Takamatsu, S,
Bulgakov, T., and Tobin, P.C. 2020. Phylogeny and taxonomy of powdery mildew on *Viburnum*
species. Mycologia. Online. https://doi.org/10.1080/00275514.2020.1739508

Braun U. 1981. Miscellaneous notes on the Erysiphaceae (II). Feddes Repertorium 92(7–8):499–513.

Braun U. 1984. A short survey of the genus Microsphaera in North America. Nova Hedwigia
39:211–243.

Braun U. 1987. A monograph of the Erysiphales (powdery mildews). Beihefte zur Nova Hedwigia
89:1–700.

Braun U. 1995. The Powdery Mildews (Erysiphales) of Europe. G. Fischer Verlag, Jena. 337 p.

Braun U, Cooke RT. 2012. Taxonomic manual of the Erysiphales (powdery mildews). Utrecht, The Netherlands: CBS-KNAW Fungal Biodiversity Centre. 707 p.

Braun U, Takamatsu S. 2000. Phylogeny of Erysiphe, Microsphaera, Uncinula (Erysipheae) and Cystotheca, Podosphaera, Sphaerotheca (Cystotheceae) inferred from rDNA ITS sequences – some taxonomic consequences. Schlechtendalia 4:1–33.

Bunkina IA. 1979. Muchnisto-rosyanye griby (sem. Erysiphaceae) Dal'nego Vostoka. Dal'nevostochny Gosudarstvenny Universitet, Vladivostok. 150 p.

Bunkina IA. 1991. Erysiphales. Pp. 11–142, in: Azbukina ZM, Ed., Nizshie rasteniya, griby i mokhoobraznye Sovetskogo Dal'nego Vostoka. Griby, Tom 2, Askomicety, Erizifal'nye, Klavitsipital'nye, Gelotsial'nye. Nauka, Leningrad.

Chen ZX, Yao YJ. 1993. Powdery mildews in Fujian, Fuzhou, China. Fujian Science and Technology Press. 120 p.

Chen GQ, Han SJ, Lai YQ, Yu YN, Zheng RY. 1987. Flora Fungorum Sinicorum. Vol. 1, Erysiphales. Science Press, Beijing. 552 p.

Clement WL, Arakari M, Sweeney PW, Edwards EJ, Donoghue MJ. 2014. A chloroplast tree for Viburnum (Adoxaceae) and its implication for phylogenetic classification and character evaluation. American Journal of Botany 101:1029–1049.

Cunnington, JH, Takamatsu S, Lawrie AC, Pascoe IG. 2003. Molecular identification of anamorphic powdery mildews (Erysiphales). Australasian Plant Pathology 32:421–428. https://doi.org/10.1071/AP03045

Darriba D, Taboada G, Doallo R, Posada D. 2012. jModelTest2: more models, new heuristics and high-performance computing. Nature Methods 9(8):772.

Donoghue MJ, Baldwin BG, Li J, Winkworth RC. 2014. Viburnum phylogeny based on chloroplast trnK intron and nuclear ribosomal ITS DNA sequences. Systematic Botany 29:188–198.

Drummond AJ, Rambaut A. 2007. BEAST: Bayesian evolutionary analysis by sampling trees. BMC Evolutionary Biology 7:214

Eliade E. 1990. Monografia Erysiphaceelor din România. Lucrările Grădinii Botanice din Bucureşti 1989–1990:105–574.

Fakirova IF. 1991. G'bute v B'lgariya, 1 tom, razred Erysiphales (Fungi Bulgaricae, 1 tomus, ordo Erysiphales). Izdatel'stvo na B'lgarskata Akademiya na Naukite. 154 p.

Farris, JS, Källersjö, M, Kluge, AG, and Bult, C. 1994, Testing of Significance of Incongruence. Cladistics, 10: 315-319. doi:10.1111/j.1096-0031.1994.tb00181.x

Felsenstein J. 1985. Confidence Limits on Phylogenies : An Approach Using the Bootstrap. Evolution 39:783–791. http://www.jstor.org/stable/2408678

Gernhard T. 2008. The Conditioned Reconstructed Process. Journal of Theoretical Biology 253:769-778.

Grigaliūnaitė B. 1997. Mycota Lithuaniae. Vol. 3, Erysiphales 1. Mokslo ir Enciklopedijų Leidybos Institutas, Vilnius. 195 p.

Harrington, TC, Wingfield BD. 1995. A PCR-based identification method for species of Armillaria. Mycologia 87:280–288. https://doi.org/Doi 10.2307/3760915

Heluta VP. 1989. Flora Gribov Ukrainy. Muchnistorosyanye griby (Flora Fungorum RSS Ucrainicae, Ascomycetes, Erysiphales). Naukova Dumka, Kiev. 256 p.

Heluta VP. 1990. Novi dlya ta CRCR taksoni boroshnisto-rosyanikh gribiv iz zapovidnika "Kedrova Pad'" (Primors'ky Kray). Ukrayins'kyi Botanichnyi Zhurnal 47(5):79–83.

Hirata T, Takamatsu S. 1996. Nucleotide sequence diversity of rDNA internal transcribed spacers extracted from conidia and cleistothecia of several powdery mildew fungi. Mycoscience 37:283–288.

Jaczewski AA. 1927. Karmanny opredelitel' gribov. Vyp. 2. Muchnisto-rosyanye griby. Mikologicheskaya Laboratoriya Imeni Professora A.A. Jaczewskogo, Gosudarstvennogo Instituta Opytnoy Agronomii, Leningrad. 626 p.

Léveillé JH. 1851. Organisation et disposition méthodique des espèces qui composent le genre Erysiphé. Annales des Sciences Naturales, Botanique, Ser. 3, 15:109–179.

Liu TZ. 2010. The Erysiphaceae of Inner Mongolia. Inner Mongolia Science and Technology Press, Chifeng. 322 p.

Magnus P. 1898. Der Mehltau auf Syringa vulgaris in Nordamerika. Berichte der Deutschen Botanischen Gesellschaft 16:63–70.

Meeboon J, Takamatsu S. 2015. Erysiphe viburni-plicati and Podosphaera photiniae, two new species of Erysiphales (Ascomycota) from Japan. Mycoscience. 56:14–23.

Mori Y, Sato Y, Takamatsu S. 2000. Evolutionary Analysis of the Powdery Mildew Fungi Using Nucleotide Sequences of the Nuclear Ribosomal DNA. Mycologia 92:74–93.

Nomura Y. 1992. Erysiphaceae of Japan. Yotsukaido C., published by the author. 476 p.

Paulech C. 1995. Flóra Slovenska, X/1, Mycota (Huby), Ascomycetes (Vreckaté), Erysiphales (Múčnatkovaré). VEDA, Bratislava. 291 p.

Rambaut A. 2009. Fig Tree ver. 1.3.1. Available at: http://tree.bio.ed.ac.uk/software/figtree. Acess Date: June 2018

Sałata S. 1985. Flora Polska, Grzyby (Mycota), Tom XV, Workowce (Ascomycetes), Mącznikowe (Erysiphales). Państwowe Wydawnictwo Naukowe, Warszawa-Kraków. 247 p.

Salmon E. 1900. A monograph of the Erysiphaceae. Memoirs of the Torrey Botanical Club 9:1–292.

Sandu-Ville C. 1967. Ciupercile Erysiphaceae din România. Studiul Monografic. Editura Academiei Republicii Socialiste România, Bucureşti. 358 p.

Scholin, CA, Herzog, M, and Anderson, DM. 1994. Identification of group- and strain-specific genetic markers for globally distributed Alexandrium (Dinophyceae). 1. RFLP analysis of SSU rRNA genes. Journal of Phycology 30:999–1011.

Seko, Y, Bolay, A, Kiss, L, Heluta, V, Grigaliunaite, B, Takamatsu, S. 2008. Molecular evidence in support of recent migration of a powdery mildew fungus on Syringa spp. into Europe from East Asia. Plant Pathology 57: 243–250

Shin HD. 1988. Erysiphaceae of Korea. Ph.D. Thesis. Seoul National University. 305 p.

Shin HD. 2000. Erysiphaceae of Korea. Plant Pathogens of Korea 2:1–320.

Silvestro D, Michalak I. 2012. raxmlGUI: a graphical front-end for RAxML. Organisms Diversity & Evolution 12:335–337.

Simonyan SA. 1994. Mikoflora Armenii. VII. Muchnistorosyanye griby Armenii (por. Erysiphales). Izdatel'stvo AN Armenii, Yerevan. 384 p.

Swofford D. 2002. PAUP*: phylogenetic analysis using parsimony (*and other methods). Sunderland, Massachusetts, Sinauer.

Takamatsu S, Kano Y. 2001. PCR primers useful for nucleotide sequencing of rDNA of the powdery mildew fungi. Mycoscience 42:135–139. https://doi.org/10.1007/BF02463987

Takamatsu S, Hirata T, Nomura Y. 1999. Phylogenetic relationships of Microsphaera and Erysiphe section Erysiphe (powdery mildews) inferred from the rDNA ITS sequences. Mycoscience 40:259–268.

Tamura K, Peterson D, Peterson N, Stecher G, Nei M, Kumar S. 2013. MEGA6: Molecular evolutionary genetics analysis using maximum likelihood, evolutionary distance, and maximum parsimony methods. Molecular Biology and Evolution 30:2725–2729. https://doi.org/10.1093/molbev/msr121

Tanda S, Nomura Y. 1978. Powdery mildews of the new hosts in Japan (V). Journal of Agriculture Science [Tokyo Nogyo Daigaku] 23(1):19–31.

Tanda S, Nomura A, Matsunami Y. 1973. Powdery mildews of the new hosts in Japan (I). Journal of Agriculture Science [Tokyo Nogyo Daigaku] 18(2):123–138.

Walsh PS, Metzger DA, Higuchi R. 1991. Chelex 100 as a medium for simple extraction of DNA for PCR-based typing from forensic material. BioTechniques 10:506–513.

Westcott, C, Horst, RK. 1990. Westcott's plant disease handbook. (5th ed. / rev. by R. Kenneth Horst. ed.). New York: Van Nostrand Reinhold.

White TJ, Bruns T, Lee S, Taylor J. 1990. Amplification and direct sequencing of fungal ribosomal RNA genes for phylogenetics. In: Innis, MA, Gelfand DH, Sninsky JJ, White TJ, Eds., PCR Protocols: A Guide to Methods and Applications. Academic Press San Diego. p. 315–332.

Winkworth RC, Donoghue MJ. 2005. Viburnum phylogeny based on combined molecular data: implications for taxonomy and biogeography. American Journal of Botany 92:653–666. doi:10.3732/ajb.92.4.653

Wu Z-Y, Raven PH, Hong D. (eds.) 2011. Flora of China. Volume 19: Cucurbitaceae through Valerianaceae, with Annonaceae and Berberidaceae. Science Press/Missouri Botanical Garden Press, Beijing/St. Louis.

Zhao ZY. 1979. Flora of the Erysiphaceae in Xingjian. Xingjiang People's Press. 151 p.

Chapter 3: A worldwide assessment of *Sawadaea bicornis* on *Acer* spp. reveals multiple haplotypes and the origin of an invasive fungal plant pathogen

Abstract

The introduction, spread, and impact of fungal plant pathogens is a critical concern in cultivated, developed, and natural landscapes. In the initial response to a novel epidemic, it is not always certain what the causative agent is. Moreover, in the case of a newly introduced pathogen, there is often a considerable lag between detection and identification, and between identification and ascertaining the invasion pathway. In this study, we were motivated by a recently reported decline in *Acer macrophyllum* (bigleaf maple) in the Pacific Northwest, and the rather sudden appearance of *A. macrophyllum* heavily infected with powdery mildew in Seattle, Washington, USA. We used morphological and genetic analyses to confirm that the pathogen causing the epidemic was *Sawadaea bicornis*. In subsequent field studies, this pathogen was found in several locations in western North America on *A. macrophyllum*, and in greenhouse studies, *A. macrophyllum* was found to be significantly more susceptible to *S. bicornis* than eight other *Acer* sp. tested. We then sequenced the ITS and LSU regions of 140 specimens of powdery mildew from throughout the world using both freshly collected and ancient herbarium specimens. Our analyses revealed seven different haplotypes that are phylogenetically split into two separate groups. The high diversity of haplotypes found in Europe coupled with sequence results from a specimen from 1864 allowed us to conclude that *S. bicornis* has a European origin. Furthermore, sequence data from a specimen from 1938 in Canada show that the

pathogen, and the most prevalent and widespread haplotype, has been present in North America for at least 82 years. We believe this to be the first study to use herbarium specimens of plant pathogens to genetically ascertain the origin and timing of an introduced plant pathogen. Examining genetic data of ancient herbarium specimens can be a useful tool in efforts to decipher the invasion dynamics of non-native plant pathogens, and address ecological, evolutionary and pathological questions related to emerging plant pathogen epidemics.

Introduction

Invasive plant pathogens can cause substantial damage to ecosystems throughout the world (Mack 2000; Ellison et al. 2005; Loo 2008; Stajich et al. 2009). Due to increases in global trade, and in particular, the importation of plants, many detrimental plant pathogens have been introduced relatively recently (Brasier 1990; Gómez-Alpizar et al. 2007; and Rellou 2018). For example, during the 1900s, the causative agents of Dutch elm disease (*Ophiostoma ulmi*) (Brasier 1990), chestnut blight (*Cryphonectria parasitica*) (Rellou 2018), and white pine blister rust (*Cronartium ribicola*) (Maloy 1997) were introduced to North America where they have caused major declines in their host trees and in the case of American chestnut, functional extinction (Anagnostakis 1987). The introduction of non-native fungal pathogens can be particularly difficult to manage due to their small size and ability to arrive without detection on asymptotic host plants (Migliorini et al. 2015; Burgess et al. 2016).

Fungi, as model organisms to study biological invasions, have often been overlooked due to their inconspicuous nature and the difficulty in identifying them to the species level. This is despite the fact that invasions by fungal organisms are thought to outnumber those by plant and animal species (Brown and Rant 2013). Moreover, the ubictious nature of fungi and their fast rate of evolution makes them valuable study organisms for elucidating ecological and evolutionary processes involved in pathogen success in new environments (Gladieux et al. 2014; Burgess et al. 2016). Herbarium specimens of fungal plant pathogens can provide unique insights into the evolutionary history of pathogen-host interactions (Yoshida et al. 2014). For example, work was recently accomplished evaluating herbarium specimens of the Oomycete pathogen *Phytopthora infestans* that found that the genotype present now is distinct from the genotype that caused the Irish potato famine (Martin et al. 2013; Yoshida et al. 2013). Among fungal pathogens, powdery mildew is an ideal model system to

study invasions due to its cosmopolitan distribution (Braun and Cook 2012), high rate of evolution (Glawe 2008), and rapid adaptation to plant hosts (Brown and Rant 2013).

Powdery mildew is known to infect >10,000 flowering plant species worldwide (Amano 1986), with an estimated 873 described species (Braun and Cook 2012). Symptoms of powdery mildew first appears on its host plants as white powdery spots that can spread over large areas of the plant, decreasing growth, and reducing flower and fruit quantity (Daughtrey and Benson 2005). Severe infections reduce the aesthetic value of ornamental plant species, and cause plant death (Westcott and Horst 1990). Powdery mildew conidia, an asexual spore stage, can aerially disperse and greatly facilitate its spread, resulting in severe epidemics over a relatively short time period (Ale-Agha et al. 2000 and 2004; Brown et al. 1991; Kiss 2005).

In recent years, tree mortality in western North America has increased at a higher rate than what is thought to be expected under historical conditions (van Mantgem et al. 2009; Cohen et al. 2016). In some tree species, fungal plant pathogens have been shown to contribute to mortality, such as Swiss needle cast, *Phaeocryptopus gaeumannii*, in Douglas-fir (Stone et al. 2008) and Arbutus canker, *Nattrassia mangiferae*, in Pacific madrone (Elliott et al. 2002). Within the Pacific Northwest, recent declines have been reported in bigleaf maple, *Acer macrophyllum* (OSU Extension 2019; Ramsey 2016; Betzen 2018). Symptoms of this decline include yellow flagging of large branches, decreased leaf size, and crown dieback (Ramsey 2016). Prior studies of bigleaf maple decline in Washington state have documented several biotic agents, including plant pathogens and insects, on declining *A. macrophyllum*; however, no biotic agents have yet been identified as a causative agent (Betzen 2018; WDNR 2016). This lack of an association between a specific biotic agent and *A. macrophyllum* decline is due, in part, to the

lack of a consistently observed biotic agent on declining trees, and the presence of decline in the absence of any detectable biotic agent (Betzen 2018).

In 2018, severe powdery mildew infections were observed on *A. macrophyllum* in and around the University of Washington campus in Seattle, Washington, USA (Fig. 1A), and in a greater rate of infection than had been previously reported (Betzen 2018; WDNR 2016). We were motivated by this observation, and the possibility that this fungal pathogen might be a contributing agent to the decline of *A. macrophyllum*. To better understand the powdery mildew infecting *A. macrophyllum* we (1) identified the powdery mildew species infecting *A. macrophyllum* from samples collected from the University of Washington campus, (2) evaluated the susceptibility of *A. macrophyllum* and other *Acer* species to this powdery mildew species, and (3) conducted a worldwide genetic analysis on herbarium and newly collected specimens of powdery mildew on *Acer* spp. The worldwide genetic analysis allowed us to ascertain the likely native range of this powdery mildew species, estimate the timing of its introduction to western Washington, and identify the different powdery mildew species haplotypes from ITS and LSU sequence data.

Materials and Methods

Species Identification

We used morphological and genetic analyses to identify the powdery mildew species infecting *A. macrophyllum* from the University of Washington campus. In late summer 2019, 519 *A. macrophyllum* trees were inspected for signs and symptoms of powdery mildew (Fig. 1). Powdery mildew was also noted on the congeneric species *A. circinatum, A. campestre,* and *A. platanoides* on campus. For identification, we collected 30 powdery mildew specimens from 30 different *A. macrophyllum* trees throughout campus during late September of 2019. Morphological examinations of the asexual morph of samples were accomplished by placing clear adhesive tape on powdery mildew colonies and setting the tape onto a slide containing a drop of distilled water. If the specimens had dried, examinations were done following the lactic acid protocol (Shin 1988). Examinations of the sexual morph were accomplished by using a clean needle to mount chasmothecia onto a microscope slide containing a 3% NaOH solution. Pictures were taken of the slides using a compound microscope with an Olympus SC50 camera attached and a Zeiss AX10. Morphological identification was done using the taxonomic keys from Braun and Cook (2012).

Genetic sequencing of specimens was conducted on the β-*tubulin* region, the intergenic spacer region (IGS), the internal transcribed spacer region (ITS), and the large ribosomal subunit (LSU) region. Sequences for the β-*tubulin* region were obtained using the primers BTF5b (5'-ATGATGGCSSACATTTTCGGTTGT-3') and BTR7a (5'-TCCATTTCGTCCATTCCTTC-3') (Ellingham et al. 2019). Sequences obtained for the IGS region were accomplished using the primers IGS-12a (5'-AGTCTGTGGATTAGTGGCCG-3')/ NS1R (5'-GAGACAAGCATATGACTAC-3')

(Carbone and Kohn 1999). Sequencing of the ITS and LSU region was accomplished according to Bradshaw and Tobin (2020). DNA extractions were done by the Chelex method (Walsh et al. 1991; Hirata and Takamatsu 1996). PCR was accomplished using the Primer pairs PM10 (5'-GGCCGGAAAGTTGTCCAAAC-3') (Bradshaw and Tobin 2020) /SPM28R (5'-GCGTTCACTTTCATTCCGCGC-3'). If PCR was unsuccessful, a nested primer approach was accomplished using the Primers AITS (5'-CGATTGAATGGCTAAGTGAGG-3') (Bradshaw and Tobin 2020)/TW14 (5'-GCTATCCTGAGGGAAACTTC-3') (Mori et al. 2000) followed by PM10/SPM28R or PM10/PM11(5'-TACCGCTTCACTCGCCGTTA-3') (for the ITS) and LSUF (5'-TAACGGCGAGTGAAGCGGTA-3')/SPM28R (for the LSU) (Bradshaw and Tobin 2020). SPM28R was generated for this study by slightly editing PM28R from Bradshaw and Tobin (2020) so that the primer would anneal to species within *Phyllactinia* and *Sawadaea*. DNA was purified by isopropanol precipitation. Purified amplicons were sent to Eurofins (Luxembourg) to be directly sequenced in both the forward and reverse direction using the successful primer pairs above. Sequences were trimmed using MUSCLE in MEGA7:Molecular Evolutionary Genetics Analysis Version 7.0 (Kumar et al. 2016) and Geneious version 11.0.2 (https://www.geneious.com).

Morphological and genetic analysis confirmed the powdery mildew species affecting *A. macrophyllum* was *Sawadaea bicornis*, which had not previously been reported in North America on *Acer macrophyllum* (see results).

Susceptibility of Acer species to Sawadaea bicornis

On the University of Washington campus, we evaluated the susceptibility of the 519 *A. macrophyllum* trees initially surveyed. Each tree was evaluated by naked eye assessments to estimate the percentage

of the leaf area that was covered by powdery mildew colonies. Additionally, we used a greenhouse setting at the Douglas Research Conservatory at the University of Washington to experimentally measure the susceptibility of nine *Acer* spp., including *A. macrophyllum*, to *S. bicornis*. Seedlings of the *Acer* spp. evaluated (*A. campestre, A. circinatum, A. davidii, A. macrophyllum, A. negundo, A. palmatum, A. pseudoplatanus, A. platanoides*, *A. pennsylvanicum,* and *A. tataricum*) were collected throughout King County, Washington, USA. Seedlings were all ~2.5cm in height. Twenty seedlings of each species were potted in Sunshine #4 potting soil (SunGro, Bellevue, WA) in 8.9×8.9X8.9cm cm pots and placed in a greenhouse in a randomized block design. Plants were watered and fertilized on an as-need basis using a sub-irrigation system to control for the effect of overhead watering on powdery mildew growth. All seedlings were applied with a soil injection of Xytect 2F™ (Imidacloprid) to prevent insect damage. Experiments were conducted between 29 June and 29 August 2019, during which time the mean temperature was 22.7 °C and the mean relative humidity was 64.0%. On 29 June, 10 plants from each species were randomly selected and inoculated with powdery mildew, while the remaining ten were used as control plants and were applied with Eagle 20W™ fungicide on a biweekly basis. Eagle 20W™ has myclobutanil as its active ingredient and was chosen due to its prevalence in the nursery industry in the Pacific Northwest (personal communications). Three control plants developed signs of powdery mildew over the course of the experiment and were discarded for analyses; no other control plants developed signs of powdery mildew.

Plants selected for the treatment were inoculated with a *S. bicornis* (haplotype 1) specimen collected from the University of Washington campus. The inoculum was made by cutting infected leaves into small pieces using a sterile blade. The leaf pieces were placed into a sterile 50 ml Falcon tube with 10ml of 0.001% Tween 20 and vortexed for 30 seconds. Spores were counted using a hemocytometer and the concentrations were adjusted to 10000 spores/ml. Inoculations were

applied onto the plant using a hand sprayer until the inoculum was visibly running off the leaf. Following the experiment, powdery mildew that formed on the *Acer* specimens were sequenced to confirm their haplotype.

Disease severity was estimated by the percentage of the entire plant colonized by powdery mildew on a weekly basis (accounting for the stem and both the front and back sides of the leaves) using naked eye assessments, which is a standard practice in powdery mildew studies (Gortari et al. 2018; Grove et al. 2000; Moparthi and Bradshaw 2020) and furthermore is as accurate as disease analysis software (Bade and Carmona 2011; Olmstead et al. 2020). Area Under the Disease Progress Curve (AUDPC) values were then estimated using protocols from the American Phytopathological Society (2019). The AUDPC is a useful tool for comparing disease intensity over time for comparison across years and among different treatments (American Phytopathological Society 2019). This type of curve is best suited when evaluating host resistance because it generates a single numerical value that accounts for disease progress over time.

The AUDPC measurements were extremely bimodally distributed between very high and very low (e.g., ~0) values. To evaluate the effect of host species on AUDPC values, we first conducted a logistic regression analysis using the presence or absence of powdery mildew as the response variable. Although there was a significant effect of host species (likelihood ratio χ^2=91.9, P<0.001), this approach was not able to differentiate differences in AUDPC values. Thus, in a subset analysis, we excluded species that were clearly resistant to *S. bicornis* (e.g., AUDPC=0). In this subset, AUDPC values were considered continuous and transformed using $\log_{10}$ to satisfy the assumptions of normality, and analyzed using ANOVA. Differences between treatment means were based on Tukey's HSD (α = 0.05). Analyses were performed using R version 3.31 (R Core Team 2017).

We also measured chlorophyll density and biomass on the last day of the experiment on inoculated and control plants. Relative chlorophyll data was measured in arbitrary units referred to as 'SPAD units' using a Konica Minolta SPAD 502 Meter (Konica Minolta, Ramsey, NJ, United States). The measurements are a suitable proxy for leaf nitrogen content (Uchino et al. 2013). Three measurements were taken per plant on different aged leaves (1st node, 2nd node, and 3rd node) and averaged to obtain a single SPAD units value. Chlorophyll data were normally distributed.

Dry above and below ground biomass was measured of the non-inoculated control and inoculated treatment plants as a proxy for the effect of *S. bicornis* on plant growth rate. The plants were first placed in buckets full of water where their roots were washed of all soil. They were then placed into brown paper bags and placed in a herbarium dryer at 37.8 °C until the plants had completely dried. Above and below ground plant matter was separated and weighed using an OHAUS BW15US scale (OHAUS, New Jersey). Biomass data were transformed using a square root transformation to satisfy the assumptions of normality. The main effects of treatment (inoculated vs control plants) and species and their interaction, were analyzed using a GLM in R to quantify the effect of powdery mildew on the SPAD units and biomass. Because this analysis was designed to test the effect of powdery mildew on susceptible host plants, only host plant species that were heavily infected with *S. bicornis*, defined as AUDPC > 100, were included for analysis; these species were *A. macrophyllum*, *A. campestre*, and *A. pseudoplatanus*.

Worldwide genetic analysis of powdery mildew on Acer spp.

A total of 107 samples of powdery mildew on *Acer* hosts were collected between 2017 and 2019 throughout the western United States (54 specimens), Germany (39 specimens), Austria (3 specimens) China (10 specimens) and New Zealand (1 specimen). Samples were collected from urban and natural landscapes. Newly collected specimens were deposited in the University of Washington Herbarium (WTU) or the Herbarium Mycology of Jilin Agricultural University (HMJA). In addition, a total of 33 herbarium specimens were evaluated from Austria, Canada, China, Czech Republic, Denmark, Hungary, Italy, New Zealand, Sweden, the United Kingdom, and Utah from the following herbariums: Canada National Mycological Herbarium (DAOM), HMJA, New York Botanical Garden Steere Herbarium (NY), The New Zealand Fungarium (PDD), National Museum of Nature and Science Tokyo (TNS) and Washington State Charles Gardner Shaw Mycological Herbarium (WSP). These additional specimens were collected between 1864-2015. All 140 specimens were sequenced as previously described and aligned with 37 additional, previously sequenced, *S. bicornis* specimens from GenBank to ascertain powdery mildew haplotypes.

We then subjected the haplotypes to phylogenetic analyses. For the phylogenetic analyses, 1-2 specimens of each haplotype were used for representative purposes. Sequences of the different haplotypes were aligned and edited using MUSCLE in MEGA7:Molecular Evolutionary Genetics Analysis Version 7.0 (Kumar et al. 2016). A partition homogeneity test (Farris et al. 1994) was conducted in PAUP 4.0a151 (Swofford 2002) to determine whether the ITS and LSU datasets were congruent with each other. A GTR+G+I evolutionary model was used for phylogenetic analyses as it is the most inclusive model of evolution and includes all other evolutionary models (Abadi et al. 2019). A MCC (maximum clade credibility) phylogenetic tree was constructed for the combined ITS and LSU rDNA using a yule process speciation model (Gernhard 2008) by Bayesian analyses, in the program BEAST version 1.10.2 (Drummond and Rambaut 2007). The resulting tree was visualized

using FigTree ver. 1.3.1 (Rambaut 2009). A maximum likelihood analysis was accomplished using raxmlGUI (Silvestro & Michalak, 2012) under the default settings with a GTR+G+I evolutionary model. Parsimony analysis was done using PAUP 4.0a151 (Swofford 2002). For the parsimony analysis, gaps were treated as missing data and sites were treated as unordered and unweighted. Bootstrap analyses were conducted using 1000 replications with the stepwise addition option set at simple (Felsenstein 1985).

Results

Species Identification

Morphological and genetic analyses conducted on powdery mildew on *A. macrophyllum*, *A. campestre,* and *A. circinatum* at the University of Washington revealed the species in question to be *S. bicornis*. The morphology (Fig. 2) matched the description of *S. bicornis* from Braun and Cook (2012). The ITS alignments aligned ~99% with *S. bicornis* specimens from New Zealand, (Accession number: MK432779), the United Kingdom (Accession number: KY661007) and the USA (Accession number: MN786324). This is the first report of *S. bicornis* on *A. macrophyllum* in the United States (Farr and Rossman 2020).

Susceptibility of Acer species to Sawadaea bicornis

Of the 519 *A. macrophyllum* trees surveyed at the University of Washington campus, 518 of them showed signs of powdery mildew. The estimated mean percentage of total leaf area of each tree infected with powdery mildew colonies was 89%.

The powdery mildew growing on the different *Acer* spp. under greenhouse conditions was sequenced as well as the specimen used as inoculum. The inoculum contained haplotype 1. The sequencing results of the powdery mildew on these *Acer* spp. showed that all of the species were infected with haplotype 1 except for *A. campestre*, which was infected by haplotype 4. Because all host plants were inoculated with haplotype 1, this is most likely due to an accidental infection with haplotype 4. Several *A. platanoides* plants were found to be infected with *S. tulasnei*, presumably as a

result of contamination, and were not included in the analysis. These results highlight the importance of genetic analyses, pre and post inoculation, when conducting pathogenicity or susceptibility experiments.

In the greenhouse experiment, signs of powdery mildew were first noted 6 days post inoculation. Among the *Acer* species tested, *A. macrophyllum* was the most susceptible to *S. bicornis* (Fig. 3). Two months post inoculation, on the last day of measurements, the average percent of each *A. macrophyllum* plant covered in powdery mildew colonies was 59%. This was more than double the second most susceptible species, *A. campestre* (20% average coverage).

After excluding resistant species (i.e., AUDPC=0), the remaining species tested in the subset were *A. campestre, A. circinatum, A. macrophyllum*, *A. negundo*, *A. palmatum, A. pennsylvanicum*, and *A. pseudoplatanus*. Among these species, I detected a significant difference in susceptibility (F=12.86, df=6, 86 P<0.001). AUDPC values for all *Acer* spp. tested are presented in Figure 3.3. I did not detect significant differences in SPAD units between the treatments (F=0.15; df=1, 48; P=0.71), among the species (F=0.6; df=2, 48; P=56), or in the interaction between treatment and species (F=1.17; df=2, 48; P=0.32). The mean SPAD units between the control and inoculated plants were 30.7 au vs 30.1 au respectively. We also did not detect significant differences in biomass between the treatments (F=1.3; df=1, 48;P=0.26), or in the interaction between treatment and species (F=0.866; df=2, 48; P=0.27). There was a species effect on biomass (F=18.5; df=2, 48; P<0.001), largely due to the differences in biomass among the *Acer* spp. I would like to note that the plants inoculated with powdery mildew had 17% less biomass on average than the non-inoculated control (6.54 g vs 7.91 g).

The ITS and/or LSU region of the powdery mildew on *Acer* specimens collected throughout the world were successfully sequenced (Fig. 4) and deposited in GenBank (GenBank accession numbers: Table 3.1). The IGS region of 16 specimens from Washington State was successfully sequenced and deposited in GenBank (MT469889-MT469904). The specimens showed some divergence from each other but did not reveal any additional haplotypes than those revealed from sequencing the ITS and LSU regions. The β-*tubulin* region of four specimens from Washington State and one specimen from Germany was successfully sequenced and deposited in GenBank (GenBank accession numbers: MT470359-MT470363). These specimens all aligned 100% with each other. The majority of the sequences attempted for the IGS and *B-tubulin* region yielded no bands in electrophoresis or inconsistent sanger sequencing results. The unsuccessful results for the IGS and *B-tubulin* regions could have resulted from the specimens having poor quality DNA (due to age), or being contaminated with other fungi. Additional research to improve the IGS and *B-tubulin* primers would facilitate their use on older powdery mildew specimens.

The specimens sequenced for this study aligned ~99% with the ITS region of four different species of powdery mildew from GenBank: *S. bicornis* (Accession number: MK432779), *S. nankinensis* (Accession number: AB353761), S. *negundinis* (Accession number: MF179623) and *S. tulasnei* (Accession number: AB193361). The *S. polyfida* specimens were only sequenced in the LSU region but aligned 100% with *S. polyfida* from GenBank (Accession number: AB193397). The *S. bicornis* specimens were sequenced on *A. campestre*, *A. circinatum*, *A. grandidentatum*, A. *macrophyllum*, *A. negundo*, *A. pseudoplatanus*, *A. platanoides*. and *A. tataricum*. This is the first report of *S. bicornis* on *A. circinatum*, and *A. grandidentatum* worldwide (Farr and Rossman 2020). The S. *negundinis* specimens

were sequenced on *A. mandshuricum, A. mono, A. negundo, A. tataricum* and *Alectryon excelsus*. This is the first report of *S. negundinis* on *A. mandshuricum, A. mono, A. tataricum* and *Alectryon excelsus* worldwide (Farr and Rossman 2020). The *S. tulasnei* specimens were sequenced on *A. macrophyllum, A. pictum, A. platanoides, A. tataricum* and *A. truncatum*, and is the first report of *S. tulasnei* on *A. pictum* (Farr and Rossman 2020). The *S. polyfida* specimens were sequenced on *A. palmatum*, which is the first report of *S. polyfida* on *A. palmatum* in China (Farr and Rossman 2020).

Five powdery mildew specimens were sequenced on *A. platanoides* from the 1890s. Four of these specimens were labeled as *S. bicornis*. However, sequence data from all four specimens revealed that they were in fact S. *tulasnei* and thus incorrectly labeled. Additionally, two powdery mildew specimens were sequenced on *Alectryon excelsus* that were labeled as *S. bicornis*. The sequence data of these specimens aligned 99% with *S. negundini*s from Iran (GenBank Acession number: MF179623). The results suggest that identification of *S. bicornis* can be extremely unreliable without sequence data, and that the identification of powdery mildews in herbaria would benefit from the use of sequence data to either confirm or correct previous identifications based upon morphology alone.

The ITS+LSU sequence alignments of 177 *S. bicornis* sequences (140 generated from this study and 37 obtained from GenBank) revealed seven distinct haplotypes (Table 3.2). The haplotype frequencies tended to differ based upon host species and locality (Fig. 3.5). Haplotype 1 was the most common haplotype sequenced and accounted for 61% of the total *S. bicornis* specimens sequenced. Haplotype 1 also had the broadest host range (eight species) and was the most common on *A. macrophyllum* (80% of the specimens sequenced on *A. macrophyllum* contained haplotype 1). The highest haplotype diversity was in Europe (6 different haplotypes) even though the greatest number of samples were taken from the United States.

The oldest specimen sequenced was from 1864 from the United Kingdom, and it aligned with haplotype 4. The oldest haplotype 1 sequenced was from the Czech Republic in 1934. The oldest specimen sequenced from North America was from 1938. The oldest North American specimen aligned with haplotype 1, revealing that haplotype 1 has been present in North America since at least 1938. Haplotype 3 was solely located in North America and was only found on *A. macrophyllum* and *A. circinatum*. Haplotype 4 was the second most frequently sequenced haplotype (19% of *S. bicornis* specimens sequenced were haplotype 4). Haplotype 4 was predominantly found on *A. campestre* (78% of the haplotype 4 specimens were on *A. campestre*). Additionally, haplotype 4 was found on 33% of the *A. circinatum* specimens sequenced. Haplotypes 6 and 7 were confined to *A. platanoides* in Europe.

A phylogenetic tree was constructed from 13 *S. bicornis* specimens, three *S. negundinis* specimens and two *S. tulasnei* specimens. The specimens for the phylogenetic analyses were chosen so that each *S. bicornis* haplotype was represented. *Sawadaea nakinensis* was selected as an outgroup taxon. The result of the partition homogeneity test showed no direct conflict between the ITS and LSU rDNA regions (*P*=0.9). All tree topologies were similar and only the representative maximum clade credibility tree is illustrated in Figure 3.6. The phylogenetic analyses revealed that *S. bicornis* can be split into two major groups of haplotypes with high support. Group one contains haplotypes 1-3 and Group two contains haplotypes 4-7. The phylogenetic analyses also show that there is high support that haplotypes 2, 3 5, and 6 belong in clades of their own.

Discussion

Powdery mildew caused by *S. bicornis* (haplotype 1) was collected at several locations in the Pacific Northwest (Fig. 3.4), and the epidemic recently observed from the University of Washington campus could be widespread throughout this region. *Acer macrophyllum* trees are also particularly susceptible to *S. bicornis* (Fig. 3.3). The percentage of leaf area on *A. macrophyllum* infected with *S. bicornis* is comparable to severe powdery mildew epidemics reported in agricultural systems. For example, greenhouse studies of powdery mildew on cherry trees, caused by *Podosphaera cerasi*, and powdery mildew on wine grapes, caused by *Erysiphe necator,* reported similar maximum disease percentage to that of powdery mildew on *Acer macrophyllum* (50% on cherry trees, 76% on wine grapes and 59% on *Acer macrophyllum*) (Moparthi and Bradshaw 2020; Singh et al. 2017). We noted that we did not detect differences in SPAD units or biomass in seedlings infected with *S. bicornis*, possibly due to the short time window (two months) of the greenhouse experiment, but it was clear that *A. macrophyllum* was heavily infested during this time period, and more susceptible to *S. bicornis* than the other *Acer* spp. I tested (Fig. 3.3). Past research on powdery mildew in other systems has shown the link between powdery mildew infection, which would be proxied by AUDPC values in this study, and reduced fitness (Enright and Cipollini 2007; Royse et al. 1980). Also, although considerable research on powdery mildew has been conducted in annual cropping systems (Austin et al. 2006; Cao 2015; Carisse et al. 2013), little attention has been given to the long-term effects of powdery mildews on ecologically important, long-lived plant species such as *A. macrophyllum*. Future research should address these long-term effects, and evaluate *A. macrophyllum* seedlings collected from throughout western North America to locate resistant populations.

We used the ITS and LSU regions to determine the different haplotypes of *S. biconris* and its origin. Past studies have similarly, primarily, used the internal transcribed region to identify haplotypes of fungal species (Duarte et al. 2012; Seena et al. 2010). The ITS used in tandem with the IGS and *B-*

tubulin regions was recently used by Brewer and Milgroom (2010) to determine the spread and origin of *E. necator*. The premise of this approach is that the native origin of a pathogen is expected to have higher diversity than in introduced locations due to genetic bottleneck effects (Dlugosch and Parker 2008; Nei et al.1975). I observed such a bottleneck effect in our study in which haplotype 1 is dominant in North America and was the only haplotype present in New Zealand (Figs. 3.4 and 3.5). Based on the genetic diversity from samples, *S. bicornis* is most likely native to Europe where the haplotype diversity is the greatest (Fig. 3.4). Also, *S. bicornis* was first described in 1819 on *A. campestre* in Germany (Braun and Cook 2012), and the oldest sequenced specimen in the current study dated to 1864 from a sample from Europe. In contrast, the oldest sequenced *S. bicornis* specimen in North America I detected in this study was from 1938.

Despite the presence of *S. bicornis* in North America from at least 1938, it was not first reported, using morphological approaches, in the USA, until 2003 from Norway maple (*Acer platanoides* L.), an introduced tree from Europe (Nischwitz and Newcombe 2003). However, I note that all of the specimens I examined from herbaria that were labeled as *S. bicornis* on *A. platanoides* were in fact, based on genetic data, *S. tulasnei*. *Sawadaea tulasnei* has only minor morphological differences from *S. bicornis*. Regardless, *S. bicornis* was first reported in the USA in 2003, and never on *A. macrophyllum* until this study (Farr and Rosmman 2020). Given the extent to which we observed powdery mildew on *A. macrophyllum* in the Western USA (Fig. 3.4), and the lack of a confirmed report (until this study), it is likely that the current epidemic has a recent origin. Moreover, with the current prevalence of *S. bicornis* on *A. macrophyllum* in Washington (Fig. 3.4) and the high susceptibility of *A. macrophyllum* to *S. bicornis* (Fig. 3.3), it also seems likely that the spread of *S. bicornis* throughout Washington is a relatively recent event.

Even though the epidemic in Washington most likely occurred recently, we note that the haplotype causing the epidemic was introduced in North America at least by 1938 based on a herbarium specimen sequenced from British Columbia, Canada. The movement of plant material facilitates the introduction of non-native pathogens (Freinkel 2007; Kliejunas 2010; Maloy 1997). *Acer platanoides* (Norway Maples) has been reportedly grown in the USA as early as 1756 (Leighton 1976), but haplotypes 6 and 7, which are the only haplotypes found to infect *A. platanoides* (Fig 5), have not been located in the USA. Thus, it is unlikely that the powdery mildew affecting *A. macrophyllum* was introduced in the 1700s or later from *A. platanoides*. *Acer Pseudoplatanus* (Sycamore maple), which is the *Acer* sp. most associated with haplotype 1 was introduced in New York and New Jersey by at least 1870 (Harper's Bazaar 1870) and New Zealand by 1880 (CABI 2020). It is possible that *A. Pseudoplatanus* was a vehicle on which haplotype 1 was introduced to New Zealand and to the USA around this time. It is also likely that haplotypes 1 and 4 arrived in North America from two separate introductions, and that haplotype 3 evolved in North America from Haplotype 1 as they are both in group 1 (Fig. 3.5). Alternate explanations are that haplotype 3, which was only present in the USA (Fig. 3.4), has a North American origin, or is present in Europe but was not detected in this study. Additionally, as haplotype 1 was the most frequently sampled (Fig. 3.5), it is possible that this haplotype is the most virulent; indeed, Niu et al. (2016) observed that the most virulent mutants tend to dominate in the environment. To that note, haplotype 3 seems to be much less virulent than haplotype 1 based on its lower incidence in the USA (e.g., 80% of *A. macrophyllum* specimens sequenced contained haplotype 1).

Plant pathogens are an important component of forest ecosystems worldwide, and non-native plant pathogens pose especially considerable threats to these ecosystems (Ploetz et al. 2013). Detecting and identifying plant pathogens and determining if an epidemic is a result of a native or non-native

plant pathogen remains a challenge to the forest management community. To our knowledge, this is the first study that used sequence data from old herbarium specimens of plant pathogens to assist in determining the invasion year and native locality of a common, detrimental fungal plant pathogen. Older herbarium specimens and the genetic data they contain can be valuable resource in efforts to ascertain the arrival and spread of detrimental plant pathogens, as well as provide insights on the epidemiology of plant diseases, and address a broad range of ecological, evolutionary and pathological questions relating to disease. They also complement field-collection efforts to better understand the spread and impact of plant pathogens.

References

Abadi, S. Azouri, D., Mayrose, I., and Pupko, T. 2019. Model selection may not be a mandatory step for phylogeny reconstruction. Nature Communications, 10: 1-11.

Ale-Agha, N., Braun, U., Feige, B. and Jage, H. 2000. A new powdery mildew disease on Aesculus spp. introduced in Europe. Cryptogamie Mycologie 21: 89–92.

Ale-Agha, N., Bolay, A., Braun, U., Feige, B., Jage, H., Kummer, V., Lebeda, A., Piatek, M., Shin, H.-D. and Zimmermannova-Pastircakova, K. 2004. Erysiphe catalpae and Erysiphe elevata in Europe. Mycological Progress 3: 291–296.

Amano, K. 1986. Host Range and Geographical Distribution of the Powdery Mildew Fungi. 2nd ed., Scientific Societies Press.

Anagnostakis, S.L. 1987. Chestnut blight: the classical problem of an introduced pathogen. Mycologia 79: 23–37.

American Phytopathological Society. 2019. Calculating the area under the disease progress curve to quantify disease progress. https://www.apsnet.org/edcenter/disimpactmngmnt/topc/ EcologyAndEpidemiologyInR/DiseaseProgress/Pages/AUDPC.aspx

Austin, C. N., Lakso, A. N., Seem, R. C., Riegel, D. A., Gadoury, D. M., and Wilcox, W. F. 2006. Vineyard Shading Increases Severity of Grapevine Powdery Mildew. Phytopathology 96: S6.

Bade, C., and Carmona, M. 2011. Comparison of methods to assess severity of common rust caused by Puccinia sorghi in maize. Tropical Plant Pathology 36: 264-266.

Betzen, J. 2018. Bigleaf Maple Decline. M.S. Thesis, University of Washington.

Bradshaw, M., and Tobin P. 2020. Sequencing herbarium specimens of a common detrimental plant pathogen (powdery mildew) Phytopathology. First Look. doi: 10.1094/PHYTO-04-20-0139-PER.

Brasier, C. M. 1990. China and the origins of Dutch elm disease: an appraisal. Plant Pathology 39: 5–16. doi: 10.1111/j.1365-3059.1990.tb02470.x.

Braun, U., and Cook, R. 2012. The Taxonomic Manual of the Erysiphales (Powdery Mildews). CBS Biodiversity series No.11.

Brewer, M., and Milgroom, M. (2010). Phylogeography and population structure of the grape powdery mildew fungus, Erysiphe necator, from diverse Vitis species. BMC Evolutionary Biology 10: 268.

Brown, J.K.M., Jessop, A.C., and Rezanoor, H.N. 1991. Genetic uniformity in barley and its powdery mildew pathogen. Proc R Soc B 246: 83–90.

Brown, J. K. M., and Rant, J. C. 2013. Fitness costs and trade-offs of disease resistance and their consequences for breeding arable crops Plant Pathology 62: 83–95. doi: 10.1111/ppa.12163.

Burgess, T.I., Crous, C.J., Slippers, B., Hantula, J., and Wingfield, M.J. 2016. Tree invasions and biosecurity: eco-evolutionary dynamics of hitchhiking fungi. AoB PLANTS 8: plw076

CABI. 2020. *Acer pseudoplatanus* (Sycamore Maple). In: Invasive Species Compendium. Wallingford, UK: CAB International. https://www.cabi.org/isc/datasheet/2884#5F599ECF-F36F-49E9-9FFE-28BF79DA106F.

Cao, X., Yao, D., Xu, X., Zhou, Y., Ding, K., Duan, X., Fan, J., and Luo, Y. 2015. Development of Weather- and Airborne Inoculum-Based Models to Describe Disease Severity of Wheat Powdery Mildew. Plant Disease 99: 395-400.

Carbone I, Kohn LM. 1999. A method for designing primer sets for speciation studies in filamentous ascomycetes. Mycologia. 91:553–556.

Carisse, O., Morissette-Thomas, V., and Van Der Heyden, H. 2013. Lagged Association Between Powdery Mildew Leaf Severity, Airborne Inoculum, Weather, and Crop Losses in Strawberry. Phytopathology 103: 811-21.

Cohen W.B., Yang Z., Stehman S.V., Schroeder T.A., Bell D.M., Masek J.G., Huang C. and Meigs G.W. 2016. Forest disturbance across the conterminous United States from 1985–2012: The emerging dominance of forest decline. For Ecol Manag, 360: 242-252.

Daughtrey, M.L., and Benson D. 2005. Principles of plant health management for ornamental plants. Annual Review of Phytopathology 43:141–169.

Dlugosch, K.M., Parker, I.M. 2008. Founding events in species invasions: genetic variation, adaptive evolution, and the role of multiple introductions. Mol Ecol. 17: 431–449. doi: 10.1111/j.1365-294X.2007.03538.x.

Duarte, S., Seena, S., Bärlocher, F., Cássio, F., Pascoal, C., and Stajich, J. 2012. Preliminary Insights into the Phylogeography of Six Aquatic Hyphomycete Species (Phylogeography of Aquatic Fungi) 7:9 e45289. doi:10.1371/journal.pone.004528.9

Drummond, A., & Rambaut, A. 2007. BEAST: Bayesian evolutionary analysis by sampling trees. BMC Evolutionary Biology. 7: 214.

Ellingham, O., David, J., and Culham, A. 2019. Enhancing identification accuracy for powdery mildews using previously underexploited DNA loci. Mycologia 111: 798-812.

Elliott M., Edmonds R.L. and May S. 2002. Role of fungal diseases in decline of Pacific madrone. Northwest Science 76: 293-303

Ellison, A. M. et al. 2005. Loss of foundation species : consequences for the structure and dynamics of forested ecosystems. Frontiers in Ecology and the Environment 3: 479–486.

Enright, S., and Cipollini, D. 2007. Infection by powdery mildew *Erysiphe cruciferarum* (Erysiphaceae) strongly affects growth and fitness of *Alliaria petiolata* (Brassicaceae). American Journal of Botany 94: 1813-820.

Farr, D. F. and Rossman, A. Y. 2020. Fungal Databases, U.S. National Fungus Collections, ARS, USDA. Available at: https://nt.ars-grin.gov/fungaldatabases/ (Accessed: 15 May 2020).

Felsenstein, J. 1985. Confidence Limits on Phylogenies : An Approach Using the Bootstrap. Evolution. 39: 783–791.

Freinkel, S. 2007. American Chestnut: The Life, Death, and Rebirth of a Perfect Tree. in. University of California Press.

Gernhard T. 2008. The Conditioned Reconstructed Process. Journal of Theoretical Biology 253:769-778.

Gladieux, P., Feurtey, A., Hood, M.E., Snirc, A., Clavel, J., Dutech, C., Roy, M., and Giraud, T. 2014. The population biology of fungal invasions. Molecular Ecology, 24: 1969–1986. doi: 10.1111/mec.13028.

Glawe, D. A. 2008. The Powdery Mildews: A Review of the World's Most Familiar (Yet Poorly Known) Plant Pathogens. Annual Review of Phytopathology 46: 27–51. doi: 10.1146/annurev.phyto.46.081407.104740.

Gómez-Alpizar, L., Carbone, I. and Ristaino, J. B. 2007. An Andean origin of Phytophthora infestans inferred from mitochondrial and nuclear gene genealogies. Proceedings of the National Academy of Sciences of the United States of America 104: 3306–11. doi: 10.1073/pnas.0611479104.

Gortari, F., Guiamet, J., and Graciano, C. 2018. Plant–pathogen interactions: Leaf physiology alterations in poplars infected with rust (Melampsora medusae). Tree Physiology 38: 925-935.

Grove, G.G., Boal, R.J., and Bennett, L. H. 2000. Managing powdery mildew of cherry in Washington orchards and nurseries with spray oils. Online. Plant Health Progress doi: 10.1094/PHP-2000-0728-01-RS.

Harper's Bazaar (1870). Harper's Bazaar. A respository of Fashion. Pleasure, and Instruction. New York, Saturday, August 20, 1870. (3): 530, Mentions *A. pseudoplatanus* as 'a tree best suited for tree plantings' in New York

Hirata, T., and Takamatsu, S. 1996. Nucleotide sequence diversity of rDNA internal transcribed spacers extracted from conidia and cleistothecia of several powdery mildew fungi. Mycoscience 37: 283-288.

Kiss., L. 2005. Powdery Mildew as Invasive Plant Pathogens: New Epidemics Caused by Two North American Species in Europe. Mycological Research 109: 259-260.

Kliejunas, J. 2010. Sudden Oak Death: A Summary of the Literature, U.S. Forest Service. United States Department of Agriculture.

Kumar, S., Stecher, G., and Tamura, K. 2016. MEGA7: Molecular Evolutionary Genetics Analysis Version 7.0 for Bigger Datasets. Molecular Biology and Evolution 33: 1870-1874.

Leighton, A. 1976. American Gardens in the Eighteenth Century. Houghton Mifflin Company, Boston. 514

Loo, J. A. 2008. Ecological impacts of non-indigenous invasive fungi as forest pathogens. Biological Invasions. 11: 81–82. doi: 10.1007/s10530-008-9321-3.

Mack, R. N. 2000. Cultivation fosters plant naturalization by reducing environmental stochasticity. Biological Invasions, 2: 111–122. doi: 10.1023/A:1010088422771.

Martin, M., Cappellini, E., Samaniego, J., Zepeda, M., Campos, P., Seguin-orlando, A., . . . Gilbert, M. 2013. Reconstructing genome evolution in historic samples of the Irish potato famine pathogen. Nature Communications 4: 2172.

Maloy, O. C. 1997. White Pine Blister Rust Control IN North America: A Case History, Annual Review of Phytopathology 35: 87–109. doi: 10.1146/annurev.phyto.35.1.87.

Michael D. Martin, Enrico Cappellini, Jose A. Samaniego, et al. 2013. Reconstructing genome evolution in historic samples of the Irish potato famine pathogen. Nature Communications, 4(1), 2172.

Migliorini, D., Ghelardini, L., Tondini, E., Luchi, N., and Santini, A. 2015. The potential of symptomless potted plants for carrying invasive soilborne plant pathogens. Diversity and Distributions 21: 1218-1229.

Moparthi, S., and Bradshaw, M. 2020. Fungicide efficacy trials for the control of powdery mildew (*Podosphaera cerasi*) on sweet cherry trees (*Prunus avium*). Biocontrol Science and Technology. 1-12. doi:10.1080/09583157.2020.1755616.

Mori, Y., Sato, Y., and Takamatsu, S. 2000. Evolutionary analysis of the powdery mildew fungi using nucleotide sequences of the nuclear ribosomal DNA. Mycologia 92: 74-93.

Nei, M., Maruyama, T., and Chakraborty, R. 1975. The bottleneck effect and genetic variability in populations. Evolution 29: 1–10. doi: 10.2307/2407137.

Niu, X., Zhao, X., Ling, K.S., Levi, A., Sun, Y., and Fan, M. 2016. The FonSIX6 gene acts as an avirulence effector in the *Fusarium oxysporum* f. sp. *niveum*-watermelon pathosystem. Sci Rep. 6: 28146. pmid:27320044

Nischwitz, C., and Newcombe, G. 2003. First Report of Powdery Mildew (Sawadaea bicornis) on Norway Maple (Acer platanoides) in North America. Plant Disease 87: 451.

Olmstead, J., Lang, G., and Grove, G. 2001. Assessment of Severity of Powdery Mildew Infection of Sweet Cherry Leaves by Digital Image Analysis. HortScience, 36: 107-111.

OSU Extension. 2019. Bigleaf maple decline. https://extension.oregonstate.edu/forests/health-managment/bigleaf-maple-decline.

Ploetz, R.C., Hulcr, J., Wingfield, M.J., de Beer, Z.W (2013) Destructive tree diseases associated with ambrosia and bark beetles: Black swan events in tree pathology? Plant Dis. 97:856-872.

R Core Team. 2017. R: A language and environment for statistical computing. R Foundation for Statistical Computing, Vienna, Austria. http://www.R-project.org/

Rambaut A. 2009. Fig Tree ver. 1.3.1. Available at: http://tree.bio.ed.ac.uk/software/figtree.

Ramsey, A. Aug. 2016 "Bigleaf Maple Decline, Update and Next Steps." Tree Link News: https://dnrtreelink.wordpress.com/2016/08/10/bigleaf-maple-decline-update-and-nextsteps/.

Rellou, J. 2018. Introduced Species Summary Project, Columbia University. Available at: http://www.columbia.edu/itc/cerc/danoff-burg/invasion_bio/inv_spp_summ/Cryphonectria_parasitica.htm (Accessed: 14 November 2018).

Royse, D.J., Gregory, L.V., Ayers, J.E., and Cole. H. 1980. Powdery Mildew of Wheat: Relation of Yield Components to Disease Severity. Canadian Journal of Plant Pathology 2:131-36.

Seena, S., Pascoal, C., Marvanova, L., Cassio., F. 2010. DNA barcoding of fungi: a case study using ITS sequences for identifying aquatic hyphomycete species. Fungal Diversity 44: 77–87.

Silvestro, D., and Michalak, I. 2012. RaxmlGUI: A graphical front-end for RAxML. Organisms Diversity & Evolution. 12: 335-337.

Singh, P.N., Singh, S.K., Tetali, S.P., and Lagashetti, A.C. 2017. Biocontrol of powdery mildew of grapes using culture filtrate and biomass of fungal isolates. Plant Pathology & Quarantine 7:181-189.

Stajich, J. E., Berbee, M.L., Blackwell, M., Hibbett, D.S., James, T.Y., Spatafora., J.W., and Taylor, J.W. 2009. The fungi. Current Biology, 19: 840–845.

Stone J.K., Coop L.B. & Manter D.K. 2008. Predicting effects of climate change on Swiss needle cast disease severity in Pacific Northwest forests. Can J Plant Pathol 30: 169-176.

Uchino, H., Watanabe, T., Ramu, K., Sahrawat, K.L., Marimuthu, S., Wani, S. P., and Osamu, I. 2013. Calibrating chlorophyll meter (SPAD-502) reading by specific leaf area for estimating leaf nitrogen concentration in sweet sorghum. Journal of Plant Nutrition 36: 1640–1646. doi: 10.1080/01904167.2013.799190

van Mantgem P.J., Stephenson N.L., Byrne J.C., Daniels L.D., Franklin J.F., Fulé P.Z., Harmon M.E., Larson A.J., Smith J.M., Taylor A.H., and Veblen T.T. 2009. Widespread increase of tree mortality rates in the western United States. Science 323:521-524.

WDNR. 2016. Forest Health Highlights in Washington. United States Department of Agriculture: https://www.dnr.wa.gov/publications/rp_fh_2015_forest_health_highlights.pdf

Walsh, P., Metzger, D., and Higuchi, R. 1991. Chelex 100 as a medium for simple extraction of DNA for PCR-based typing from forensic material. BioTechniques 10: 506-13.

Westcott, C., and Horst, R.K. 1990. Westcott's plant disease handbook. (5th ed. / rev. by R. Kenneth Horst. ed.). New York: Van Nostrand Reinhold.

Yoshida, K., Schuenemann, V., Cano, L., Pais, M., Mishra, B., Sharma, R., . . . Baulcombe, D. 2013. The rise and fall of the Phytophthora infestans lineage that triggered the Irish potato famine. Elife 2, Elife, 2013 May 28, Vol.2.

Yoshida, K., Burbano, H., Krause, J., Thines, M., Weigel, D., Kamoun, S., and Heitman, J. 2014. Mining Herbaria for Plant Pathogen Genomes: Back to the Future. PLOS Pathogens 10(4), E1004028.

Chapter 4: Host evolutionary history dictates susceptibility to disease: Evolution of susceptibility in the Asteraceae to the powdery mildew *Golovinomyces latisporus*.

Abstract

The host range and virulence of pathogens are dependent on interactions with their hosts, and are hypothesized to have evolved as products of a coevolutionary arms race. An understanding of the factors that affect host range and pathogen virulence is becoming more crucial as introduced pathogens infect novel hosts, causing substantial damage to ecosystems. Powdery mildews are detrimental pathogens found worldwide in managed and natural systems. *Golovinomyces latisporus* is a powdery mildew especially damaging to plants within Asteraceae, and in particular plants within *Helianthus*. In this study, I evaluated 126 species within Asteraceae to measure the role of host plant morphological traits and evolutionary history on their suitability and susceptibility to *G. latisporus*. I observed a phylogenetic signal to both host range and susceptibility between and within major clades of the Asteraceae. Phylogenetic statistical methods showed that chlorophyll density, biomass, stomatal index and trichome density were not correlated to disease severity, thus providing evidence that phylogenetic structure, and not plant morphology, is the most reliable predictor of host susceptibility to pathogens. This work sheds light on the role that evolutionary history plays in the plant susceptibility to disease and underscores the relative unimportance of host plant traits in the pathogenicity of powdery mildew.

Introduction

The ability for a pathogen to cause disease, and the amount of disease caused, are dependent on a variety of host-pathogen interactions (Gilbert and Parker 2016). The biological and genetic factors associated with disease are hypothesized to have evolved as products of a coevolutionary arms race between pathogens and their hosts (Anderson et al. 2010). Plant pathogens are known to decrease the fitness of their hosts, resulting in evolutionary pressures on plants to evolve different modes of defense (Goss and Bergelson 2007). Plants defend themselves against pathogens through morphological adaptations (constitutive defenses), and the production of constitutive and induced chemicals (Thaler et al. 1999; Zaynab et al. 2018). An understanding of the factors that affect host range and virulence of pathogens is a crucial avenue of research. This is especially the case for introduced plant pathogens affecting novel plant hosts given the extent to which these novel interactions are causing damage to ecosystems throughout the world (Mack 2000; Ellison et al. 2005; Loo 2008; Stajich et al. 2009).

In recent years, there has been an increase in reports of the damage and spread of the common fungal pathogen, powdery mildew, in both agricultural and natural settings (Ale-Agha et al. 2000 and 2004; Gent et al. 2013; Kiss 2005; Lipps and Madden 1989). Powdery mildews are obligate parasites (Braun and Cooke 2012) that can infect over 10,000 angiosperm species worldwide (Amano 1986). Powdery mildew is a detrimental fungal disease known to collectively affect a number of vegetables, fruits and ornamental plants (Westcott and Horst 1990). Symptoms of powdery mildew first appears on its hosts as white powdery spots that can spread over large areas of the plant and decrease its growth, and its flower and fruit quantity (Daughtrey and Benson 2005). Favorable conditions for disease expression include dense plant growth, low light and temperatures ~25°C (Gubler et al., 1999). High humidity can be favorable for infection and conidial (asexual spores) survival; however,

dry conditions are favorable for colonization, sporulation and dispersal (McGrath 2017). Severe

infections can lead to the death of the plant, and control costs can exceed hundreds of millions of

dollars in California alone (Sambucci et al. 2014).

Multiple genera of plants within Asteraceae are known to be infected by powdery mildew, including

Coreopsis, Helianthus, *Xanthium* and *Zinnia.* Powdery mildews are especially detrimental to *Helianthus*

annuus where they have been reported to reduce agricultural yields (Kontaxis 1986). The Asteraceae

is the largest family of flowering plants with over 418 genera and 2,413 described species. Plants

within Asteraceae are morphologically diverse (Funk et al. 2009). The genus *Helianthus* (sunflowers)

contains 52 species of annual or perennial plants native throughout North America and are found

worldwide (Heiser et al. 1969; Schilling 2006). *Helianthus* species are grown ornamentally as well as

agriculturally for their oil and seeds. It is also a good model system for studies in evolutionary

ecology, and specifically, the evolution of host defense since its species contain a broad range of

morphological attributes and chemical compounds (Mason and Donovan 2015; Mason et al. 2016).

The objectives of this research were to test whether the success of a pathogen to multiple genera

within Asteraceae is a function of (1) the morphological traits of the host plant and/or (2) the

evolutionary history of the host plants. In particular, I evaluated if host evolutionary history is a

predictor for powdery mildew host range and virulence within the Asteraceae.

Methods

The powdery mildew used for inoculum in this study underwent multi-locus phylogenetic and morphological evaluations, and was identified as *Golovinomyces latisporus* (U. Braun) (Qiu et al. 2020).

Greenhouse Experiments

Two separate greenhouse experiments were conducted. One to evaluate the host range of *G. latisporus* and one to evaluate the susceptibility of different species of Asteraceae, listed in Table 1, to *G. latispous*. In the host range experiment 126 species were evaluated, and 62 of these species were evaluated for their susceptibility.

Wild collected seeds were ordered from the U.S. National Plant Germplasm System (2019). Seeds were planted per the recommendations supplied by the U.S. National Plant Germplasm at the Douglas Research Conservatory at the University of Washington. After germination, seedlings were potted in Sunshine #4 potting soil (SunGro, Bellevue WA) in 8.9 × 8.9 cm pots.

Plants were inoculated with a *G. latisporus* specimen growing on *Helianthus annuus* at the University of Washington Farm. The inoculum was made by cutting infected leaves into small pieces using a sterile blade. The leaf pieces were placed into a sterile 50 ml Falcon tube with 10ml of 0.001% Tween 20 and vortexed for 30 seconds. Spores were counted using a hemocytometer and the concentrations were adjusted to 10000 spores/ml. Spores were applied onto the plant using a hand sprayer until the inoculum suspension was visibly running off the leaf. For the host range experiment seedlings were grown for 1 month and the inoculum was applied every three days. If

powdery mildew colonies were observed from naked eye assessments the species was considered a viable host for *G. latisporus*.

For the disease severity experiments, three seedlings of susceptible Asteraceae species from Table 1 were planted in 8.9 cm pots. Severity experiments were conducted in a randomized block design. The average temperature was 22.7°C, and the average relative humidity was 64.0% in the greenhouse during the experiment. The seedlings were inoculated with powdery mildew, as described above, once, at the onset of the experiment. The plants were watered and fertilized on an as need basis using a sub-irrigation system to control for the effect of overhead watering on powdery mildew growth. To minimize insect damage, a soil injection of Xytect 2F™ (21.4% Imidacloprid) was applied to all of the seedlings.

Disease severity measurements were taken once a week for two months using naked eye assessments to estimate the percentage of the entire plant colonized by powdery mildew (accounting for the stem and both the front and back sides of the leaves). Naked eye assessments estimating disease severity based upon leaf coverage are common in powdery mildew studies (Gortari et al. 2018 ; Grove and Bennett 2000; Moparthi and Bradshaw 2020) and has been found to be as accurate as disease analysis software (Bade and Carmona 2011; Olmstead et al. 2020). Additionally, naked eye assessments are faster and more efficient than using disease analysis software, and the software often only estimates disease on leaves without considering the stem.

In the susceptibility experiments, the following plant traits were measured: relative chlorophyll content (measured as SPAD units), above and belowground biomass (as a proxy for growth rate), trichome density, stomata density, epidermal cell density, and stomatal index. Data for growth form,

host ploidy, veination pattern and native locality were acquired from Flora of North America (2020), Kallamadi and Mulpuri (2016), Mason et al. (2015), U.S. National Plant Germplasm System (2019), and Qiu et al. (2018).

Relative chlorophyll content was measured in arbitrary units refered to as 'SPAD units' using a Konica Minolta SPAD 502 Meter (Konica Minolta, Ramsey, NJ, United States). The measurements are a suitable proxy for leaf nitrogen content (Uchino et al. 2013). Three measurements were taken per leaf on different aged leaves (1st node, 2nd node, and 3rd node) on the last sampling day and then averaged to obtain a single SPAD units value.

Above and below ground biomass measurements were taken at the end of the experiment as a proxy for the growth rate of the different plant species. The plants were first placed in buckets full of water to wash the soil of the roots. They were then placed into brown paper bags, and placed in a herbarium dryer for four days at 37.8°C. Above and below ground biomass were separated and individually weighed using an OHAUS BW15US scale (OHAUS, New Jersey).

After measuring biomass, trichome and stomata counts were acquired by taking pictures of leaf peels with a compound microscope. Because plant traits are fairly conserved within species, one leaf was randomly selected from the center node of each plant (total of 3 leaves per species). Leaf peels were made by placing a thin layer of nail polish on the abaxial and adaxial leaf surface. The nail polish was removed from the leaf and placed onto a microscope slide. Pictures were taken of the slides using a compound microscope with an Olympus SC50 camera attached (Olympus Corporation, Tokyo, Japan). Trichome, stomata, and epidermal counts were calculated twice per leaf, on the upper and lower portion of selected leaves (Fig. 1) using Olympus cellSens Imaging software (Olympus

Corporation, Tokyo, Japan). The two measurements were averaged together to calculate a mean measurement per leaf. Stomatal index was calculated according to: Stomatal index=Stomata per mm^2 × 100/ (epidermal cells per mm^2 +stomata per mm^2).

Phylogenetic Inference

A species-level phylogeny of 186 species in the Asteraceae (and outgroup taxon) using a Python implementation (PyPHLAWD, Smith and Walkar 2019) of the PHLAWD pipeline (Smith and Brown 2018) was generated. Briefly, PHLAWD was used to gather sequence data from NCBI, and construct putative orthologs, perform quality filtering (i.e., eliminate sequences <300bp in length and clusters with <5 represented taxa), and concatenate the resulting sequences. Then a maximum likelihood tree was fit with 100 bootstraps using RAxML using a backbone constraint tree based on Mandel et al. (2019), Urbatsch et al. (2000), and the Angiosperm Phylogeny Group (APG IV), and finer-scale relationships were largely congruent with published phylogenies (Timme et al. 2007; Stephens et al. 2015).

Statistical Analyses

Area Under the Disease Progress Curve (AUDPC) values were calculated for the disease severity data using the formula from the American Phytopathological Society (2019). The AUDPC is a useful tool for comparing disease intensity over time (American Phytopathological Society 2019). This type of curve is best suited when evaluating host resistance because it generates a single numerical value that accounts for disease progress over time. AUDPC data were transformed using a square root transformation to satisfy the assumptions of normality, and analyzed in an ANOVA to measure the

effect of phylogenetic clade on susceptibility to *G. latisporus*. Host plant species were grouped based upon their clades presented in Figures 2 and 3. Post hoc tests were based on Tukey's HSD (α = 0.05). All analyses were performed using R version 3.31 (2017).

To determine the effect of the plant traits on disease severity, phylogenetic statistical methods were conducted to compare with conventional ANOVA. The phylogenetic statistical methods took into consideration the evolutionary relationships between host species. Conventional and Phylogenetic ANOVA were conducted to determine the effects of growth form, ploidy, veination pattern, and native locality on disease severity (calculated as AUDPC value). For the ANOVA, differences between treatment means were based on Tukey's HSD (α= 0.05). For the phylogenetic ANOVA the Phytools package (Revell 2012) in R version 3.31 (2017) was used. In the phylogenetic ANOVA differences between treatment means were based on the Holm-Bonferroni method (α = 0.05). The phylogenetic ANOVA function is based on the work of Garland et al. (1993).

Generalized linear regression was used to analyze the effect of growth rate, shoot-to-root ratio, chlorophyll density, trichome density, and stomatal index, on disease severity (calculated as AUDPC value). The traits were evaluated individually and in a model that accounted for interaction effects. Multicollinear predictor variables were not used in the same model. For phylogenetic comparative analyses, we extended zero-length terminal branches (an occasional outcome of phylogenetic inference routines) by the median of all non-zero terminal branch lengths on the tree. I performed phylogenetic generalized least squares (PGLS) regression using the *phylolm* package (Ho and Ané 2014) to assess the relationship between disease severity (AUDPC) and growth rate, shoot/root ratio, chlorophyll density, trichome density, and stomatal index.

Results

Signs of powdery mildew were first noted 6 days post inoculation. Of the 126 species tested, 57 were observed to not be suitable hosts of *G. latisporus* (as defined by visual assessments of colonies forming on the leaves), while 69 were to some extent suitable hosts of *G. latisporus*. The suitablibility of all species as hosts is denoted in Table 1. This study is the first report of host suitability for *G. latisporus* on 58 of these hosts. (Farr and Rossman 2020). All of the *Helianthus* species were susceptible to *G. latisporus*, and overall, species within *Helianthus* were the most susceptible to *G. latisporus*. However, the susceptibility within *Helianthus* ranged from *H. carnosus* as the most susceptible (AUDPC value=2308, sd=530.46) and *H. praecox* being the least (AUDPC value=4.67 , sd=5.35).

Phylogenetic clades within Asteraceae and also within *Helianthus* statistically differed in their susceptibility to *G. latisporus*. Clade A, which consists of species within the Helianthinae, was significantly more susceptible to *G. latisporus* than Clade B, Clade, C and Clade D (P<0.05; Fig. 2). Within the *Helianthus* clade, clade A-3 was more susceptible to *G. latisporus* than clade A-1 (P=0.06) (Fig. 3). The most parsimonious explanation suggested that host recognition (defined as the ability to cause noticeable disease) within Asteraceae evolved separately five times and was lost 4 times (Figs. 2-5). Whether or not host recognition of *G. latisporus* evolved in multiple separate events outside of the Asteraceae cannot be deduced from the current study as only one genus outside of Asteraceae (*Abelmoscus*) was included.

There were no statistical differences of growth form, ploidy, veination pattern and native locality on disease severity in a Phylogenetic ANOVA analysis. However, multiple differences were observed in a conventional ANOVA (Table 2). Statistically significant differences (P<0.05) of susceptibility in a

conventional ANOVA were observed based on the growth form (annual vs perennial), venation patterns and native locality. Annual species, species with a longitudinal leaf venation pattern, and species from southern North America (or outside North America) were significantly less susceptible to powdery mildew caused by *G. latisporus*. Because conventional and phylogenetic ANOVA differed in their results, it cannot be ascertained if the observed differences are due to differences in plant traits alone, or due to evolutionary history. For example, the perennial clade was highly susceptible to *G. latisporus*; however, there have only been approximately three transitions between annual and perennial growth form as sunflowers have diversified. This limits the ability to conclude that increased resistance is due to growth form and not phylogeny (common ancestor evolving resistance).

There was no significance effect of chlorophyll density, stomatal index, trichome density, growth rate and shoot-to-root ratio on plant susceptibility to *G. latisporus* in a phylogenetic least square regression analysis after accounting for multiple tests (Holm 1979), or a in a generalized linear regression, which does not account for phylogenetic relatedness. In a generalized linear regression, none of the plant traits were significant predictors of disease severity.

Discussion

Evolutionary history is a reliable predictor of host range and virulence of *G. latisporus* to species within Asteraceae. This study revealed five clades within Asteraceae that are susceptible to *G. latisporus* (Fig. 2). Within Asteraceae, the phylogenetic structure of susceptibility is seen not only at the family level, but also at the genus level. For example, taxa within Clade A (Fig. 2) are the most susceptible to *G. latisporus*. Additionally, within Clade A, Clade A-3 is the most susceptible (Fig. 3). The phylogenetic clumping of hosts reported in this study agrees with previous work that reported

that evolutionary history predicted host range (Gilbert and Webb 2007; De Vienne et al. 2009), and past work that observed that evolutionary relationships between hosts can be a valid predictor of host range and severity to fungal pathogens as well as insect herbivores (De Vienne et al. 2009; Gilbert and Webb 2007; Gilbert et al. 2015; Gilbert and Parker 2016; King and Cable 2007; Mech et al. 2019; Moore and Gotelli 1996; Perlman and Jaenike 2003). The species grown in this experiment have evolved to different climatic regimes from throughout the world. It is possible the differences in disease resistance observed are due to the different species ability to grow in a controlled greenhouse setting.

The role that constitutive morphological plant traits play in defense against powdery mildew, and whether plant morphology predicts disease, is not known, and past studies in this area have been limited and contradictory (e.g., Chattopadhyay et al. 2011; Kloos et al. 2005, and Jarosz et al. 1982). Consistent with these past contradictions, in this study, a conventional ANOVA revealed significant differences in the susceptibility of hosts based upon their growth habit (perennial vs annual), leaf venation patterns, and host geographic origin. However, there was no significant relationship between any of the plant traits tested and disease susceptibility when using a phylogenetic analyses, which accounts for phylogenetic history and the evolution of shared traits through a common ancestor. Nonetheless, the evaluation of additional traits may yield different results. For example, Mason et al. (2016) found that resistance to powdery mildew was strongly predicted by the abundance of secondary metabolites and that most morphological trait measurements, at the leaf level, were not correlated with powdery mildew resistance.

This is the first study that observed a phylogenetic structure to disease severity at the family and genus level within the same plant-pathogen system. The data presented provides evidence that

phylogeny is a critical predictor of host susceptibility to pathogens. Future work should evaluate clades of other lineages that vary in morphological traits and susceptibility to determine if other systems exhibit similar patterns of susceptibility. Additional traits, such as secondary compounds, should also be intensively evaluated.

References:

Ale-Agha, N., Braun, U., Feige, B. and Jage, H. 2000. A new powdery mildew disease on Aesculus spp. introduced in Europe. Cryptogamie Mycologie 21: 89–92.

Ale-Agha, N., Bolay, A., Braun, U., Feige, B., Jage, H., Kummer, V., Lebeda, A., Piatek, M., Shin, H.-D. and Zimmermannova-Pastircakova, K. 2004. Erysiphe catalpae and Erysiphe elevata in Europe. Mycological Progress 3: 291–296.

Amano, K. 1986. Host Range and Geographical Distribution of the Powdery Mildew Fungi. 2nd ed., Scientific Societies Press.

American Phytopathological Society. 2019. Calculating the area under the disease progress curve to quantify disease progress. https://www.apsnet.org/edcenter/disimpactmngmnt/topc/ EcologyAndEpidemiologyInR/DiseaseProgress/Pages/AUDPC.aspx

Anderson, Jonathan P., Cynthia A. Gleason, Rhonda C. Foley, Peter H. Thrall, Jeremy B. Burdon, and Karam B. Singh. 2010. Plants versus Pathogens: An Evolutionary Arms Race. Functional Plant Biology 37: 499-512.

Angiosperm Phylogeny Group. 2016. An update of the Angiosperm Phylogeny Group classification for the orders and families of flowering plants: APG IV. Botanical Journal of the Linnean Society, 181: 1–20, doi:10.1111/boj.12385

Barkley T.M., Brouillet, L., and Strother, J.L. 2006. Asteraceae. Flora of North America, New York: Oxford University Press 19: 3–69.

Chattopadhyay, S. Ali, K., Doss, S., Das, N., Aggarwal, R., Bandopadhyay, T., Sarkar, A., and Bajpai, A. 2011. Association of leaf micro-morphological characters with powdery mildew resistance in field-grown mulberry (Morus spp.) germplasm. *AoB PLANTS* 11: 1–11 doi: 10.1093/aobpla/plr002.

Daughtrey, M.L., and Benson D. 2005. Principles of plant health management for ornamental plants. Annual Review of Phytopathology 43:141–169.

De Vienne, D. M., Hood, M. E. and Giraud, T. 2009. Phylogenetic determinants of potential host shifts in fungal pathogens. Journal of Evolutionary Biology 22: 2532–2541. doi: 10.1111/j.1420-9101.2009.01878.x.

Ellison, A. M. et al. 2005. Loss of foundation species : consequences for the structure and dynamics of forested ecosystems. Frontiers in Ecology and the Environment 3: 479–486.

Farr, D. F. and Rossman, A. Y. 2020. Fungal Databases, U.S. National Fungus Collections, ARS, USDA. Available at: https://nt.ars-grin.gov/fungaldatabases/ (Accessed: 15 May 2020).

Flora of North America. 2020. Flora of North America. Accessed May 2020: http://beta.floranorthamerica.org/Main_Page

Funk, V.A,. Susanna, A., Steussy, T.F., and Bayer, R.J. 2009. Systematics, evolution, and biogeography of Compositae. Vienna (Austria): International Association for Plant Taxonomy, Institute of Botany, University of Vienna.

Garland, T., Dickerman, A.W., Janis, C.M., and Jones, J. 1993. Phylogenetic analysis of covariance by computer simulation. Systematic Biology 42: 265-92.

Gent, D. H., G. G. Grove, M. E. Nelson, S. N. Wolfenbarger, and J. L. Woods. 2014. Crop Damage Caused by Powdery Mildew on Hop and Its Relationship to Late Season Management. Plant Pathology 63: 625-39.

Gilbert, G. S. and Webb, C. O. 2007. Phylogenetic signal in plant pathogen-host range. Proceedings of the National Academy of Sciences 104: 4979–4983 doi: 10.1073/pnas.0607968104.

Gilbert GS, Briggs HM, Magarey R. 2015. The impact of plant enemies shows a phylogenetic signal. PLOS ONE 10:e0123758

Gilbert, G.S. and I.M. Parker. 2016. The evolutionary ecology of plant disease: a phylogenetic perspective. Annual Review of Phytopathology 54:549-578 doi: 10.1146/annurev-phyto-102313-045959.

Goss, E. M. and Bergelson, J. 2007. Fitness consequences of infection of *Arabidopsis thaliana* with its natural bacterial pathogen *Pseudomonas viridiflava*. Oecologia 152:71–81. doi: 10.1007/s00442-006-0631-9.

Gubler, W. D., Rademacher, M. R. and Vasquez, S. J. 1999. Control of Powdery Mildew Using the UC Davis Powdery Mildew Risk Index. APSnet Feature Articles. doi: 10.1094/APSnetFeature-1999-0199.

Heiser CBJ, Smith DM, Clevenger SB, Martin WCJ. 1969. The North American Sunflowers: Helianthus. Mem Torrey Bot Club. 22:1–218.

Holm, S. 1979. A simple sequentially rejective multiple test procedure. Scandinavian Journal of Statistics, 6: 65–70.

Jarosz, A. M., Sheets, M., and Levy, M. 1982. Cuticle Thickness in Phlox and Resistance to Powdery Mildew: An Unreliable Line of Defense. American Journal of Botany 69: 824–828.

Kallamadi, P., and Mulpuri, S. 2016. Ploidy analysis of Helianthus species by flow cytometry and its use in hybridity confirmation. The Nucleus 59:2, 123-130.

King, T. A., and Cable, J. 2007. Experimental infections of the monogenean Gyrodactylus turnbulli indicate that it is not a strict specialist. Internation Journal for Parasitology 24:185–196 doi: 10.1016/j.ijpara.2006.11.015.

Kiss., L. 2005. Powdery Mildew as Invasive Plant Pathogens: New Epidemics Caused by Two North American Species in Europe. Mycological Research 109: 259-260.

Kloos, W. E., George, C. G. and Sorge, L. K. 2005. Inheritance of powdery mildew resistance and leaf macrohair density in Gerbera hybrida HortScience 40: 1246–1251.

Kontaxis, D. 1986. Managing powdery mildew and rust on sunflower. California Agriculture July, 1986.

Lipps, P.E., and Madden, L.V. 1989. Assessment of methods of determining powdery mildew severity in relation to grain yield of winter wheat cultivars in Ohio. Phytopathology 79: 462–70.

Loo, J. A. 2008. Ecological impacts of non-indigenous invasive fungi as forest pathogens. Biological Invasions. 11: 81–82. doi: 10.1007/s10530-008-9321-3.

Mack, R. N. 2000. Cultivation fosters plant naturalization by reducing environmental stochasticity. Biological Invasions, 2: 111–122. doi: 10.1023/A:1010088422771.

Mason, C.M., and Donovan, L.A. 2015. Evolution of the leaf economics spectrum in herbs: evidence from environmental divergences in leaf physiology across Helianthus (Asteraceae). Evolution 69:2705–2720.

Mason, C.M., Bowsher, A.W., Crowell, B.L., Celoy, R.M., Tsai, C.J., and Donovan, L.A. 2016. Macroevolution of leaf defenses and secondary metabolites across the genus *Helianthus. New Phytologist* 209:1720-1733.

Mandel, J. R., Dikow, R. B., Siniscalchi, C. M., Thapa, R., Watson, L. E., and Funk, V. A. 2019. A fully resolved backbone phylogeny reveals numerous dispersals and explosive diversifications throughout the history of Asteraceae. Proceedings of the National Academy of Sciences, 116:28, 14083-14088.

McGrath, M. T. 2017. Powdery Mildew of Cucurbits fact sheet, Cornell University. Available at: http://vegetablemdonline.ppath.cornell.edu/factsheets/Cucurbits_PM.htm (Accessed: 16 May 2020).

Mech, A., et al. 2019. Evolutionary history predicts high-impact invasions by herbivorous insects. Ecology and Evolution 9:12216-12230.

Moore, J., and Gotelli, N. J. 1996. Evolutionary Patterns of Altered Behavior and Susceptibility in Parasitized Hosts Evolution, 50: 807–819.

Perlman, S. J. and Jaenike, J. 2003. Infection success in novel hosts: An experimental and phylogenetic study of Drosophila-parasitic nematodes. Evolution 57: 544–557 doi: 10.1111/j.0014-3820.2003.tb01546.x.

Qiu, F., Baack, E., Whitney, K., Bock, D., Tetreault, H., Rieseberg, L., and Ungerer, M. 2019. Phylogenetic trends and environmental correlates of nuclear genome size variation in Helianthus sunflowers The New Phytologist 221:3, 1609-1618.

Qiu, P., Liu, S., Bradshaw, M., Latham-Rooney, S., Takamatsu, S., Bulgakov, T., Tang, S., Feng, J., Temitope, T., Li, Y., Wang, L., and Braun, U. 2020. Multi-locus phylogeny and taxonomy of an unresolved, heteroenous species complex within the genus *Golovinomyces* (Ascomycota, Erysiphales), including *G. ambrosiae, G. circumfusus* and *G. spadiceus*. BMC Microbiology 20:51. doi:10.1186/s12866-020-01731-9

R Core Team. 2017. R: A language and environment for statistical computing. R Foundation for Statistical Computing, Vienna, Austria. http://www.R-project.org/

Revell, L. J. 2012. phytools: An R package for phylogenetic comparative biology (and other things). *Methods in Ecology and Evolution* **3**: 217-223.

Salimen M, Yang SM, Wilson L. 1982. Reaction of *Helianthus* species to *Erisiphe cichoracearum*. Plant Disease 66: 572–573.

Sambucci, Olena S., Alston, J., and Fuller, K. 2014. The Costs of Powdery Mildew Management in Grapes and the Value of Resistant Varieties: Evidence from California. California – Center for Wine Economics, Robert Mondavi Institute: http://vinecon.ucdavis.edu/2014/09/11/the-costs-of-powdery-mildew-management-in-grapes-and-the-value-of-resistant-varieties-evidence-from-california/.

Schilling, E. 2006. Helianthus. Flora of North America, New York: Oxford University Press 21:141.

Smith, S. A. and J. W. Brown. 2018. Constructing a broadly inclusive seed plant phylogeny. American Journal of Botany 105:3 1–13.

Smith, S. A. and J. F. Walker. 2019. Py PHLAWD: A python tool for phylogenetic dataset construction. *Methods in Ecology and Evolution* 10: 104-108.

Stajich, J. E., Berbee, M.L., Blackwell, M., Hibbett, D.S., James, T.Y., Spatafora., J.W., and Taylor, J.W. 2009. The fungi. Current Biology, 19: 840–845.

Stephens, J. D., Rogers, W. L., Mason, C. M., Donovan, L. A., and Malmberg, R. L. 2015. Species tree estimation of diploid Helianthus (Asteraceae) using target enrichment. American Journal of Botany 102:6 910-920.

Thaler, J., Fidantsef, S., Duffey, A., and Bostock, L. 1999. Trade-Offs in Plant Defense Against Pathogens and Herbivores: A Field Demonstration of Chemical Elicitors of Induced Resistance. Journal of Chemical Ecology, 25: 1597-1609.

Timme, R. E., Simpson, B. B., and Linder, C. R. 2007. High‐resolution phylogeny for Helianthus (Asteraceae) using the 18S‐26S ribosomal DNA external transcribed spacer. American Journal of Botany 94:11 1837-1852.

Tung H., L. S., and Ané, C. 2014. A linear-time algorithm for Gaussian and non-Gaussian trait evolution models. Systematic biology, 63: 397-408.

Urbatsch, L. E., Baldwin, B. G., and Donoghue, M. J. 2000. Phylogeny of the coneflowers and relatives (Heliantheae: Asteraceae) based on nuclear rDNA internal transcribed spacer (ITS) sequences and chloroplast DNA restriction site data. Systematic Botany, 539-565.

U.S. National Plant Germplasm System. 2019. The U.S. National Plant Germplasm System. Accessed January-October,2019. : https://npgsweb.ars-grin.gov/gringlobal/search.aspx

Westcott, C., and Horst, R.K. 1990. Westcott's plant disease handbook. (5th ed. / rev. by R. Kenneth Horst. ed.). New York: Van Nostrand Reinhold.

Zaynab, M., Fatima, M., Abbas, S., Sharif, Y., Umair, M., Zafar, M., and Bahadar, K. 2018. Role of secondary metabolites in plant defense against pathogens. Microbial Pathogenesis 124: 198-202.

Tables

Chapter 1:

Table 1.1: List of taxa, hosts, vouchers, Genbank accession numbers and references of the sequences used in this study.

Taxa	Host	Voucher	ITS Sequence	LSU Sequence	References
Arthrocladiella mougeotii	*Lycium chinense*	MUMH 851	AB329690	AB329690	Takamatsu et al. 2008a
A. mougeotii	*Lycium chinense*	MUMH 135	AB022380	AB022379	Mori et al. 2000
Blumeria graminis	*Triticum aestivum*	MUMH1707	AB273542	AB273542	Inuma et al. 2007
B. graminis	*Poa nemoralis*	MUMH1040	AB273560	AB273560	Inuma et al. 2007
Brasiliomyces malachrae	*Malvastrum coromandelianum*	MUMH3093	LC191217	LC191217	Cabrera et al. 2018
Bulbomicroidium bauhiniicola	*Bauhinia macranthera*	MUMH6844	LC222311	LC222311	Marmolejo et al. 2018
Byssoascus striatosporus (outgroup)	Found within soil	CBS 642.66	MH858902	AB040688	Sugiyama and Mikawa 2001
Caespitotheca forestalis	*Schinopsis balansae*	MUMH1461	AB193466	AB193467	Unpublished
Cystotheca lanestris	*Quercus canbyi*	MUM6845	LC222312	LC222312	Marmolejo et al. 2018
Cystotheca kusanoi	*Quercus serrata*	TUAMH1286	MG865465	MG865614	Cho et al. 2018
Cystotheca wrightii	*Quercus glauca (ITS)*	MUMH137	AB000932	AB022355	Mori et al. 2000
Erysiphe alphitoides	*Quercus macranthera*	MUMH7008	LC270838	LC270838	Abasova et al. 2018
Erysiphe aquilegiae	*Ranunculus japonicus*	MUMH0287	LC009942	LC009942	Takamatsu et al. 2015

Erysiphe asiatica	*Castanopsis diversifolia*	MUMH4992	AB622218	NG_059210	Meeboon et al. 2012
Erysiphe betae	*Ambrina ambrsioides*	MUMH0395	LC009946	LC009946	Takamatsu et al. 2015
Erysiphe hydrangeae	*Hydrangea paniculata*	MUMH514	LC028983	LC028983	Takamatsu et al. 2015
Erysiphe japonica var. crispulae	*Quercus crispula*	MUM4163	AB701301	AB701306	Meeboon and Takamatsu 2013
Erysiphe japonica var. japonica	*Quercus serrata*	MUMH4582	AB701302	AB701305	Meeboon and Takamatsu 2013
Erysiphe necator	*Vitis vinifera*	MUMH530	LC028996	LC028996	Takamatsu et al. 2015
Erysiphe polygoni	*Polygonum aviculare*	MUMH7036	LC328322	LC328322	Abasova et al. 2018
Erysiphe psuedoviburni	*Viburnum tinus*	WTUF71044	MN431629	MN431629	Bradshaw et al. 2020
Erysiphe trina	*Quercus agrifolia*	MUMH114	AB022351	AB022350	Mori et al. 2000
Golovinomyces latisporus	*Helianthus tuberosus*	MUMH942	AB769419	AB769419	Takamatsu et al. 2015
Golovinomyces artemisiae	*Altermisia vulgalis*	MUMH6849	LC217864	LC217864	Bradshaw et al. 2017
Golovinomyces cichoracearum	*Scorzonera hispanica*	MUMH759	AB077682	AB077681	Matsuda and Takamatsu 2003
Leveillula buddlejae	*Buddleja asiatica*	MUMH7069	LC306655	LC306655	Adhikari et al. 2018
Leveillula elaeagni	*Elaeagnus orientale*	LE192668	AB042642	AB042642	Khodaparast et al. 2001
Leveillula taurica	*Alkanna* cf. *orientalis*	MUMH4898	AB667863	AB667863	Khodaparast et al. 2011
Microidium phyllanthi	*Phyllanthus amarus*	MUM1782	LC259487	AB120755	To-anun et al. 2005

Microidium phyllanthi-reticulati	*Phyllanthus reticulatus*	MUMH1761	LC259486	AB120758	Meeboon and Takamatsu 2017a
Neoerysiphe galeopsidis	*Phlomis tuberosa*	MUMH4676	AB498940	AB498940	Heluta et al. 2010
Neoerysiphe hiratae	*Cacalia delphiniifolia*	MUMH552	AB329669	AB329669	Takamatsu et al. 2008a
Neoerysiphe nevoi	*Tolpis virgata*	MUMH4679	AB498974	AB498974	Heluta et al. 2010
Parauncinula polyspora	*Quercus serrata*	MUMH5223	LC222320	LC222320	Meeboon et al. 2017
Parauncinula septata	*Quercus serrata*	MUMH4840	LC222317	LC222317	Meeboon et al. 2017
Phyllactinia adesmiae	*Adesmia volckmannii*	MUMH1938	LC108834	LC108834	Takamatsu et al. 2016
Phyllactinia guttata	*Corylus* sp.	MUMH927	AB080565	AB080463	Takamatsu et al. 2008b
Phyllactinia lagerstroemiae	*Lagerstroemia speciosa*	MUMH3342	LC177379	LC177379	Meeboon and Takamatsu 2017b
Phyllactinia leveilluloides	*Quercus potosina*	MUMH6549	LC108847	LC108847	Takamatsu et al. 2016a
Phyllactinia obclavata	*Hyandroanthus impetiginosus*	MUMH1876	LC108832	LC108832	Takamatsu et al. 2016a
Pleochaeta polychaeta	*Celtis tala*	MUMH3040	LC108835	LC108835	Takamatsu et al. 2016a
Pleochaeta shiraiana	*Celtis sinensis*	MUMH1742	LC108831	LC108831	Takamatsu et al. 2016a
Pleochaeta turbinata	*Platycyamus regnellii*	VIC26558	AB218773	AB218773	Liberato et al. 2006
Podosphaera amelanchieris	*Amelanchier laevis*	MUM4968	AB525927	AB525927	Takamatsu et al. 2010
Podosphaera aphanis	*Fragaria* sp.	—	MF919433	MF919433	Moparthi et al. 2019
Podosphaera clandestina	*Crataegus* sp.	—	MG062783	MG062783	Moparthi et al. 2019
Podosphaera epilobii	*Epilobium ciliatum*	MUMH1873	AB525926	AB525926	Takamatsu et al. 2010

Pseudoidium javanicum	Acalypha argentea	MUMH5152	AB733592	AB733596	Meeboon et al. 2013b
Pseudoidium javanicum	Acalypha wilkesiana var. marginata	MUMH5559	NR_137528	AB733597	Meeboon et al. 2013b
Sawadaea bicornis	Acer campestre	WTUF71965	MT162616	MT162616	Current Study
S. tulasnei	Acer mono var. marmoratum	MUMH1051	AB193386	AB193399	Hirose et al. 2005
Takamatsuella circinata	Acer sp.	—	DQ066421	—	Unpublished

LE=Herbarium of Komarov Botanical Institute, MUMH=Mie University Mycological Herbarium, VIC=Herbarium of the Universidade Federal de Vicosa, Brazil, TUAMH=Tokyo University of Agriculture Herbarium

Table 1.2: Commonly used primers for the sequencing of the powdery mildews.

Specifity[1]	Primers	Sequence	Recommendations	References
	PM7	5'-RYYGACCCTCCCACCCGTGY-3'	*Erysiphe[2], Leveillula, Phyllactinia[2]*	Seko et al. 2008
	PM6	5'-GYCRCYCTGTCGCGAG-3'	*Arthrocladiella, Erysiphe[2], Podosphaera[2]*	Takamatsu and Kano 2001
	PM5	5'-TTGCTTTGGCGGGCCGGG-3'	*Arthrocladiella, Cystotheca, Erysiphe[2], Podosphaera[2]*	Takamatsu and Kano 2001
	PM3	5'-GKGCTYTMCGCGTAGT-3'	*Erysiphe[2], Leveillula[2], Phyllactinia[2],Podosphaera, Sawadaea*	Mori et al. 2000
	PM10	5'-GGCCGGAAAGTTGTCCAAAC-3'	All genera except *Brasiliomyces, Neoerysiphe,* and *Pleochaeta[2]*	Current Study
	PM28R	5'-ACGTTCACTTTCATTCCGCG-3'	All genera except *Caespitotheca, Cystotheca, Erysiphe[2], Leveillula,* and *Sawadaea[2]*	Current Study
	PM1	5'-TCGGACTGGCCYAGGGAGA-3'	All genera except *Brasiliomyces, Caespitotheca, Cystotheca, Leveillula[2], Phyllactinia[2],* or *Pleochaeta*	Cunnington et al. 2003
	PM2	5'-TCACTCGCCGTTACTGAGGT-3'	All genera except *Caespitotheca, Leveillula[2], Phyllactinia, Pleochaeta* or *Pseudoidium javanicum*	Cunnington et al. 2003
	RPM2	5'-ACCTCAGTAACGGCGAGTGA-3'	All genera except *Caespitotheca, Leveillula[2], Phyllactinia, Pleochaeta* or *Pseudoidium javanicum*	Current Study
	PM11	5'-TACCGCTTCACTCGCCGTTA-3'	All genera except *Pseudoidium javanicum*	Current Study
	PM28F	5'-TAACGGCGAGTGAAGCGGTA3'	All genera except *Pseudoidium javanicum*	Current Study
	NL1	5'-AGTAACGGCGAGTGAAGCGG-3'	All genera	Mori et al. 2000
	NL2	5'-TACTTGTTCGCTATCGGTCT-3'	All genera except *Erysiphe[2], Golovinomyces[2]* or *Phyllactinia[2]*	Mori et al. 2000
	NL3	5'-AGACCGATAGCGAACAAGTA-3'	All genera except *Erysiphe[2], Golovinomyces[2]* or *Phyllactinia[2]*	Mori et al. 2000
	AITS	5'-CGATTGAATGGCTAAGTGAGG-3'	All genera	Current Study
	LSU1	5'-ACCCGCTGAACTTAAGCATA-3'	All genera except *Pseudoidium javanicum*	Scholin et al. 1994
	LSU2	5'-CCTTGGTCCGTGTTTCAAGA-3'	All genera	Scholin et al. 1994
	NLP2	5'-GGTCCCAACAGCTATGCTCT-3'	All genera except *Caespitotheca, Golovinomyces[2], Microidium, Leveillula, Pleochaeta[2],* or *Phyllactinia[2]*.	Mori et al. 2000
	TW13	5'-GGTCCGTGTTTCAAGACG-3'	All genera	Taylor and Bruns (1999)
	TW14	5'-GCTATCCTGAGGGAAACTTC-3'	All genera	Mori et al. 2000
	T3	5'-ACGCTCGAACAGGCATGCCC-3'	All genera except *Caespitotheca, Cystotheca,* or *Parauncinula*	Hirata and Takamatsu 1996
	T4	5'-TCAACAACGGATCTCTTGGC-3'	All genera except *Parauncinula*	Hirata and Takamatsu 1996

122

ITS5	5'-GGAAGTAAAAGTCGTAACAAGG-3'	All genera except *Caespitotheca*	White et al. 1990
ITS1	5'-TCCGTAGGTGAACCTGCGG-3'	All genera	White et al. 1990
ITS4	5'-TCCTCCGCTTATTGATATGC-3'	All genera	White et al. 1990

[1] Relative specificity is an approximation

[2] Amplifies some species within the genus

Information on these primers ability to anneal to *Takamatsuella* spp. and *Pseudoidium javanicum* is lacking due to the limited availability of sequences in GenBank from these genera

123

Table 1.3: Primer pairs for sequencing the ITS and LSU regions of the powdery mildews.

Primer Pairs	Successful Annealing Temperature
AITS/ITS4	55°
AITS/TW14	52°
AITS/PM11	55°
ITS5/ITS4	55°
ITS1/TW14	52°
ITS1/ITS4	55°
ITS1/PM11	55°
ITS1/PM2	57°
ITS1/PM6[1]	52°
ITS1/T3	55°
LSU1/LSU2	53°
NL3/NLP2	54°
NL1/TW14	52°
T4/PM2	56°
PM3/TW14[2]	52°
PM3/NLP2[2]	52°
PM1/ITS4[1]	52°
PM1/PM2[2]	55°
PM1/T3[1]	58°
PM10/PM11	56°
PM10/PM2	56°
PM10/PM28R	56°
PM10/ITS4	55°
PM28F/LSU2	55°

PM28F/PM28R	56°
RPM2/LSU2	55°
RPM2/NLP2	56°
PM5/NLP2	56°
PM5/PM6[1]	52°
PM7/ITS4[1]	52°

[1]Primer set is not reliable
[2]Fresh samples are needed
Successful annealing temperatures and primer pairs were determined generating sequences for Bradshaw et al. (2016), Moparthi et al. (2017), Bradshaw (2018), Braun et al. (2018), Moparthi et al. (2018 a and b), Moparthi et al. (2019), Bradshaw et al. (2020), Qiu et al. (2020) and the current study.

Table 1.4: Taxa, vouchers, collection year, primer pairs, and Genbank accession numbers of specimens sequenced for this study.

Taxa	Vouchers	Collection Year	Primer Pairs ITS	LSU	Genbank Accession	Genbank Blast Results
Arthrocladiella mougeotii	WTUF072395	2018	PM10/PM28R	PM10/PM28R	MT162619	99.9% with *Arthrocladiella mougeotii* (AB329690)
Blumeria graminis	WSP71368	1899	AITS/TW14->PM10/PM28R	AITS/TW14->PM10/PM28R	MT162611	97% with *Blumeria graminis* (AB273567)
Blumeria graminis	WSP2353	1899	AITS/TW14->PM10/PM28R	AITS/TW14->PM10/PM28R	MT162612	97% with *Blumeria graminis* (AB273567)
Blumeria graminis	WSP2385	1915	AITS/TW14->PM10/PM28R	AITS/TW14->PM10/PM28R	MT162613	99.9% with *Blumeria graminis* (AB273555)
Blumeria graminis	WSP2381	1889	AITS/PM11->PM10/ITS4	No Attempt	MT162614	100% with *Blumeria graminis* f. sp. *tritici* (MN861088)
Blumeria graminis	WSP18503	1918	AITS/PM11->PM10/ITS4	No Attempt	MT162615	100% with *Blumeria graminis* f. sp. *tritici* (MN861088)

Erysiphe sp.	WSP51968	1963	PM10/PM2 and AITS/TW13->PM5/NL2	PM28F/PM28R and AITS/TW13->PM5/NL2	MT095112	95% with *Erysiphe symphoricarpi* (LC009970)
Erysiphe sp.	WSP25887	1949	PM10/PM2 and AITS/TW13->PM5/NL2	PM28F/PM28R and AITS/TW13->PM5/NL2	MT095111	95% with *Erysiphe symphoricarpi* (LC009970)
Erysiphe sp.	WSP3941	1912	PM10/PM2	PM28F/PM28R	MT095113	95% with *Erysiphe symphoricarpi* (LC009970)
Erysiphe sp.	DAOM90461	1941	AITS/TW14->PM10/PM28R	AITS/TW14->PM10/PM28R	MT095100	99% with *Erysiphe corylacearum* (LC270863)
Erysiphe sp.	DAOM67867	1959	AITS/TW14->PM10/PM28R	AITS/TW14->PM10/PM28R	MT095099	98% with *Erysiphe corylacearum* (LC009928)
Erysiphe sp.	DAOM152249	1927	ITS1/PM2->PM5/ITS4	RPM2/NLP2->PM28F/PM28R	MT095101	99% with *Erysiphe corylacearum* (MN822722)
Erysiphe sp.	DAOM207741	1927	ITS1/PM2->PM5/ITS4	RPM2/NLP2->PM28F/PM28R	MT095096	99% with *Erysiphe corylacearum* (MN822722)

Golovinomyces verbenae	WSP13634	1941	PM10/PM11	No Attempt	MT162618	99.8% with *Golovinomyces* sp. (LC076840)
Phyllactinia guttata	WTUF072463	2018	AITS/TW14->PM10/PM28R	AITS/TW14->PM10/PM28R	MT162617	100% with *Phyllactinia guttata* (AB080563)
Podosphaera physocarpi	WTUF071972	2018	PM10/PM28	PM10/PM28	MT106655	99% with *Podosphaera cerasi* (MG183669)
Sawadaea bicornis	WTUF071965	2018	PM10/PM11	PM28F/LSU2	MT162616	91% with *Sawadaea nankinensis* (AB353760)
Sawadaea tulsanei	DAOM142798	1894	AITS/PM11->PM10/ITS4	No Attempt	MT162610	100% with *Sawadaea tulasnei* (AB193385)

DAOM= Canadian National Mycological Herbarium, WSP= Charles Gardener Shaw Mycological Herbarium, WTU= University of Washington Herbarium.

Chapter 2:

Table 2.1: List of hosts, origin of specimens, vouchers, Genbank accession numbers and references of the sequences used in this study.

Host	Country of origin	Vouchers[a]	Fungal name	DNA accession numbers		References
				ITS	LSU	
Amphicarpaea edgeworthii	Japan	MUMH0056	*Erysiphe glycines*	LC009910	LC009910	Takamatsu et al. (2015)
Aquilegia sp.	Argentina	BCRU00359	*E. aquilegiae*	LC009883	LC009883	Takamatsu et al. (2015)
Betula pubescens	Ukraine	MUMH2563/DB53533	*E. ornata* var. *ornata*	LC010034	LC010034	Takamatsu et al. (2015)
B. pubescens	Ukraine	MUMH2565/DB53525	*E. ornata* var. *ornata*	LC010036	LC010036	Takamatsu et al. (2015)
B. pubescens	Ukraine	MUMH2564/DB53512	*E. ornata* var. *europaea*	LC010035	LC010035	Takamatsu et al. (2015)
B. pubescens	Ukraine	MUMH2566/DB12835	*E. ornata* var. *europaea*	LC010037	LC010037	Takamatsu et al. (2015)
B. pubescens	Ukraine	MUMH2560/DB53529	*E. ornata* var. *ornata*	LC010032	LC010032	Takamatsu et al. (2015)
Chamaesyce nutans	Japan	MUMH4646	*E. euphorbiae*	LC010073	LC010073	Takamatsu et al. (2015)
Chloranthus serratus	Japan	MUMH202	*E. chloranthi*	LC009931	LC009931	Takamatsu et al. (2015)
Clematis apiifolia	Japan	MUMH277	*E. aquilegiae*	LC009938	LC009938	Takamatsu et al. (2015)
Desmodium lanum	Japan	MUMH0396	*E. glycines*	LC009948	LC009947	Takamatsu et al. (2015)
Isodon trichocarpus	Japan	MUMHs87	*E. huayinensis*	LC010080	LC010080	Takamatsu et al. (2015)
I. umbrosus	Japan	MUMH4644	*E. huayinensis*	LC010072	LC010072	Takamatsu et al. (2015)
Sambucus sieboldiana	Japan	MUMH17	*E. vanbruntiana*	AB015925	LC009909	Takamatsu et al. (1999)
Sedum pallescens	Russia	MUMH2577	*E. sedi*	LC010047	LC010047	Takamatsu et al. (2015)
Sedum sp.	Russia	MUMH2576	*E. sedi*	LC010046	LC010046	Takamatsu et al. (2015)

129

Viburnum carlesii	Germany	GLM-81204	*E. viburni*	MN431620	MN431620	Current Study
V. edule	USA	WTU-F-71043	*E. viburni*	MN431627	MN431627	Current Study
V. edule	USA	WTU-F-71047	*E. viburniphila*	MN431632	MN431632	Current Study
V. lantana	Germany	GLM-F103736	*E. viburni*	MN431618	MN431618	Current Study
V. odoratissimum var. *awabuki*	South Korea	KUS-F27310	*E. pseudoviburni*	MN431595	MN431595	Current Study
V. odoratissimum var. *awabuki*	South Korea	KUS-F27319	*E. pseudoviburni*	MN431596	MN431596	Current Study
V. opulus	Germany	GLM-F99785	*E. viburni*	MN431621	MN431621	Current Study
V. opulus	Germany	GLM-F74776	*E. viburni*	MN431619	MN431619	Current Study
V. opulus	USA	WTU-F-71034	*E. viburni*	MN431624	MN431624	Current Study
V. opulus	USA	WTU-F-71035	*E. viburni*	MN431625	MN431625	Current Study
V. opulus	USA		*E. viburni*	MN431626	MN431626	Current Study
V. opulus subsp. calvescens	China	HMJAU91800	*E. miranda*	MN431597	MN431597	Current Study
V. opulus subsp. calvescens	China	HMJAU91801	*E. miranda*	MN431598	MN431598	Current Study
V. opulus subsp. calvescens	China	HMJAU91802	*E. miranda*	MN431599	MN431599	Current Study
V. opulus subsp. calvescens	China	HMJAU91803	*E. miranda*	MN431600	MN431600	Current Study
V. sargentii	Russia	MUMH2561	*E. miranda*	LC010033	LC010033	Takamatsu et al. (2015)
V. sargentii	South Korea	KUS-F31068	*E. miranda*	MN431616	MN431616	Current Study
V. sargentii	South Korea	KUS-F26341	*E. miranda*	MN431601	MN431601	Current Study
V. sargentii	South Korea	KUS-F26825	*E. miranda*	MN431602	MN431602	Current Study
V. sargentii	South Korea	KUS-F27331	*E. miranda*	MN431603	MN431603	Current Study

V. sargentii	South Korea	KUS-F27861	*E. miranda*	MN431605	MN431605	Current Study
V. sargentii	South Korea	KUS-F29514	*E. miranda*	MN431607	MN431607	Current Study
V. sargentii	South Korea	KUS-F29802	*E. miranda*	MN431609	MN431609	Current Study
V. sargentii	South Korea	KUS-F29939	*E. miranda*	MN431610	MN431610	Current Study
V. sargentii	South Korea	KUS-F30630	*E. miranda*	MN431611	MN431611	Current Study
V. sargentii	South Korea	KUS-F31014	*E. miranda*	MN431612	MN431612	Current Study
V. sargentii	South Korea	KUS-F31019	*E. miranda*	MN431613	MN431613	Current Study
V. sargentii	South Korea	KUS-F31077	*E. miranda*	MN431617	MN431617	Current Study
V. sieboldii	Japan	MUMH1	*E. pseudoviburni*	LC009904	LC009904	Takamatsu et al. (2015)
V. tinus	USA	WTU-F-71044	*E. viburniphila*	MN431629	MN431629	Current Study
V. tinus	USA	WTU-F-71045	*E. viburniphila*	MN431630	MN431630	Current Study
V. tinus	USA	WTU-F-71046	*E. viburniphila*	MN431631	MN431631	Current Study
V. tinus	Russia	HAL 3304F	*E. viburni*	MN431623	MN431623	Current Study
V. tinus	Switzerland	HAL 000355	*E. viburniphila*	MN431628	MN431628	Current Study
V. plicatum	Japan	MUMH794	*E. viburni-plicati*	AB863612	AB863612	Meeboon and Takamatsu (2015)
V. plicatum	Japan	MUMH249	*E. viburni-plicati*	AB863613	AB863613	Meeboon and Takamatsu (2015)
Weigela hortensis	Japan	TPU-1669	*E. diervillae*	AB015931	LC010087	Takamatsu et al. (1999)

[a] BCRU: Universidad Nacional del Comahue, Argentina; HAL: Martin-Luther-University, Gemany; MUMH: Mie University, Mycological Herbarium, Japan; TPU: Herbarium of Toyama Prefectural University, Japan; WTU: Washington Territorial Herbarium, USA.

Chapter 3:

Table 3.1: List of hosts, haplotype numbers, vouchers, fungal species and Genbank accession numbers of specimens evaluated in this study.

Host	Haplotype Numbers	Collection Year	Country of origin	Voucher[a]	Fungal species	DNA accession numbers	
						ITS	LSU
A. campestre	4	2004	Budapest	MUMH688	*S. bicornis*	AB193362	
A. campestre	1	1934	Czech Republic	NY 2945250	*S. bicornis*	MT462324	MT462324
A. campestre	5	1980	Denmark	DAOM 183717	*S. bicornis*	MT462323	MT462323
A. campestre	4	2019	Germany	WTU-F-072519	*S. bicornis*	MT462321	MT462321
A. campestre	4	2019	Germany	WTU-F-072518	*S. bicornis*	MT462320	MT462320
A. campestre	4	2019	Germany	WTU-F-072516	*S. bicornis*	MT462319	MT462319
A. campestre	4	2019	Germany	WTU-F-072515	*S. bicornis*	MT462318	MT462318
A. campestre	4	2019	Germany	WTU-F-072513	*S. bicornis*	MT462317	MT462317
A. campestre	4	2019	Germany	WTU-F-072509	*S. bicornis*	MT462316	MT462316
A. campestre	4	2019	Germany	WTU-F-072507	*S. bicornis*	MT462315	MT462315
A. campestre	4	2019	Austria	WTU-F-072501	*S. bicornis*	MT462314	MT462314
A. campestre	4	2019	Germany	WTU-F-072491	*S. bicornis*	MT462312	MT462312
A. campestre	4	2019	Germany	WTU-F-072481	*S. bicornis*	MT462311	MT462311
A. campestre	4	2004	Germany	MUMH1061	*S. bicornis*	AB193378	
A. campestre	4	1960	Italy	DAOM 105731	*S. bicornis*	MT462325	MT462325
A. campestre	1		United Kingdom		*S. bicornis*	KY660801	

A. campestre	4	2015	United Kingdom		*S. bicornis*	KY661118	
A. campestre	4	2015	United Kingdom		*S. bicornis*	KY660992	
A. campestre	4	2015	United Kingdom		*S. bicornis*	KY660856	
A. campestre	4	2015	United Kingdom		*S. bicornis*	KY661113	
A. campestre	4	2015	United Kingdom		*S. bicornis*	KY660997	
A. campestre	4	2015	United Kingdom		*S. bicornis*	KY660857	
A. campestre	4	2015	United Kingdom		*S. bicornis*	KY660804	
A. campestre	4	2015	United Kingdom		*S. bicornis*	KY660803	
A. campestre	4	2018	Washington, USA	WTU-F-71965	*S. bicornis*	MT462322	MT462322
A. campestre	4	2019	Germany	WTU-F-072496	*S. bicornis*	MT462313	MT462313
A. circinatum	1	2018	Washington, USA	WTU-F-073133	*S. bicornis*	MT462332	MT462332
A. circinatum	1	2018	Washington, USA	WTU-F-072529	*S. bicornis*	MT462327	MT462327
A. circinatum	1	2018	Washington, USA	WTU-F-072525	*S. bicornis*	MT462326	MT462326
A. circinatum	1	2018	Washington, USA	WTU-F-072535	*S. bicornis*	MT462328	MT462328
A. circinatum	3	2018	Washington, USA		*S. bicornis*	MT462334	MT462334
A. circinatum	1	2018	Washington, USA	WTU-F-073117	*S. bicornis*	MT462329	MT462329
A. circinatum	3,4	2018	Washington, USA	WTU-F-073120	*S. bicornis*	MT462330	MT462330
A. circinatum	4	2018	Washington, USA	WTU-F-073130	*S. bicornis*	MT462331	MT462331
A. circinatum	4	2018	Washington, USA		*S. bicornis*	MT462333	MT462333
A. grandidentatum	1	1995	Utah, USA	NY 2943699	*S. bicornis*	MT462335	MT462335

A. grandidentatum	1	1994	Utah, USA	NY 2943701	*S. bicornis*	MT462424	MT462424
A. grandidentatum	1	1991	Utah, USA	NY 2943700	*S. bicornis*	MT462336	MT462336
A. grandidentatum	1		Utah, USA		*S. bicornis*	MN786324	
A. macrophyllum	1	2019	California, USA	WTU-F-073128	*S. bicornis*	MT462364	MT462364
A. macrophyllum	1	1951	Canada	DAOM 34191	*S. bicornis*	MT462368	MT462368
A. macrophyllum	1	1994	Canada	DAOM 221751	*S. bicornis*	MT462369	MT462369
A. macrophyllum	1	2013	Canada		*S. bicornis*	KC291614	
A. macrophyllum	1	1951	Canada	DAOM 34165	*S. bicornis*	MT462370	MT462370
A. macrophyllum	1	1938	Canada	DAOM 5470	*S. bicornis*	MT462371	MT462371
A. macrophyllum	1	2019	Oregon, USA	WTU-F-072522	*S. bicornis*	MT462339	MT462339
A. macrophyllum	1	2019	Oregon, USA	WTU-F-072523	*S. bicornis*	MT462340	MT462340
A. macrophyllum	1	2019	Oregon, USA	WTU-F-072521	*S. bicornis*	MT462338	MT462338
A. macrophyllum	1	2019	Oregon, USA	WTU-F-072520	*S. bicornis*	MT462337	MT462337
A. macrophyllum	1	2018	Washington, USA	WTU-F-073121	*S. bicornis*		MT462433
A. macrophyllum	1	2018	Washington, USA	158	*S. bicornis*		MT462442
A. macrophyllum	1,3	2018	Washington, USA	WTU-F-073111	*S. bicornis*		MT462440
A. macrophyllum	1,3	2018	Washington, USA	WTU-F-073105	*S. bicornis*		MT462437
A. macrophyllum	1	2018	Washington, USA	WTU-F-073122	*S. bicornis*	MT462358	MT462358
A. macrophyllum	1,3	2018	Washington, USA	WTU-F-072528	*S. bicornis*		MT462435
A. macrophyllum	1,3	2018	Washington, USA	WTU-F-072527	*S. bicornis*		MT462434

A. macrophyllum	1,3	2018	Washington, USA	WTU-F-073109	*S. bicornis*		MT462439
A. macrophyllum	3	2018	Washington, USA	WTU-F-073108	*S. bicornis*		MT462438
A. macrophyllum	3	2018	Washington, USA	WTU-F-073112	*S. bicornis*		MT462441
A. macrophyllum	1	2018	Washington, USA	WTU-F-072531	*S. bicornis*		MT462436
A. macrophyllum	1	2018	Washington, USA	WTU-F-073129	*S. bicornis*	MT462365	MT462365
A. macrophyllum	1	2018	Washington, USA	WTU-F-073104	*S. bicornis*	MT462351	MT462351
A. macrophyllum	1	2018	Washington, USA	WTU-F-073103	*S. bicornis*	MT462350	MT462350
A. macrophyllum	1	2018	Washington, USA	WTU-F-073102	*S. bicornis*	MT462349	MT462349
A. macrophyllum	1	2018	Washington, USA	WTU-F-072534	*S. bicornis*	MT462345	MT462345
A. macrophyllum	1	2018	Washington, USA	WTU-F-073118	*S. bicornis*	MT462356	MT462356
A. macrophyllum	1	2018	Washington, USA	WTU-F-073101	*S. bicornis*	MT462348	MT462348
A. macrophyllum	1	2018	Washington, USA	WTU-F-072526	*S. bicornis*	MT462342	MT462342
A. macrophyllum	1	2018	Washington, USA	WTU-F-073124	*S. bicornis*	MT462360	MT462360
A. macrophyllum	1	2018	Washington, USA	WTU-F-073126	*S. bicornis*	MT462362	MT462362
A. macrophyllum	1	2018	Washington, USA	WTU-F-072524	*S. bicornis*	MT462341	MT462341
A. macrophyllum	1	2018	Washington, USA	WTU-F-072533	*S. bicornis*	MT462344	MT462344
A. macrophyllum	1	2018	Washington, USA	WTU-F-073119	*S. bicornis*	MT462357	MT462357
A. macrophyllum	1	2018	Washington, USA	WTU-F-072536	*S. bicornis*	MT462346	MT462346
A. macrophyllum	1,3	2018	Washington, USA	WTU-F-072530	*S. bicornis*	MT462343	MT462343
A. macrophyllum	3	2018	Washington, USA	519	*S. bicornis*	MT462366	MT462366

A. macrophyllum	1	2018	Washington, USA	WTU-F-073114	S. bicornis	MT462355	MT462355
A. macrophyllum	1	2018	Washington, USA	WTU-F-073123	S. bicornis	MT462359	MT462359
A. macrophyllum	1	2018	Washington, USA	WTU-F-073107	S. bicornis	MT462353	MT462353
A. macrophyllum	3	2018	Washington, USA	WTU-F-073125	S. bicornis	MT462361	MT462361
A. macrophyllum	3	2018	Washington, USA	WTU-F-073106	S. bicornis	MT462352	MT462352
A. macrophyllum	1,3,4	2018	Washington, USA	WTU-F-073131	S. bicornis	MT462367	MT462367
A. macrophyllum	1	2018	Washington, USA	WTU-F-073100	S. bicornis	MT462347	MT462347
A. negundo	1	2019	Germany	WTU-F-072493	S. bicornis	MT462372	MT462372
A. negundo	1	2019	Germany	WTU-F-072510	S. bicornis	MT462373	MT462373
A. negundo	1	2013	New Zealand	PDD 97186	S. bicornis	MT462375	MT462375
A. negundo	1	2019	New Zealand	WTU-F-073132	S. bicornis	MT462374	MT462374
A. platanoides	6	2018	Germany	WTU-F-072498	S. bicornis	MT462384	MT462384
A. platanoides	6	2019	Germany	WTU-F-072503	S. bicornis	MT462387	MT462387
A. platanoides	6	2019	Germany	WTU-F-072486	S. bicornis	MT462379	MT462379
A. platanoides	7	2019	Austria	WTU-F-072502	S. bicornis	MT462385	MT462385
A. platanoides	7	2019	Germany	WTU-F-072494	S. bicornis	MT462382	MT462382
A. platanoides	7	2019	Germany	WTU-F-072490	S. bicornis	MT462381	MT462381
A. platanoides	7	2019	Germany	WTU-F-072482	S. bicornis	MT462377	MT462377
A. platanoides	7	2019	Germany	WTU-F-072489	S. bicornis	MT462380	MT462380
A. platanoides	7	1995	Switzerland		S. bicornis	AF298540	

A. pseudoplatanus	1	2019	Germany	WTU-F-072511	*S. bicornis*	MT462396	MT462396
A. pseudoplatanus	1	2019	Germany	WTU-F-072508	*S. bicornis*	MT462408	MT462408
A. pseudoplatanus	1	1999	United Kingdom	TNS 87522	*S. bicornis*	MT462409	MT462409
A. pseudoplatanus	1	2015	United Kingdom		*S. bicornis*	KY660727	
A. pseudoplatanus	4	1947	Germany	NY294244	*S. bicornis*	MT462398	MT462398
A. pseudoplatanus	1	2008	Austria	WSP 071781	*S. bicornis*	MT462410	MT462410
A. pseudoplatanus	1	2019	Germany	WTU-F-072517	*S. bicornis*	MT462414	MT462414
A. pseudoplatanus	1	2019	Germany	WTU-F-072514	*S. bicornis*	MT462413	MT462413
A. pseudoplatanus	1	2019	Germany	WTU-F-072512	*S. bicornis*	MT462412	MT462412
A. pseudoplatanus	1	2019	Germany	WTU-F-072483	*S. bicornis*	MT462402	MT462402
A. pseudoplatanus	1	2019	Austria	WTU-F-072500	*S. bicornis*	MT462406	MT462406
A. pseudoplatanus	1	2019	Germany	WTU-F-072497	*S. bicornis*	MT462405	MT462405
A. pseudoplatanus	1	2019	Germany	WTU-F-072488	*S. bicornis*	MT462404	MT462404
A. pseudoplatanus	1	2019	Germany	WTU-F-072485	*S. bicornis*	MT462403	MT462403
A. pseudoplatanus	1	2019	Germany	WTU-F-072505	*S. bicornis*	MT462407	MT462407
A. pseudoplatanus	1	2019	Germany	WTU-F-072480	*S. bicornis*	MT462401	MT462401
A. pseudoplatanus	1	2019	Germany	WTU-F-072478	*S. bicornis*	MT462400	MT462400
A. pseudoplatanus	1	2019	Germany	WTU-F-072477	*S. bicornis*	MT462399	MT462399
A. pseudoplatanus	1		New Zealand	PDD 105910	*S. bicornis*	MK432779/ MT462397	MT462397

A. pseudoplatanus	2	2004	United Kingdom	MUMH904	*S. bicornis*	AB193380	
A. pseudoplatanus	1	2015	United Kingdom		*S. bicornis*	KY660984	
A. pseudoplatanus	1	2015	United Kingdom		*S. bicornis*	KY661006	
A. pseudoplatanus	1	2015	United Kingdom		*S. bicornis*	KY661005	
A. pseudoplatanus	1	2015	United Kingdom		*S. bicornis*	KY661004	
A. pseudoplatanus	1	2015	United Kingdom		*S. bicornis*	KY661001	
A. pseudoplatanus	1	2015	United Kingdom		*S. bicornis*	KY661000	
A. pseudoplatanus	1	2015	United Kingdom		*S. bicornis*	KY660999	
A. pseudoplatanus	1	2015	United Kingdom		*S. bicornis*	KY660996	
A. pseudoplatanus	1	2015	United Kingdom		*S. bicornis*	KY660993	
A. pseudoplatanus	1	2015	United Kingdom		*S. bicornis*	KY660990	
A. pseudoplatanus	1	2015	United Kingdom		*S. bicornis*	KY660989	
A. pseudoplatanus	1	2015	United Kingdom		*S. bicornis*	KY660988	
A. pseudoplatanus	1	2015	United Kingdom		*S. bicornis*	KY660986	
A. pseudoplatanus	1	2015	United Kingdom		*S. bicornis*	KY660802	
A. pseudoplatanus	1	2015	United Kingdom		*S. bicornis*	KY660722	
A. pseudoplatanus	1	2015	United Kingdom		*S. bicornis*	KY660995	
A. pseudoplatanus	1	2015	United Kingdom		*S. bicornis*	KY660987	
A. pseudoplatanus	1	2015	United Kingdom		*S. bicornis*	KY660985	
A. pseudoplatanus	4	1947	United Kingdom	DAOM 152865	*S. bicornis*	MT462411	MT462411

A. saccharinum	1	2019	Germany	WTU-F-072492	*S. bicornis*	MT462415	MT462415
A. tataricum	1	1930	Hungary	NY2945253	*S. bicornis*	MT462416	MT462416
A. tsinglingense	2	2013	China		*S. bicornis*	KR048114	
Acer campestre	7	2004	Armenia	MUMH1062	*S. bicornis*	AB193379	
Acer sp.	1			NY2935821	*S. bicornis*	MT462417	MT462417
Acer sp.	4	1959	United Kingdom	DAOM 140250	*S. bicornis*	MT462418	MT462418
Acer sp.	4	1864	United Kingdom	NY2945434	*S. bicornis*	MT462419	MT462419
A. buergerianum		2019	China	HMJAU-PM91883	*S. nankinensis*	MT462310	MT462310
A. mandshuricum		2005	China	HMJAU00446	*S. negundinis*		MT462443
A. mono		2005	China	HMJAU00746	*S. negundinis*		MT462444
A. negundo		2017	China	HMJAU-PM91882	*S. negundinis*		MT462445
A. negundo		2017	China	HMJAU-PM91881	*S. negundinis*		MT462446
A. negundo		2017	China	HMJAU-PM91880	*S. negundinis*		MT462447
A. negundo		2017	China	HMJAU-PM91879	*S. negundinis*		MT462448
A. negundo		2014	China	HMJAU02219	*S. negundinis*		MT462449
A. negundo		2013	China	HMJAU02207	*S. negundinis*		MT462450
A. negundo		2011	China	HMJAU00794	*S. negundinis*		MT462451
A. tataricum		2011	China	HMJAU-00749	*S. negundinis*	MT462420	MT462420
Alectryon excelsus		2015	New Zealand	PDD 106188	*S. negundinis*	MT462421	MT462421
Alectryon excelsus		2007	New Zealand	PDD 93793	*S. negundinis*	MT462422	MT462422

A. palmatum	2018	China	HMJAU-PM91885	*S. polyfida*		MT462453
A. palmatum	2018	China	HMJAU-PM91884	*S. polyfida*		MT462452
A. macrophyllum	2018	Washington, USA	WTU-F-073113	*S. tulasnei*	MT462354	MT462354
A. macrophyllum	2018	Washington, USA	WTU-F-073127	*S. tulasnei*	MT462363	MT462363
A. pictum	2018	China	HMJAU-PM91889	*S. tulasnei*		MT462457
A. platanoides	2019	Germany	WTU-F-072503	*S. tulasnei*	MT462386	MT462386
A. platanoides	2019	Germany	WTU-F-072486	*S. tulasnei*	MT462378	MT462378
A. platanoides	2019	Germany	WTU-F-072479	*S. tulasnei*	MT462376	MT462376
A. platanoides	2019	Germany	WTU-F-072506	*S. tulasnei*	MT462388	MT462388
A. platanoides	2019	Germany	WTU-F-072498	*S. tulasnei*	MT462383	MT462383
A. platanoides	1892	Sweden	DAOM 142794	*S. tulasnei*	MT462391	MT462391
A. platanoides	1892	Sweden	DAOM 142796	*S. tulasnei*	MT462395	MT462395
A. platanoides	1895	Sweden	DAOM 142795	*S. tulasnei*	MT462392	MT462392
A. platanoides	1894	Sweden	DAOM 142798	*S. tulasnei*	MT462393	MT462393
A. platanoides	1892	Sweden	DAOM 142799	*S. tulasnei*	MT462394	MT462394
A. platanoides	2019	Washington, USA	WTU-F-072532	*S. tulasnei*		MT462454
A. platanoides	2019	Washington, USA	WTU-F-073116	*S. tulasnei*	MT462390	MT462390
A. platanoides	2019	Washington, USA	WTU-F-073110	*S. tulasnei*	MT462389	MT462389
A. platanoides	2019	Germany	WTU-F-72494	*S. tulasnei*	MT462425	MT462425
A. tataricum	2018	China	HMJAU-PM91888	*S. tulasnei*		MT462456

A. tataricum	2019	China	HMJAU-PM91886	*S. tulasnei*		MT462455
A. truncatum	2015	China	HMJAU-PM91878	*S. tulasnei*		MT462458
A. truncatum	2005	China	HMJAU00450	*S. tulasnei*	MT462423	MT462423

Table 3.2: Haplotypes and polymorphic sites among isolates of S. bicornis based on sequences of the ITS and LSU genomic regions.

HAPLOTYPE	POLYMORPHIC SITES[1] 1 2 3/ 4 5 6 / 7 8 9 / 10 GAT/GCA/CCT/C	PREDOMINANT HOST AND REGION
1	* * * / * * * / * * */ *	Worldwide on a variety of hosts
2	T * * / * * * / * * */ *	China and Europe on *Acer tsinglingense* and *Acer pseudoplatnoides*
3	* * * / * * G / * * C/ *	North America on *Acer macrophyllum* and *Acer circinatum*.
4	* G A / A * G / * T C / T	Europe and North America on *Acer campestre* and *Acer circinatum*.
5	* G A / A G G / * T C / T	Europe on *Acer campestre*
6	* G A / A * * / T T C / T	Europe on *Acer platanoides* and *A. campestre*
7	* G A / A * * / * T C / T	Europe on *Acer platanoides*

[1]Within the ITS region of *Sawadaea bicornis* specimens submitted to Genbank, **site one** is located at nucleotide number 1, **site two** is at nucleotide 5, **site three** is at nucleotide 53, **site four** is at nucleotide 74, **site five** is at nucleotide 116, **site six** is at nucleotide 338, **site seven** is at nucleotide 446, **site eight** is at nucleotide 461, **site nine** is at nucleotide 932 and **site ten** is at nucleotide 1004.

Chapter 4:

Table 4.1: A list of the species, Grin Accession numbers and results of the host range test, of the different taxa evaluated in this study.

Species	Grin Accession Number	Host to *G. latisporus*
Abelmoschus caillei	PI 489996	-
Abelmoschus esculentus	PI 538081	+
Abelmoschus manihot	PI 497169	+
Acamptopappus sphaerocephalus	W6 55157	-
Achillea alpina	W6 43984	-
Agoseris grandiflora	W6 55699	-
Ambrosia dumosa	W6 55748	+
Anaphalis margaritacea	W6 55826	-
Anisocarpus madioides	W6 55711	-
Artemisia borealis	W6 44017	-
Artemisia frigida	W6 55311	-
Artemisia ludoviciana	W6 55285	-
Artemisia tilesii	W6 44020	-
Artemisia tridentate	W6 55287	-
Baccharis sarothroides	W6 55856	+
Baileya multiradiata	Ames 31297	-
Baileya pleiradiata	Ames 31298	-
Balsamorhiza hookeri	W6 55214	+
Bebbia juncea	W6 56017	+

Chaenactis carphoclinia	W6 55647	-
Chaenactis stevioides	W6 55542	-
Coreopsis delphiniifolia	PI 667447	+
Coreopsis major	PI 667398	+
Coreopsis palmata	PI 667298	+
Coreopsis pubescens	PI 667445	+
Coreopsis tinctoria	PI 667433	+
Coreopsis tripteris	PI 667379	+
Coreopsis verticillata	PI 667439	+
Echinacea pallida	PI 631309	-
Echinacea simulata	PI 631308	-
Encelia farinose	W6 55744	+
Ericameria nauseosa	W6 55964	-
Erigeron acris	W6 44116	-
Erigeron pumilus	W6 55617	-
Geraea canescens	W6 55740	-
Grindelia squarrosa	W6 55309	-
Gutierrezia microcephela	W6 55789	-
Helenium amarum	PI 667461	-
Helianthella uniflora	Ames 32505	-
Helianthus angustifolius	PI 435355	+
Helianthus annuus	PI 597899	+
Helianthus argophyllus	PI 649862	+

Helianthus arizonensis	PI 653549	+	145
Helianthus atrorubens	PI 468655	+	
Helianthus bolanderi	PI 673142	+	
Helianthus californicus	PI 664602	+	
Helianthus carnosus	PI 649956	+	
Helianthus cusickii	PI 664657	+	
Helianthus debilis subsp. cucumerifolius	PI 597908	+	
Helianthus debilis subsp. debilis	PI 597909	+	
Helianthus debilis subsp. silvestris	PI 435651	+	
Helianthus debilis subsp. tardiflorus	PI 468689	+	
Helianthus debilis subsp. vestitus	PI 468693	+	
Helianthus decapetalus	PI 468697	+	
Helianthus divaricatus	PI 664603	+	
Helianthus eggertii	PI 649974	+	
Helianthus exilis	PI 435644	+	
Helianthus floridanus	PI 468715	+	
Helianthus giganteus	PI 649984	+	
Helianthus heterophyllus	PI 664727	+	
Helianthus laevigatus	PI 503226	+	
Helianthus maximiliani	PI 650002	+	
Helianthus microcephalus	PI 650012	+	
Helianthus mollis	PI 650013	+	
Helianthus nuttallii	PI 592349	+	

Helianthus nuttallii subsp. nuttallii	PI 586905	+
Helianthus occidentalis	PI 435788	+
Helianthus occidentalis subsp. plantagineus	PI 494591	+
Helianthus pauciflorus subsp. pauciflorus	PI 494612	+
Helianthus pauciflorus subsp. subrhomboideus	PI 664605	+
Helianthus petiolaris	PI 597923	+
Helianthus petiolaris sunsp. petiolaris	PI 613761	+
Helianthus praecox	PI 413176	+
Helianthus praecox subsp. hirtus	PI 435854	+
Helianthus praecox subsp. praecox	PI 435847	+
Helianthus praecox subsp. runyonii	PI 435849	+
Helianthus radula	PI 468871	+
Helianthus salicifolius	PI 664758	+
Helianthus simulans	PI 435880	+
Helianthus smithii	PI 664699	+
Helianthus strumosus	PI 435888	+
Helianthus tuberosus	PI 650091	+
Heliomeris multiflora	W6 55678	+
Heterotheca villosa	W6 56421	-
Hymenoxys odorata	W6 55547	-
Lactuca serriola	W6 37142	-
Lasthenia gracilis	W6 55494	-
Layia platyglossa	W6 55488	-

Leucanthemum vulgare	PI 667405	-
Madia sativa	W6 55713	-
Melampodium leucanthum	W6 55501	+
Microseris douglasii	W6 55687	-
Monarda fistulosa	Ames 32579	-
Monolopia stricta	W6 55489	-
Nothocalais troximoides	W6 55215	-
Packera multilobata	W6 55184	-
Parthenium argentatum	W6 2189	+
Parthenium incanum	PARL 788	+
Rafinesquia neomexicana	W6 55729	-
Ratibida pinnata	PI 673957	-
Ratibida tagetes	W6 56394	+
Rudbeckia hirta	PI 667348	-
Rudbeckia laciniata	PI 667356	-
Rudbeckia mohrii	PI 667450	-
Rudbeckia mollis	PI 667358	-
Rudbeckia occidentalis	W6 55815	-
Rudbeckia triloba	PI 667354	-
Sanvitalia abertii	W6 55552	+
Solidago wrightii	W6 55870	-
Stenotus armerioides	W6 55290	-
Symphyotrichum novae-angliae	PI 667296	-

Tanacetum camphoratum	Ames 29955	-
Taraxacum kok-saghyz	W6 35156	-
Thelesperma megapotamicum	W6 55561	-
Thymophylla pentachaeta	W6 55559	-
Townsendia incana	W6 55618	-
Viguiera dentata	W6 55842	+
Xanthisma gracile	W6 55657	-
Xanthisma grindelioides	W6 55623	-
Xanthium spinosum	KSB: 114253	+
Xanthium strumarium	W6 30049	+
Xylorhiza tortifolia	W6 55755	-
Xylorhiza venusta	W6 55182	-
Zinnia bicolor	PI 613039	+
Zinnia elegans	PI 586635	+
Zinnia peruviana	PI 410404	+

Table 4.2: Results of Conventional and Phylogenetic ANOVA evaluating the effects of plant host traits on susceptibility to *G. latisporus*.

Plant Trait	AUDPC Means			
Growth Form	Annual		Perennial	
	475.8^{a1}		832.67^{a2}	
Ploidy	Diploid (2n)	Tetraploid (4n)	Hexaploid (6n)	
	804.44^{a1}	284.833^{a1}	743.08^{a1}	
Venation Patterns	Intermediate/Variable	Longitudinal	Palmate	Pinnate
	1040.28^{a34}	2144.37^{a4}	350.73^{a2}	463.46^{a23}
Native Locality	Northern and Southern North America	Southern North America	Outside North America	
	714.72^{a1}	349.44^{a2}	35.29^{a2}	

Means within rows with the same number are not statistically different ($p<0.05$) in an ANOVA

Means within rows with the same letter are not significantly different ($p<0.05$) in a Phylogenetic ANOVA

Chapter 1:
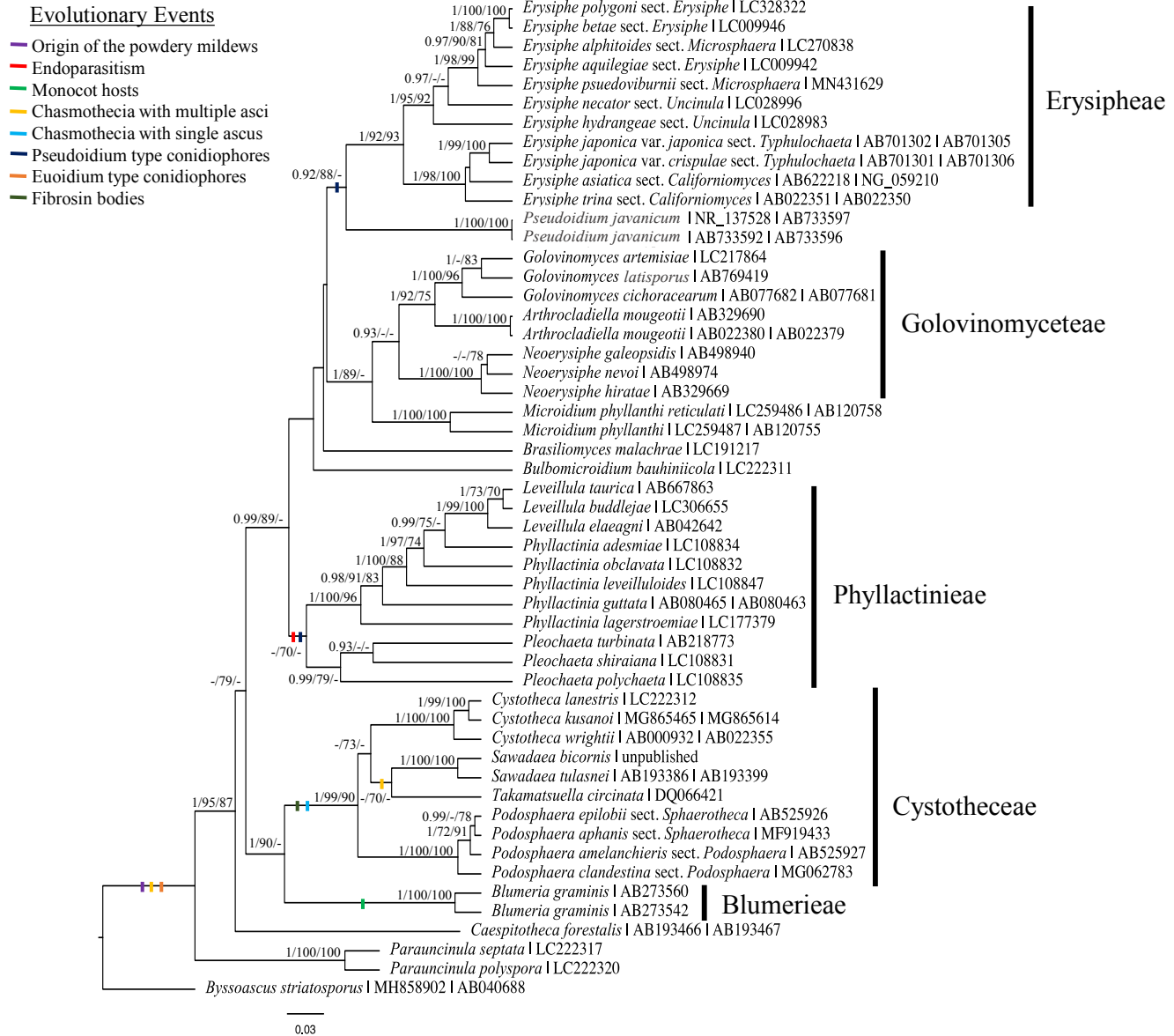
Figure 1.1: An ITS+LSU phylogenetic tree of powdery mildew specimens from each Erysiphaceae genus showing the five powdery mildew tribes. There is no support that *Parauncinula* is part of the Erysiphaceae clade. Posterior probabilities ≥ 90 are displayed followed by bootstrap values greater than 70% for the maximum likelihood (ML) and maximum parsimony (MP) analyses. Evolutionary events were added to the tree based on information from Braun and Cook (2012) and Takamatsu (2013b).
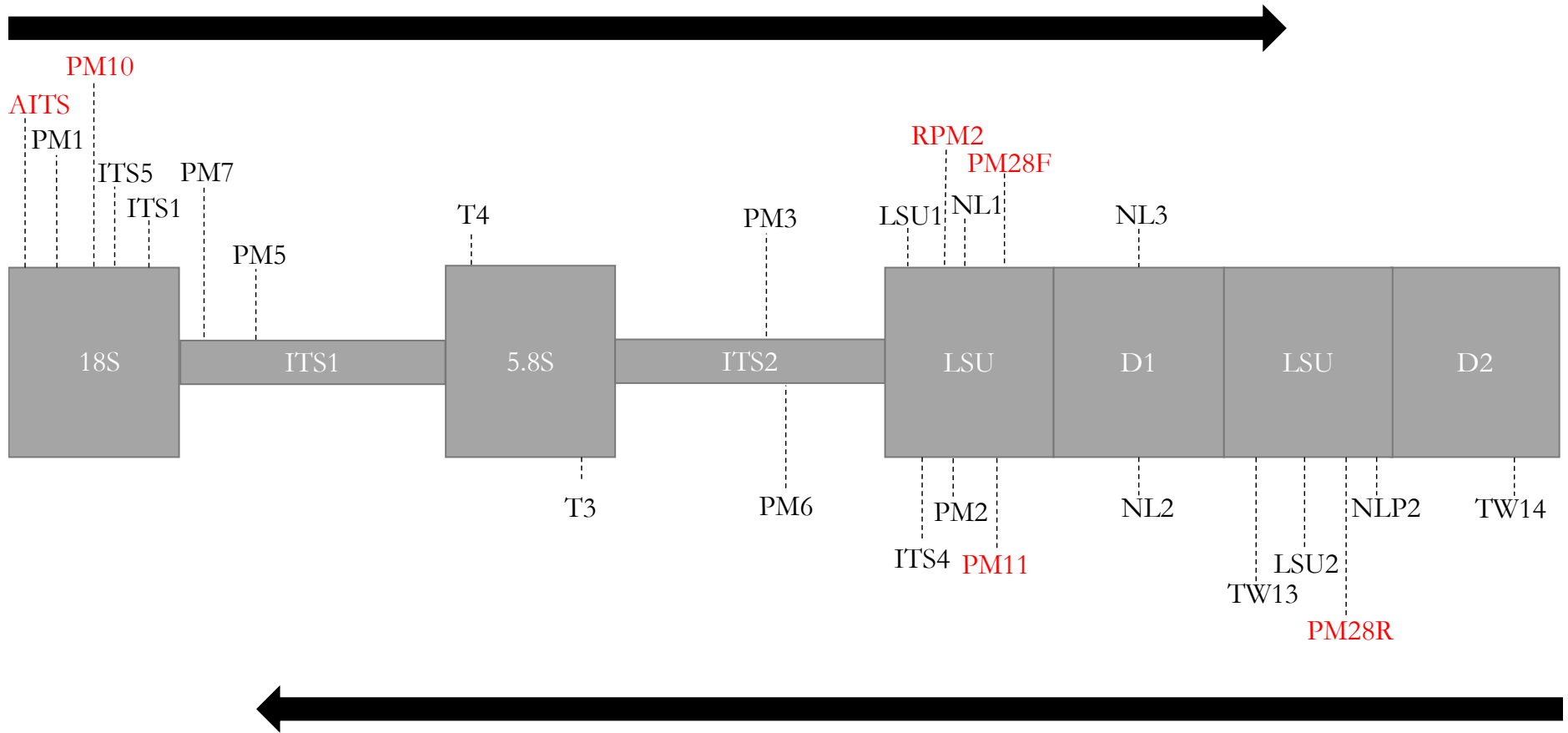
Figure 1.2: Map of primers for sequencing the ITS + LSU regions of the powdery mildews. Primers in red were generated for this study. The exact position of the primers is an approximation. Primers with 'PM' in their label are specific to powdery mildews.
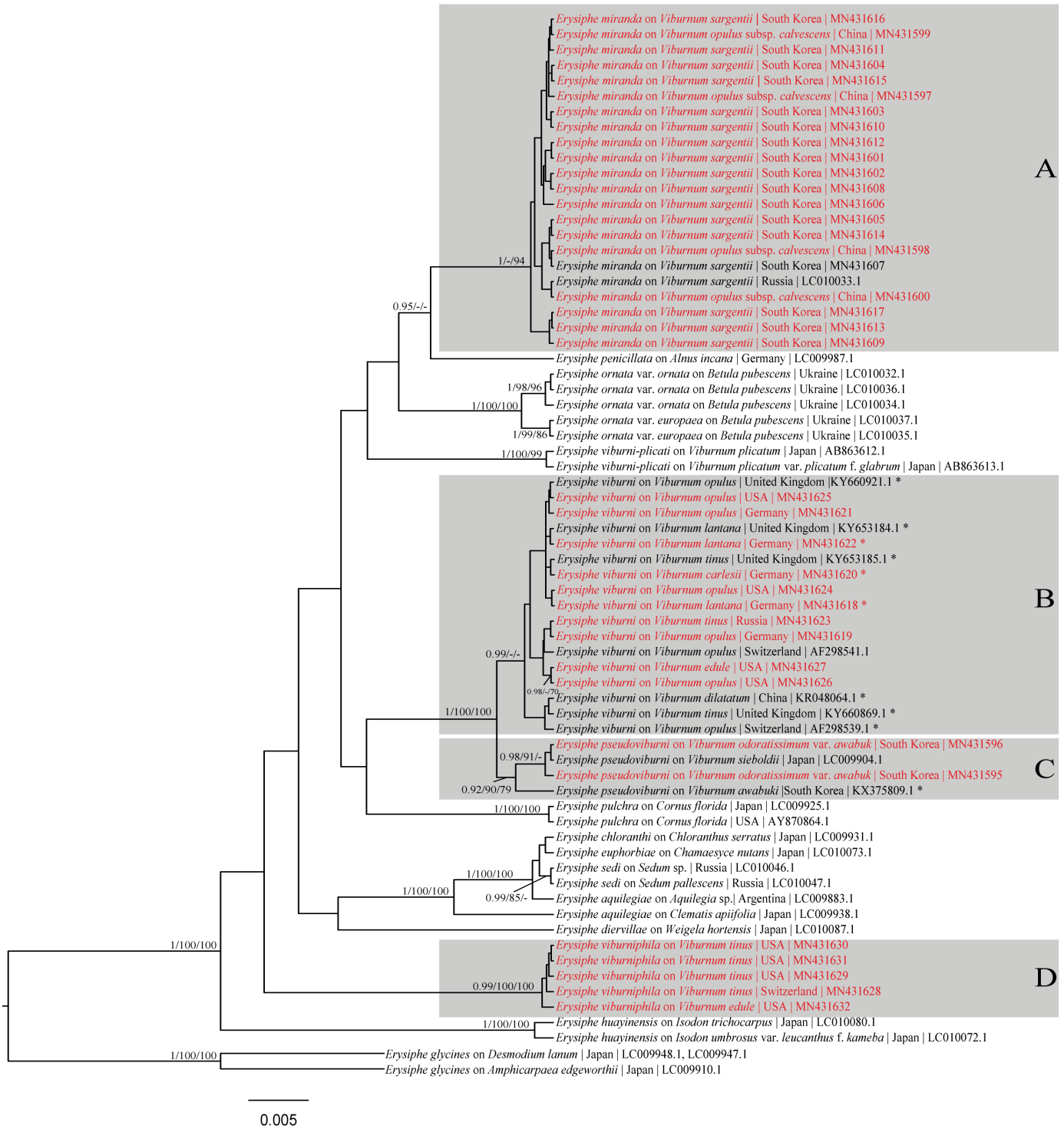
Figure 2.1: Bayesian maximum clade credibility tree of sequences from the combined rDNA ITS regions and the divergent domains D1 and D2 of the LSU rDNA. Posterior probabilities $\geq$ 90 are displayed followed by bootstrap values greater than 70% for the maximum likelihood (ML) and maximum parsimony (MP) analyses conducted. Sequences in red were obtained for this study. A) Clade consisting of *Erysiphe miranda.* B) Clade consisting of numerous taxa previously referred to as *Erysiphe hedwigii* and *Erysiphe viburni.* Taxa denoted with an * were previously identified as *Erysiphe hedwigii.* C) Clade consisting of an undesribed species, *Erysiphe pseudoviburni.* D) Clade consisting of an undescribed species, *Erysiphe viburniphila.*
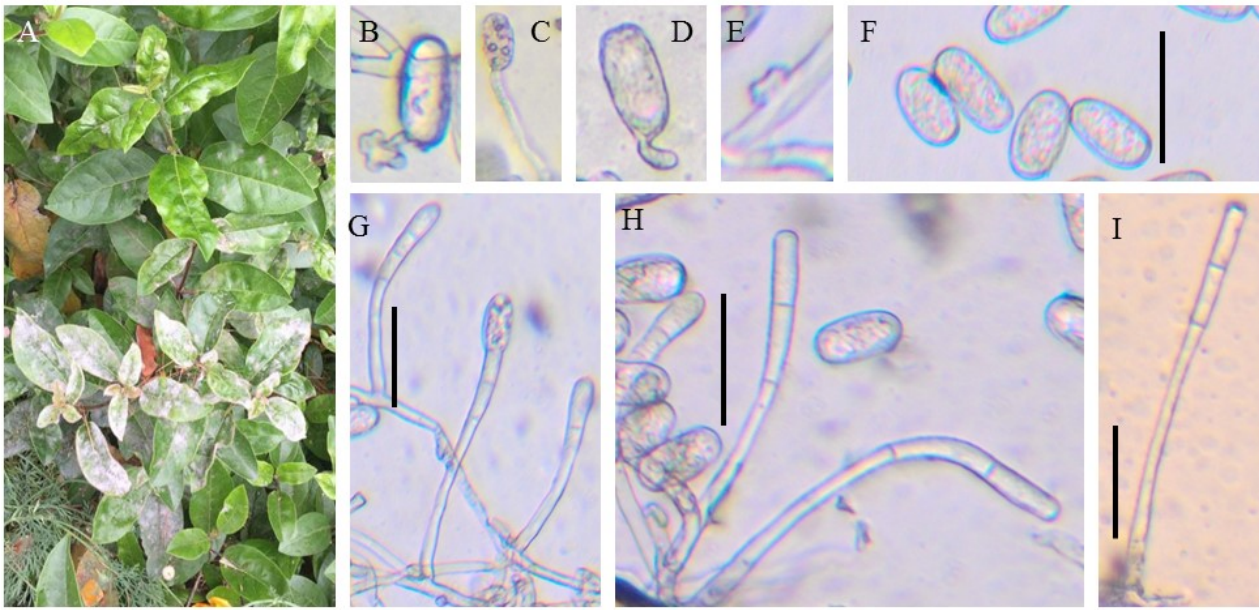
Figure 2.2: *Erysiphe viburniphila* on *Viburnum tinus* from North America. A. Powdery mildew on *V. tinus*. B–D. Germtubes, E. Appressoria. F. Conidia. G–I. Conidiophores. Bars=50 μm.
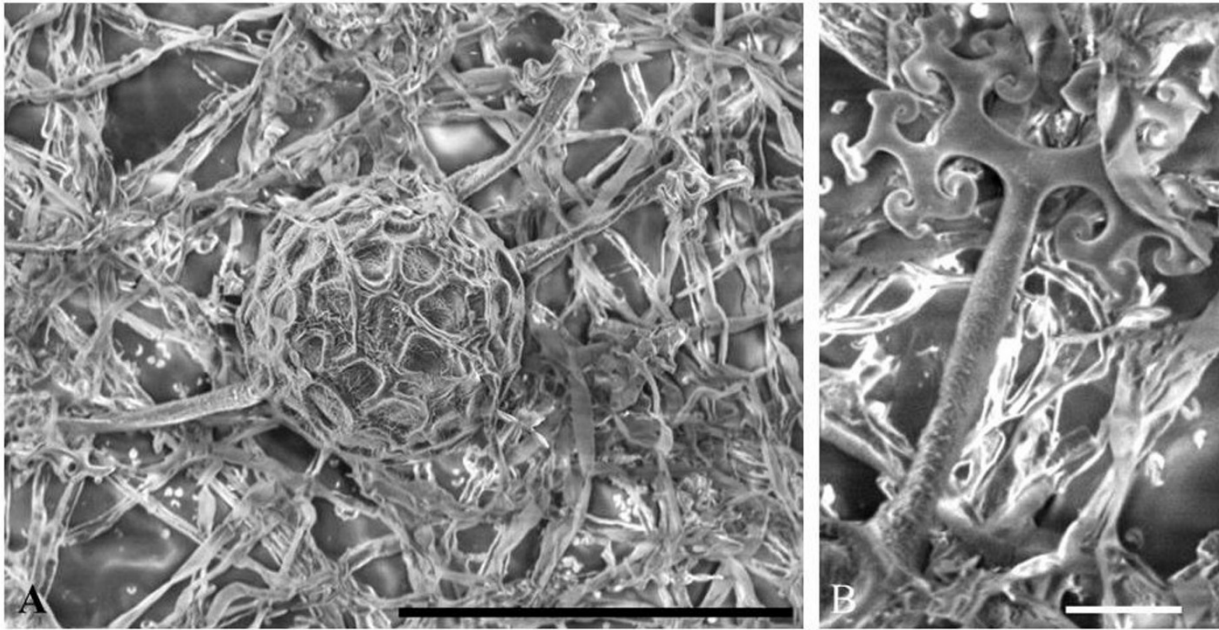
Figure 2.3: Scanning electron microscope photos of *Erysiphe viburniphila* on *Viburnum tinus* from Switzerland. A.

Chasmothecium. B. Appendage. Bars: A=100 μm, B= 20 μm. Figure taken from Bradshaw et al. (2020).
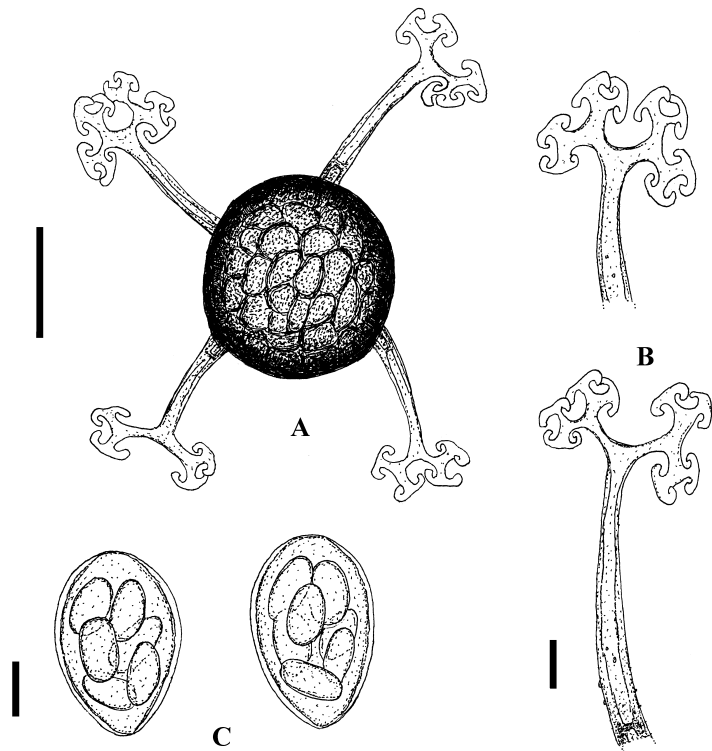
Figure 2.4: Illustration of the sexual morph of *Erysiphe viburniphila* on *Viburnum tinus* from Switzerland. A. Chasmothecium. B. Appendages. C. Asci with ascospores. Bars: A=50 μm, B and C=20 μm. Figure taken from Bradshaw et al. (2020).
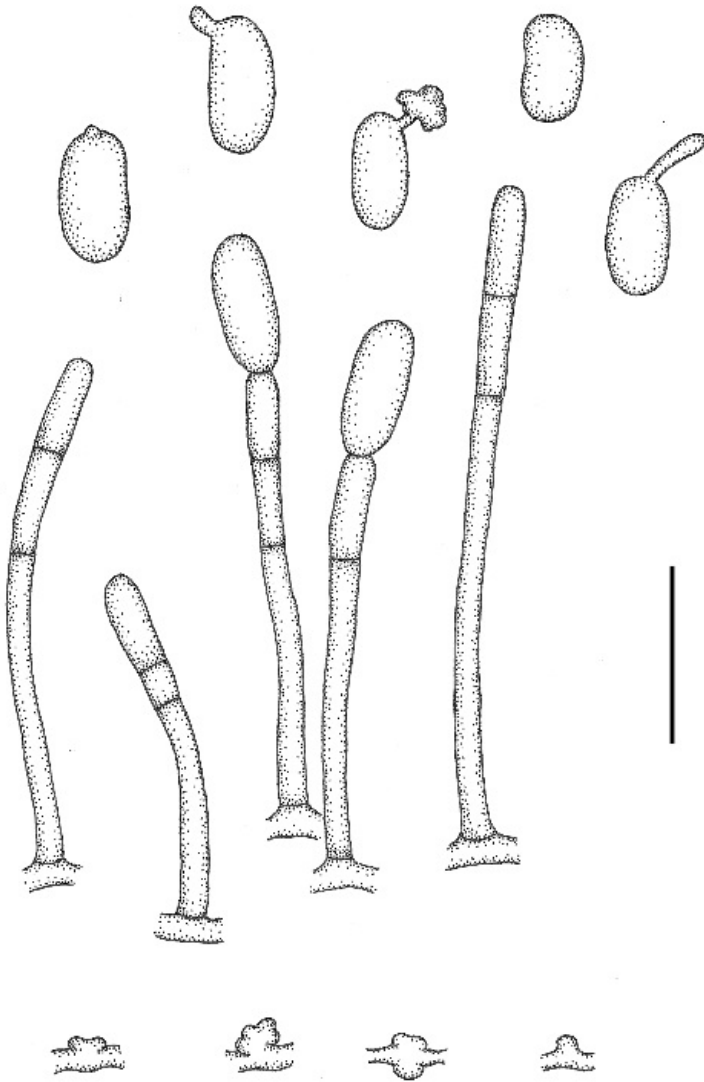
Figure 2.5: Illustration of the asexual morph of *Erysiphe viburniphila* on *Viburnum tinus* from the USA. Bar= 50 µm.

Figure taken from Bradshaw et al. (2020).
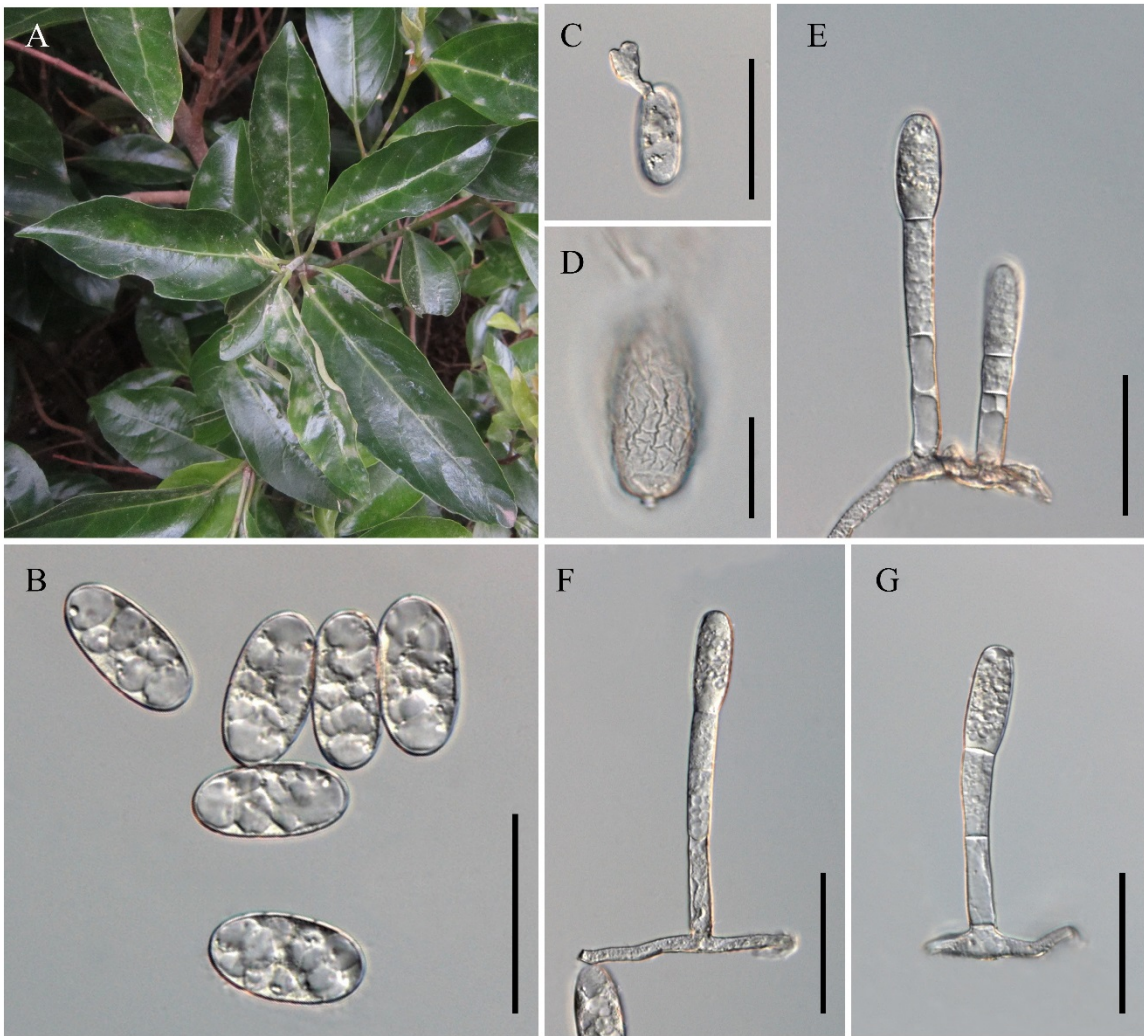
Figure 2.6: *Erysiphe pseudoviburni* on *V. odoratissimum* var. *awabuki*. A. Powdery mildew colonies on *V. odoratissimum* var. *awabuki*. B. Conidia. C. Conidia with germ tube. D. Surface structure of a wrinkled conidium. E–F. Conidiophores. Bars: B–C and E–G=50 μm and D= 50 μm. Figure taken from Bradshaw et al. (2020).
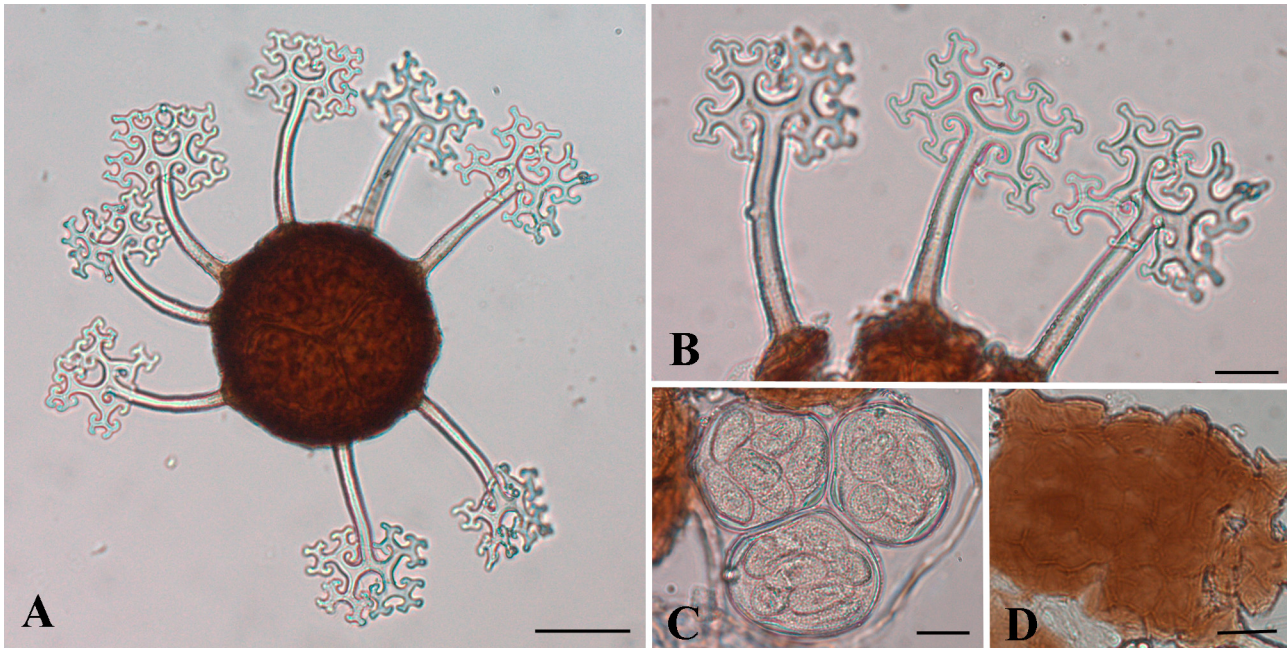
Figure 2.7: *Erysiphe pseudoviburni* on *V. sieboldii*. A. Chasmothecium. B. Appendages. C. Asci and ascospores. D. Outer peridium cell layer. Bars: A=40 μm and B–D=20 μm. Figure taken from Bradshaw et al. (2020).
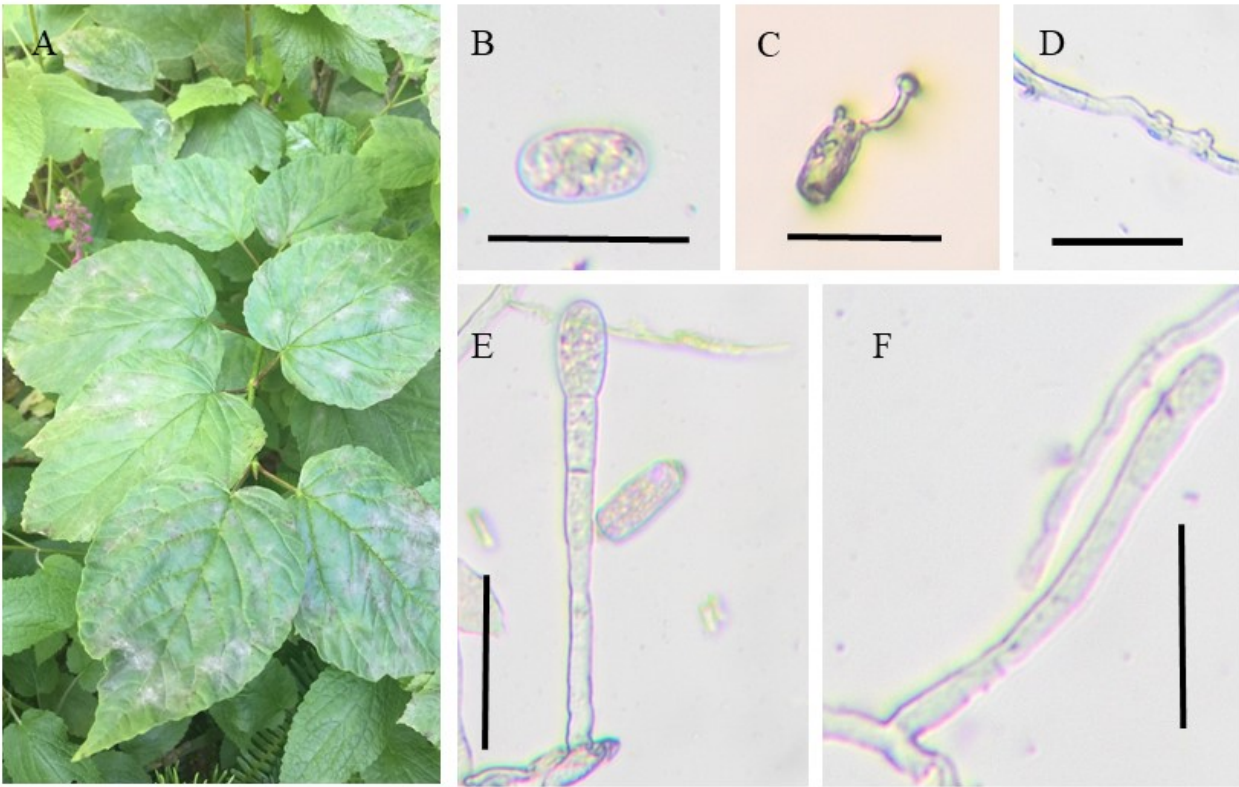
Figure 2.8: *Erysiphe viburni* on *Viburnum edule*. A. Powdery mildew colonies on *Viburnum edule*. B. Conidia. C. Conidia with germtube. D. Appresssoria. E–F. Conidiophores. Bars=50 μm.
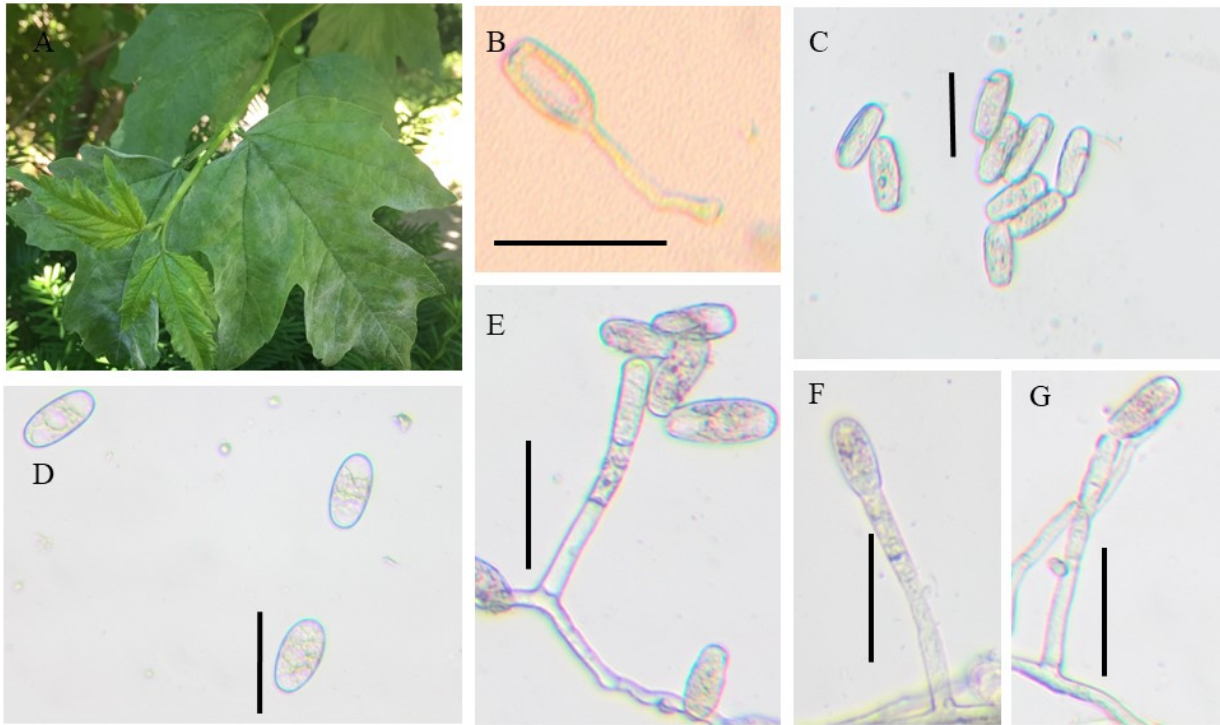
Figure 2.9: *Erysiphe viburni* on *Viburnum opulus*. A. Powdery mildew on *Viburnum opulus*. B. Germtube. C–D. Conidia. E–F. Conidiophores. Bars=50 μm.
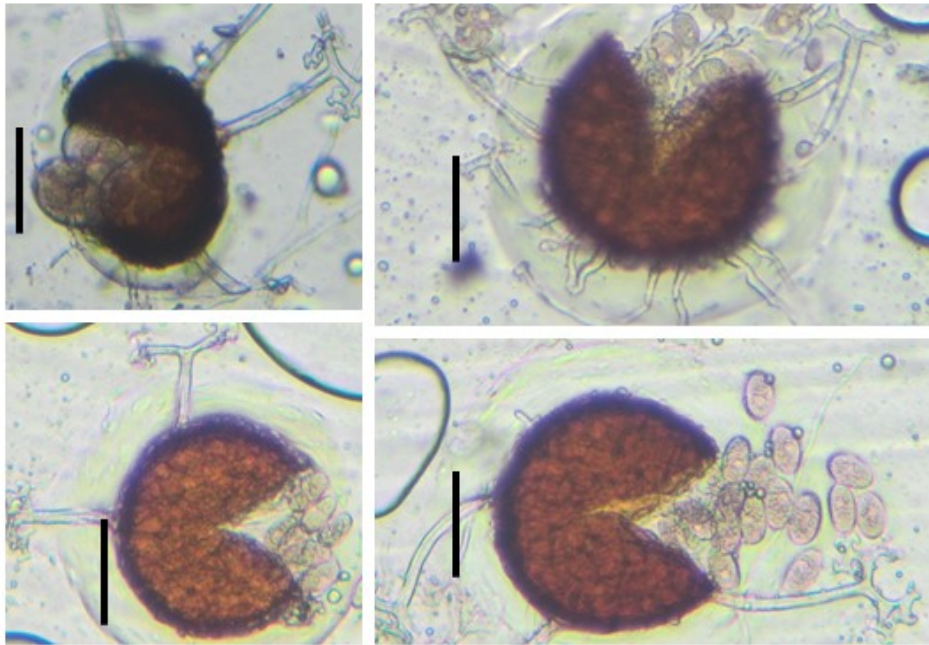
Figure 2.10: *Erysiphe viburni* on *Viburnum opulus*. Chasmothecia with asci and ascospores. Bars=50 μm.
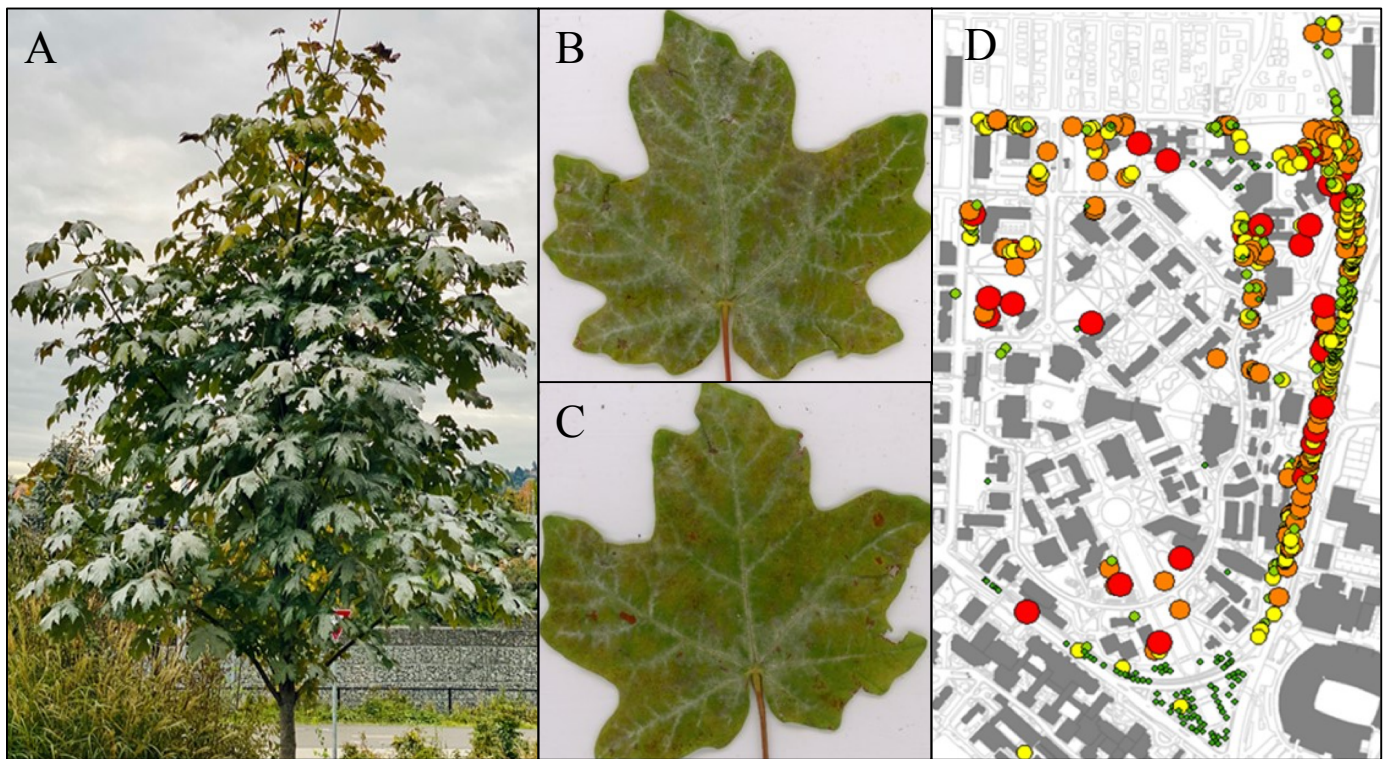
Figure 3.1: *Acer macrophyllum* infected with powdery mildew on the University of Washington Campus (A) *Acer macrophyllum* tree infected with *S. bicornis*; (B-C) Signs and symptoms of *S. bicornis* on *A. macrophyllum* leaves; (D) Location of the 519 *A. macrophyllum* trees evaluated for this study (size and color of circles is proportion to the tree diameter at breast height).
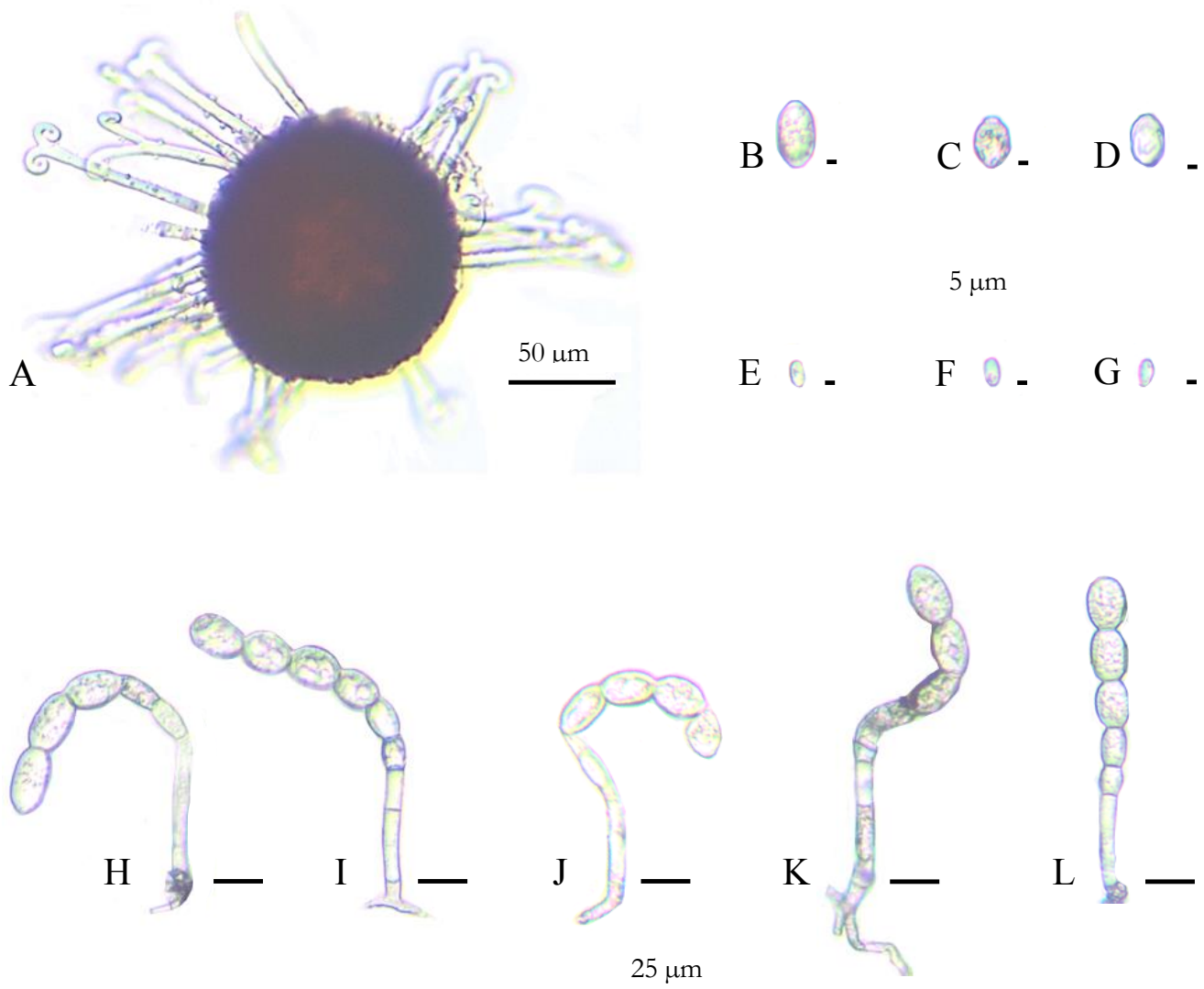
Figure 3.2. *Sawadaea bicornis* (A) chasmothecia (B-D) conidia, (E-G) microconidia, (H-L) conidiophores. Scale bars: A= 50 μm, B-G=5 μm, H-L=25 μm.
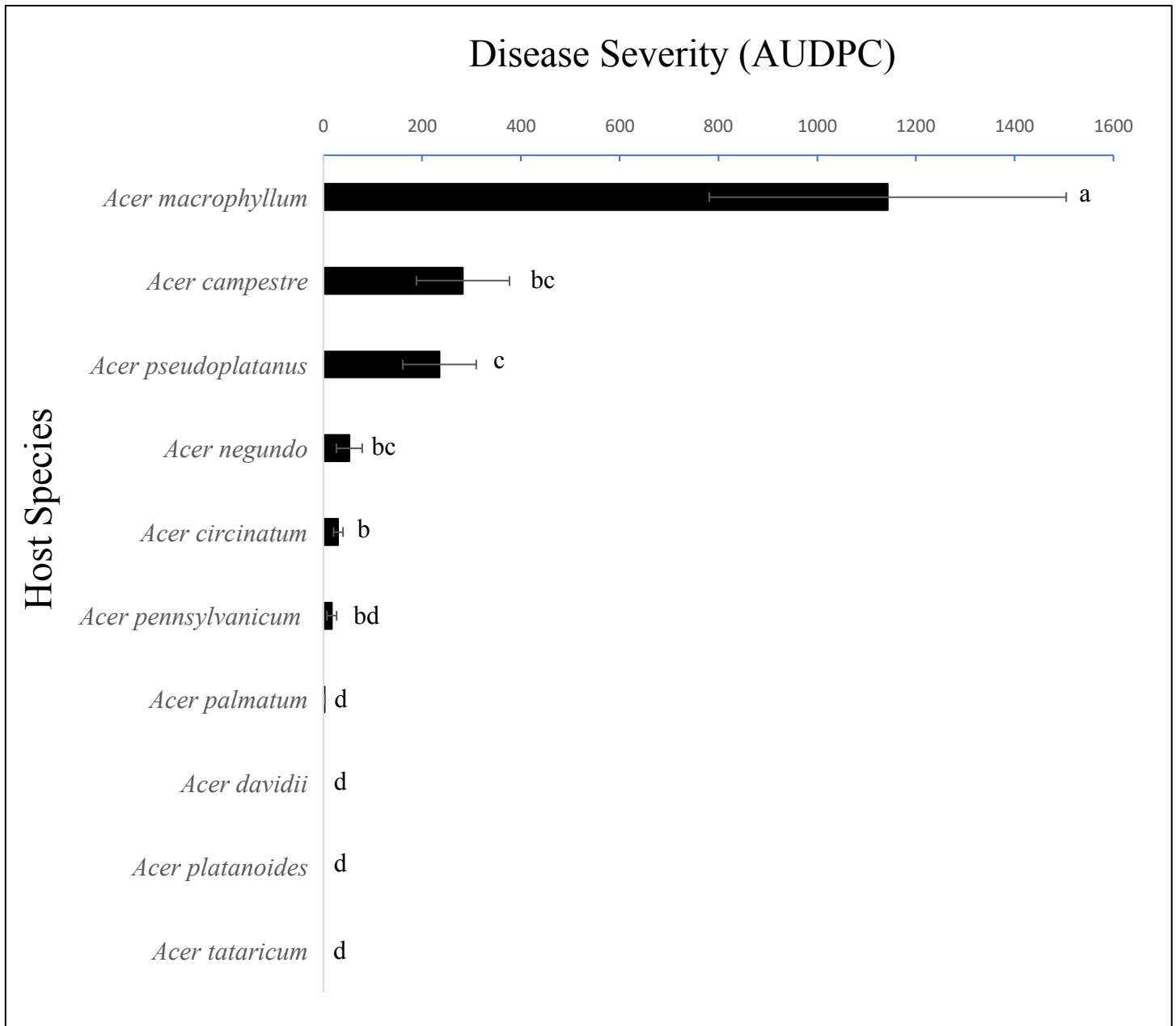
Figure 3.3: Bar graph evaluating the susceptibility of different *Acer* species to *S. bicornis*. Bars with different letters are significantly different from each other (P<0.05).
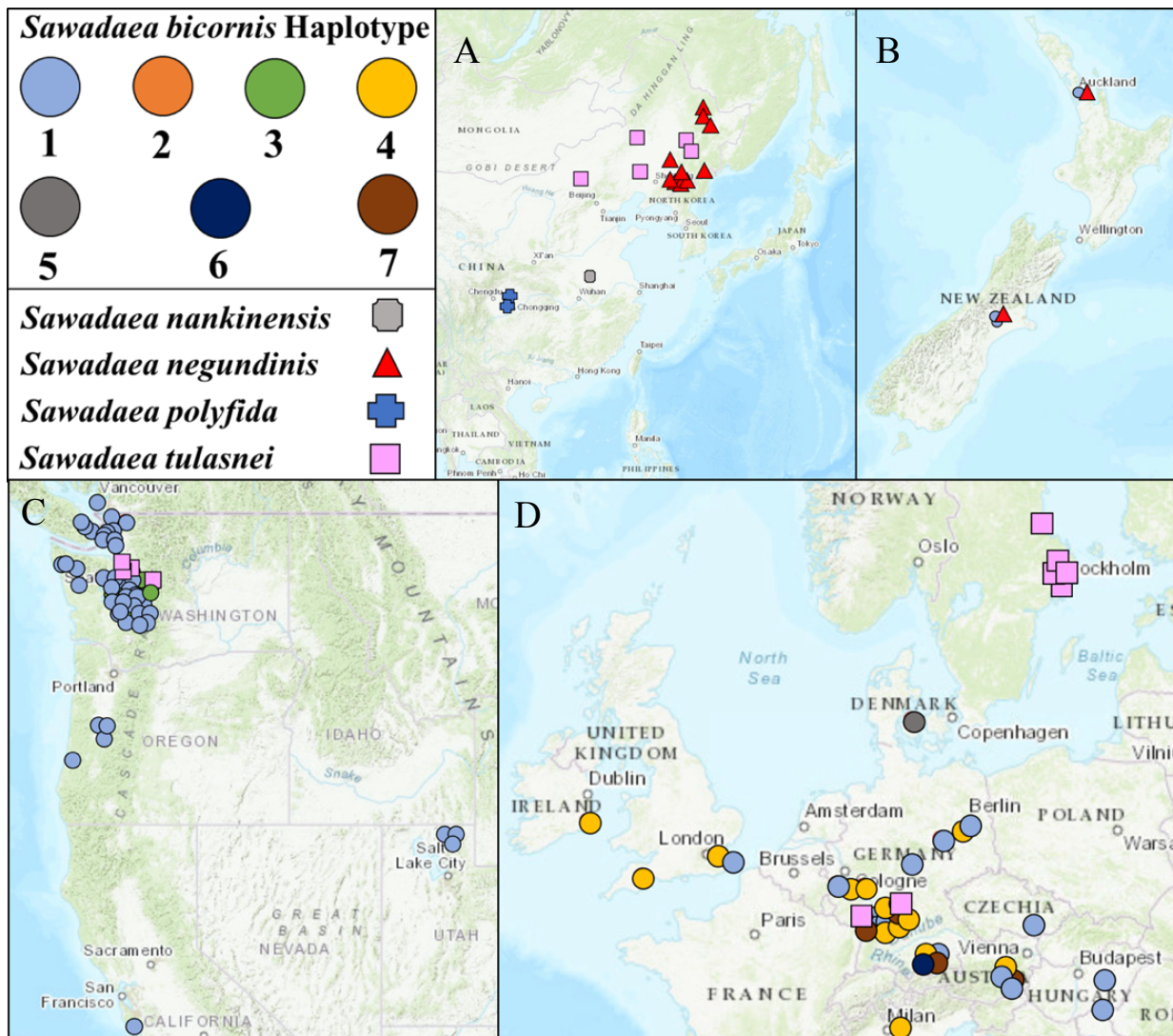
Figure 3.4: Locations, ITS/LSU haplotype numbers and species of the different powdery mildew specimens collected and sequenced for this study in (A) China, (B) New Zealand, (C) North America, and (D) Europe.
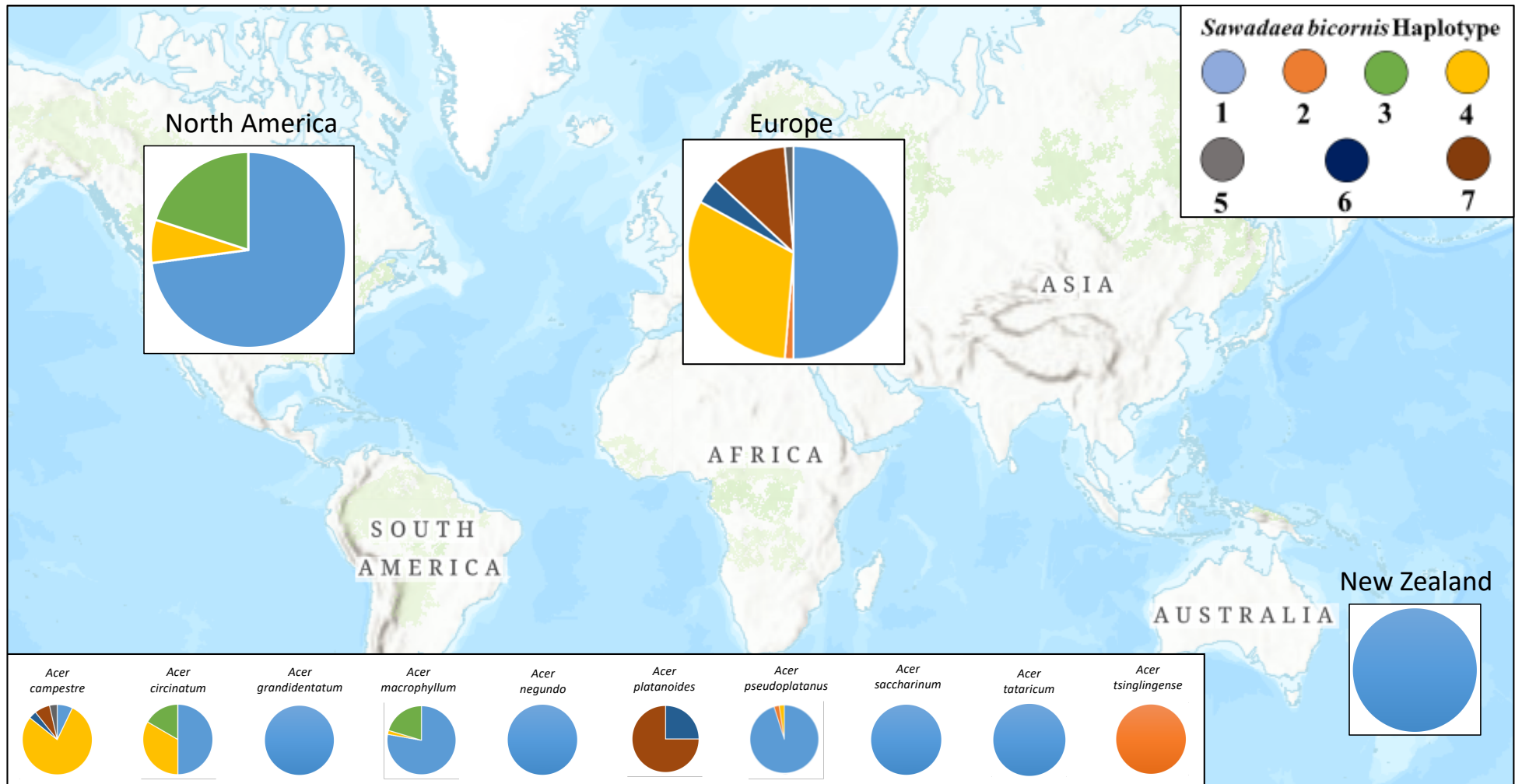
165

Figure 3.5: ITS/LSU haplotype frequency of *S. bicornis* specimens collected for this study based on location and host species.
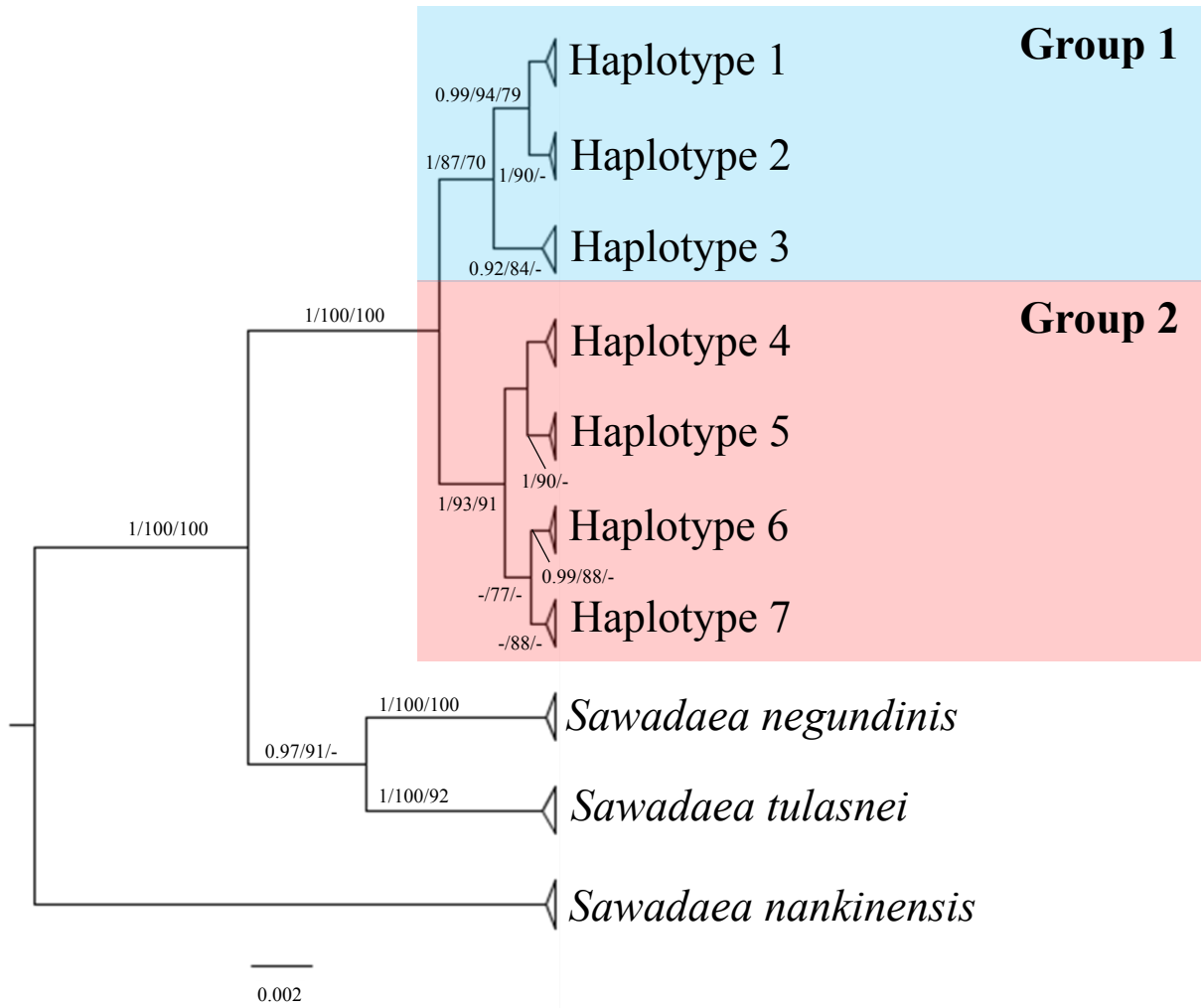
Figure 3.6: An ITS+LSU phylogenetic tree representing the different haplotypes and species of powdery mildew collected for this study. Posterior probabilities ≥ 90 are displayed followed by bootstrap values greater than 70% for the maximum likelihood (ML) and maximum parsimony (MP) analyses. *Sawadaea nankinensis* was used as an outgroup taxon. Analyses revealed two major groups of *S. bicornis* haplotypes.
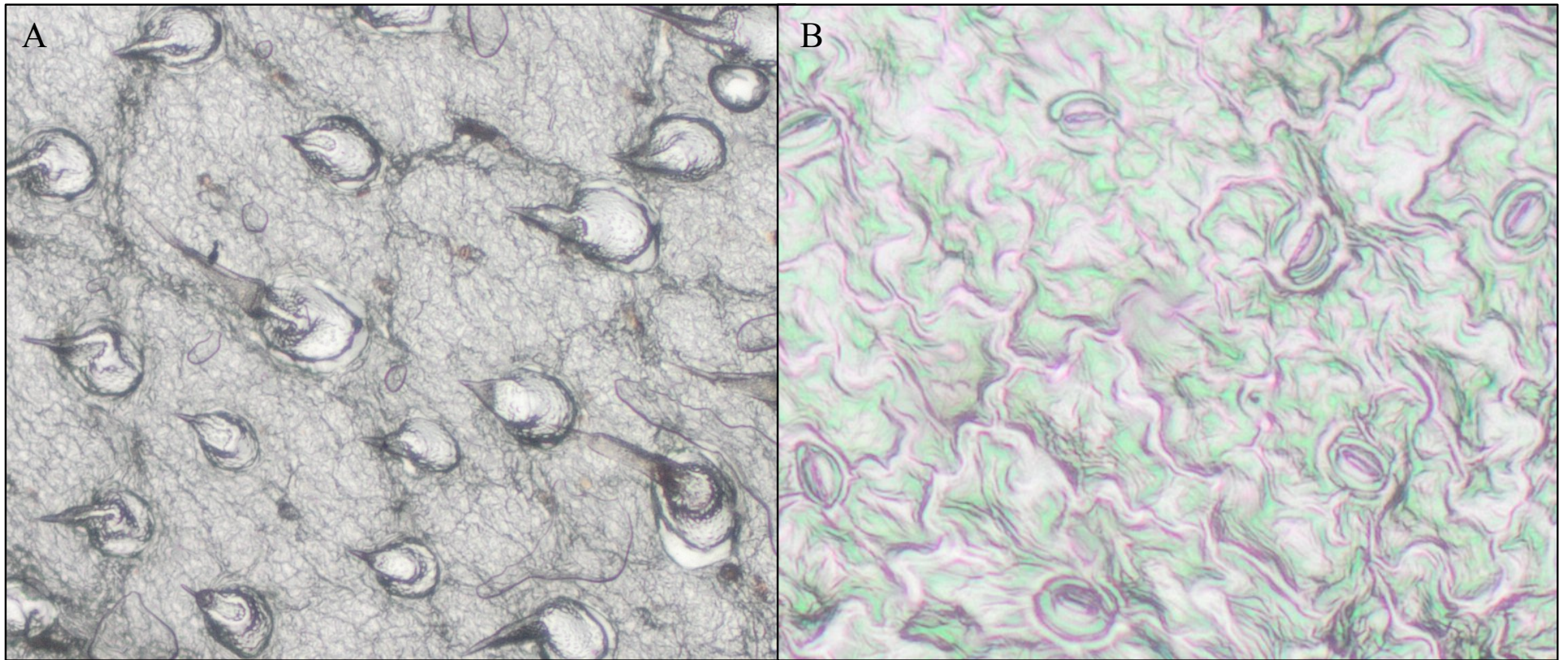
Figure 4.1: Pictures of leaf peels under a compound microscope showing A. trichomes and B. epidermal and stomata cells.
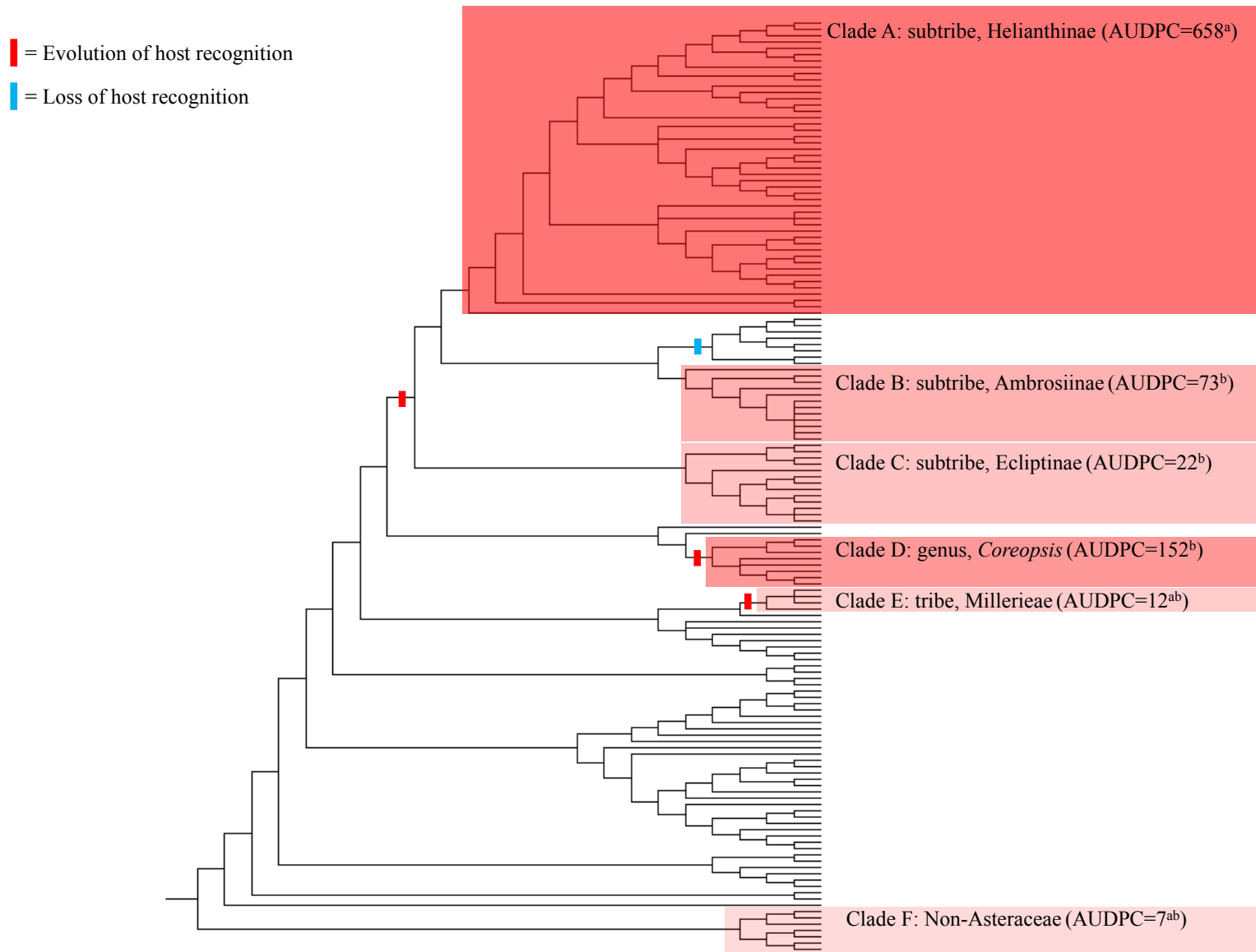
Figure 4.2: A phylogenetic tree of the Asteraceae with major evolutionary events added based on a parsimonious approach. The average susceptibility of the species within the highlighted clades to *G. latisporus* is presented as an Area Under the Disease Progress Curve value. Darker colors signify higher susceptibility values. Taxa within clade A (composed of mainly *Helianthus* spp.) are the most susceptible. Clades with the same letters are not statistically different in an ANOVA (P<0.05). Evolutionary events of taxa not in the Asteraceae were not included.

Figure 4.3: A zoomed in portion of the phylogenetic tree presented in Figure 4.2. Evolutionary events added based on a parsimonious approach. Taxa in red font were tested in this study to be hosts of *G. latisporus* and taxa in purple font were previously reported as hosts. The average susceptibility of the species within the highlighted clades to *G. latisporus* is presented as an Area Under the Disease Progress Curve value. Clades with the different letters are nearly significantly different in an ANOVA (P=0.06). Clade A-1 (which primarily consists of Annual species is less susceptible to disease than clade A-3 (which primarily consists of Perennial species.
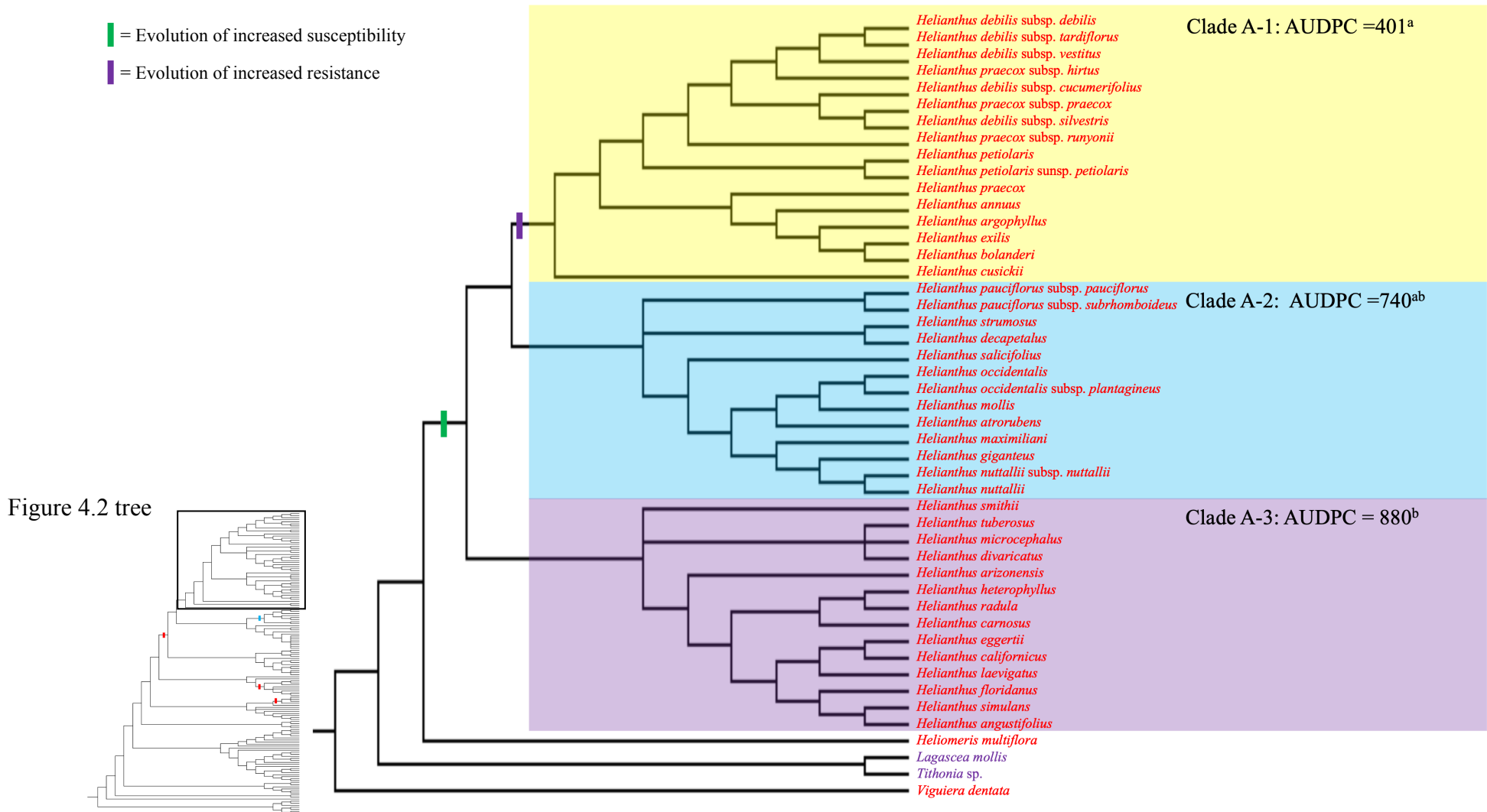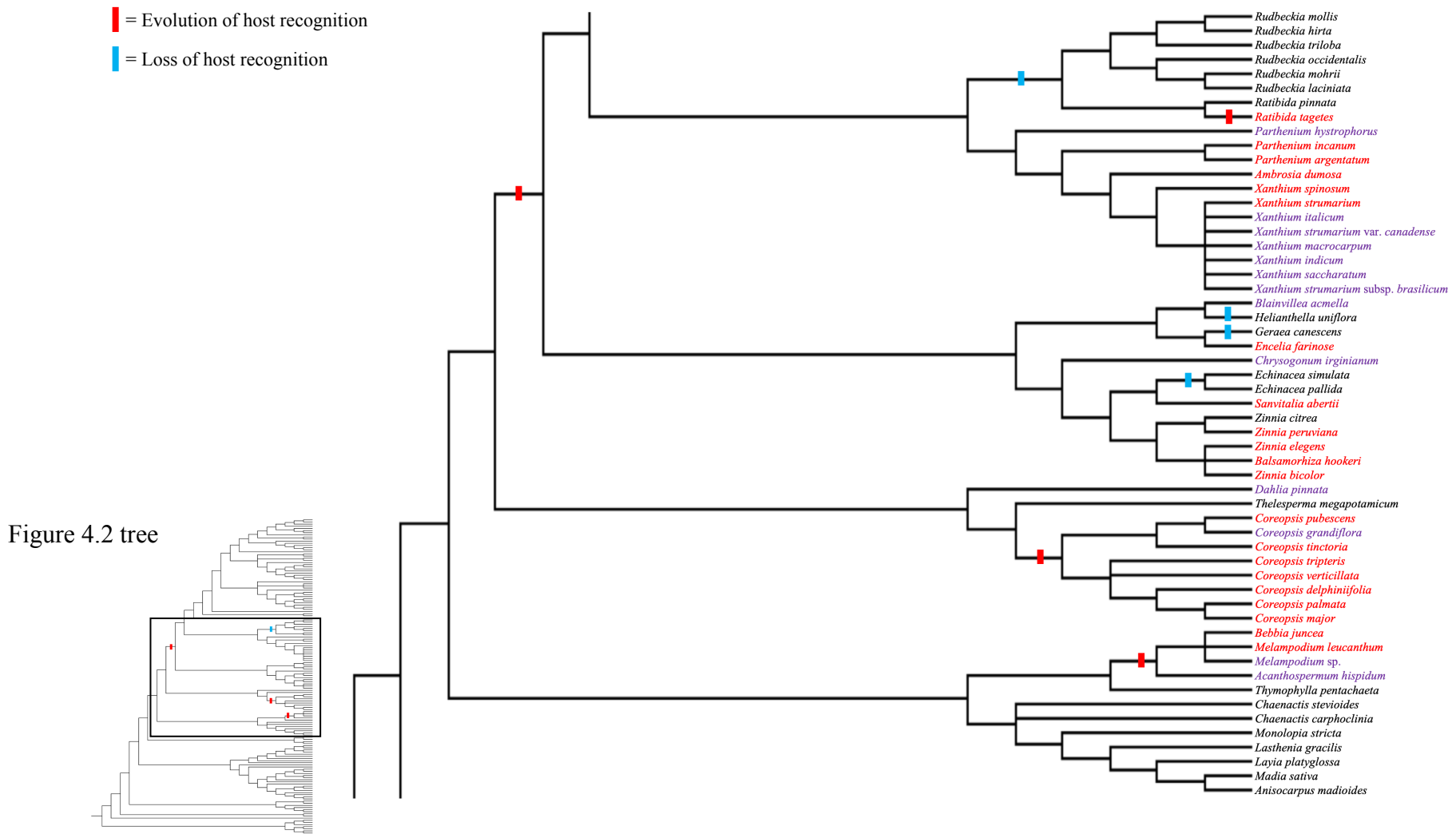
Figure 4.4: A zoomed in portion of the phylogenetic tree presented in Figure 4.2. Evolutionary events added based on a parsimonious approach. Taxa in red font were tested in this study to be hosts of *G. latisporus* and taxa in purple font were previously reported as hosts. *Dhalia pinnata* was recently shown to be a host of *G. ambrosiae,* not *G. latisporus* (which was reported in the past; Qiu et al. 2020). Host recognition was gained and lost throughout the Asteraceae.

= Evolution of host recognition

= Loss of host recognition

Figure 4.2 tree

Baileya multiradiata
Baileya pleiradiata
Hymenoxys odorata
Helenium amarum
Artemisia tilesii
Artemisia ludoviciana
Artemisia borealis
Artemisia frigida
Artemisia tridentate
Tanacetum camphoratum
Leucanthemum vulgare
Achillea alpina
Packera multilobata
Anaphalis margaritacea
Baccharis sarothroides
Xanthisma gracile
Xanthisma grindelioides
Xylorhiza venusta
Xylorhiza tortifolia
Grindelia squarrosa
Symphyotrichum novae-angliae
Townsendia incana
Gutierrezia microcephela
Erigeron pumilus
Erigeron acris
Heterotheca villosa
Ericameria nauseosa
Acamptopappus sphaerocephalus
Stenotus armerioides
Solidago wrightii
Lactuca serriola
Taraxacum kok-saghyz
Rafinesquia neomexicana
Microseris douglasii
Agoseris grandiflora
Nothocalais troximoides
Sesamum indicum
Monarda fistulosa
Persicaria decipiens
Abelmoschus esculentus
Abelmoschus caillei
Abelmoschus manihot
Cyamopsis soraloides
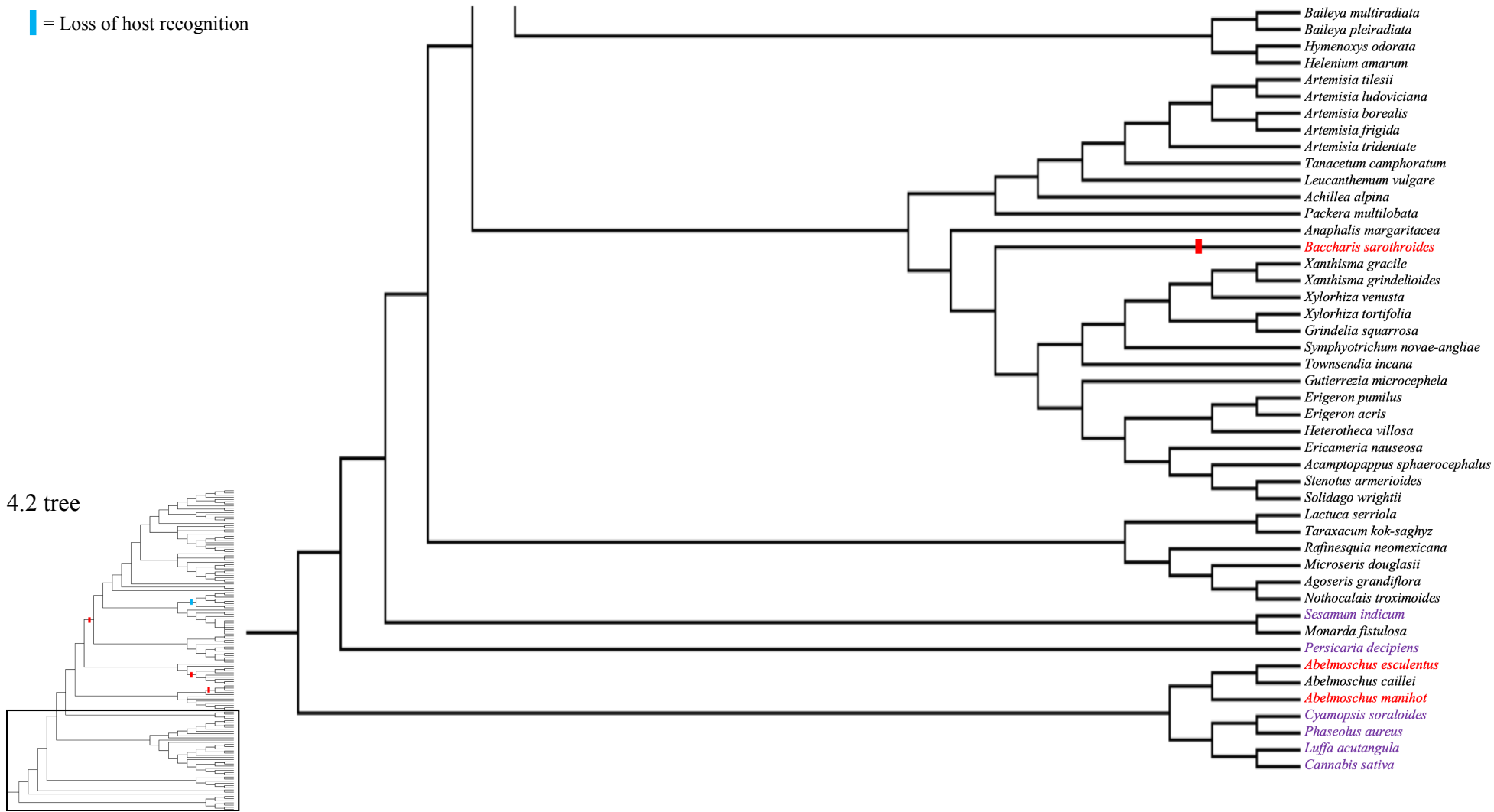Phaseolus aureus
Luffa acutangula
Cannabis sativa

Figure 4.5: A zoomed in portion of the phylogenetic tree presented in Figure 4.2. Evolutionary events added based on a parsimonious approach. Taxa in red font were tested in this study to be hosts of *G. latisporus* and taxa in purple font were previously reported as hosts. Evolutionary events of taxa not in the Asteraceae were not included.
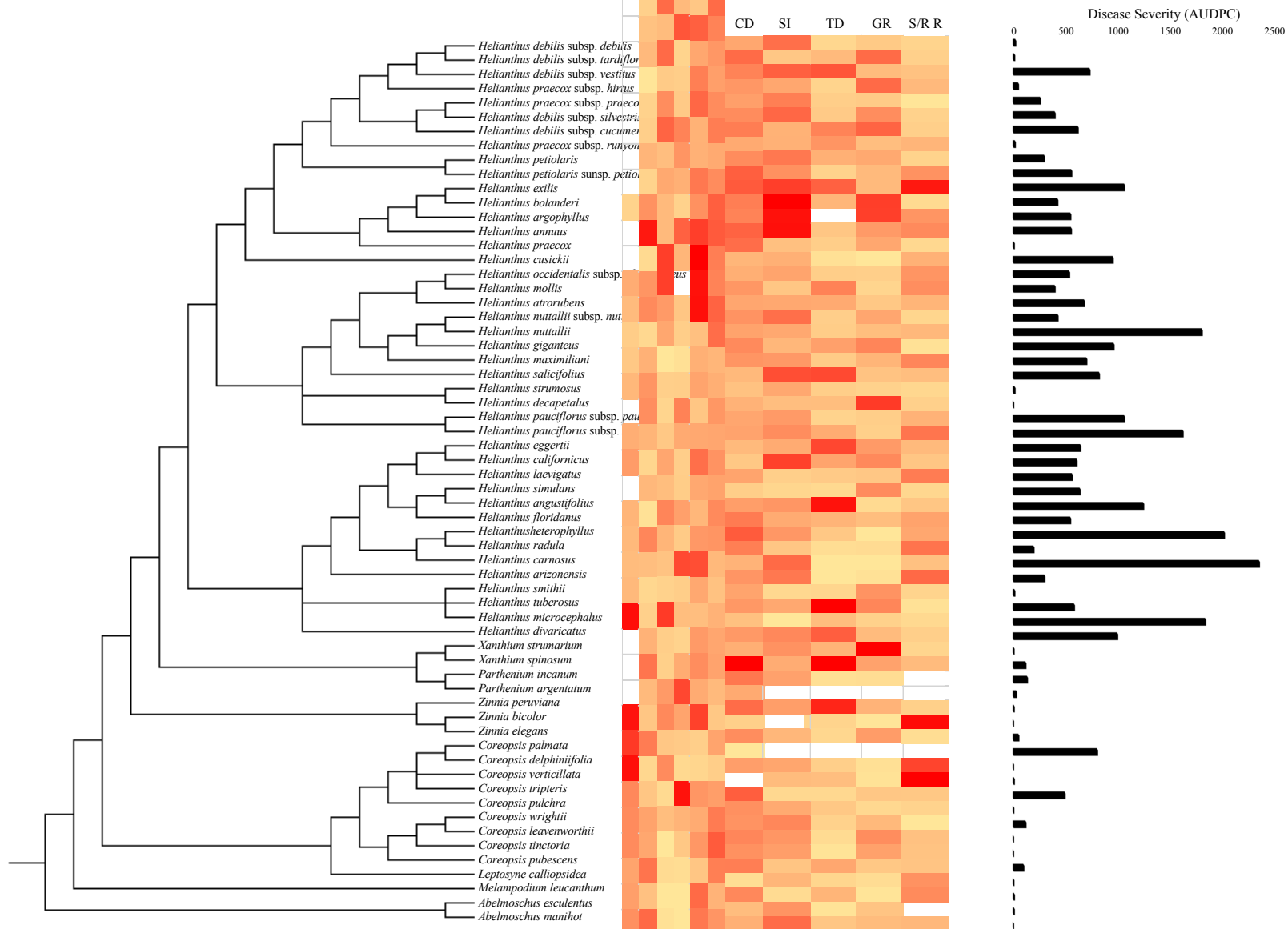
Figure 4.6: Phylogeny of the taxa that were evaluated for their susceptibility to *G. latisporus* in this study. The disease severity of the different taxa are shown in a bar graph to the right. Susceptibility is presented as an AUDPC, the Disease Progress Curve value. A heat map is shown of the average value for each of the different traits measured in this study. CD=Chlorophyll Density, SI=Stomatal Index, TD=Trichome Density, GR=Growth Rate, S/R R=Shoot-to-Root Ratio.

173